ADVANCED MATERIALS TECHNOLOGIES
www.advmattechnol.de

3D Printable Hydrogel Bioelectronic Interfaces for Healthcare Monitoring and Disease Diagnosis: Materials, Design Strategies, and Applications

*Sayan Deb Dutta, Keya Ganguly, Aayushi Randhawa, Tejal V. Patil, Hojin Kim, Rumi Acharya, and Ki-Taek Lim**

In recent years, additive manufacturing tools, such as 3D printing, has gained enormous attention in biomedical engineering for developing ionotropic devices, flexible electronics, skin-electronic interfaces, and wearable sensors with extremely high precision and sensing accuracy. Such printed bioelectronics are innovative and can be used as multi-stimuli response platforms for human health monitoring and disease diagnosis. This review systematically discusses the past, present, and future of the various printable and stretchable soft bioelectronics for precision medicine. The potential of various naturally and chemically derived conductive biopolymer inks and their nanocomposites with tunable physico-chemical properties is also highlighted, which is crucial for bioelectronics fabrication. Then, the design strategies of various printable sensors for human body sensing are summarized. In conclusion, the perspectives on the future advanced bioelectronics are described, which will be helpful, particularly in the field of nano/biomedicine. An in-depth knowledge of materials design to functional aspects of printable bioelectronics is demonstrated, with an aim to accelerate the development of next-generation wearables.

1. Introduction

Wearable electronics are essential medical diagnostic tools, limiting the shortcomings raised by ambiguous, faulty, and delayed diagnostic results.[1–5] These devices are looking forward to playing a vital role in precision medicine due to their direct ability to monitor the physiological changes of an individual through the skin.[6,7] These electronics' extreme flexibility and sensitivity could be an ideal source for designing future novel biomedical devices.[8–12] Most commercially available wearable medical devices initially relied on silicon-based microelectronics because of their unique design, rigidity, and flexibility, which could afford robust and reliable functionality for clinical and preclinical applications.[4,13,14] However, the inconvenient wiring and inadequate integration of silicon electronics with human skin make it nearly unusable for mobile and long-term personalized monitoring. Moreover, conventional electronic devices need additional straps and/or adhesive tapes to hold onto the skin surface, making it inconvenient for diagnosis.[4,15,16] Remarkably, the mismatch originated from the improper electronic-skin interface or poor adhesion,[17–20] which creates significant challenges in developing next-generation skin-integrated wearable devices for biomedical applications.[4,21,22]

Researchers mainly focus on developing novel and tactile wearable skin patches for multi-faceted applications. An "electronic skin patch" or "E-skin" patch can be defined as a multifunctional system to detect the physiological responses of the human body, such as temperature, pressure, pH, heart-beat, and many other electrophysiological signals, by integrating conductive electrodes, various sensors, power supply, and internet of things (IoT) sensors to communicate, visualize, and analyze the signals.[18,23–28] In robotics and prosthetics, the E-skin is also known as tactile skin. Therefore, an ideal "E-skin" should have the following key features, including 1) multiple sensors distributed over the entire body to analyze multiple types of touch sensing (e.g., 45k touch or pressure-sensitive receptors/1.5 m^2 area of skin); 2) exact placement of the sensors to achieve different levels of sensitivity; 3) soft, stretchable, and integrated substrate to adjust in the three dimensional (3D)-microenvironment of the human body; 4) capability to analyze a large amount of data through mobile devices (e.g., analyzing real-time data through IoT mobile devices, such as cell phones, computer, and other gadgets); 5) energy-efficient, cost-effective, and low-power

S. D. Dutta, K. Ganguly, A. Randhawa, T. V. Patil, H. Kim, R. Acharya, K.-T. Lim
Department of Biosystems Engineering
Kangwon National University
Chuncheon 24341, Republic of Korea
E-mail: ktlim@kangwon.ac.kr
S. D. Dutta, K.-T. Lim
Institute of Forest Sciences
Kangwon National University
Chuncheon 24341, Republic of Korea
A. Randhawa, T. V. Patil, R. Acharya, K.-T. Lim
Interdisciplinary Program in Smart Agriculture
Kangwon National University
Chuncheon 24341, Republic of Korea
The ORCID identification number(s) for the author(s) of this article can be found under https://doi.org/10.1002/admt.202301874

DOI: 10.1002/admt.202301874

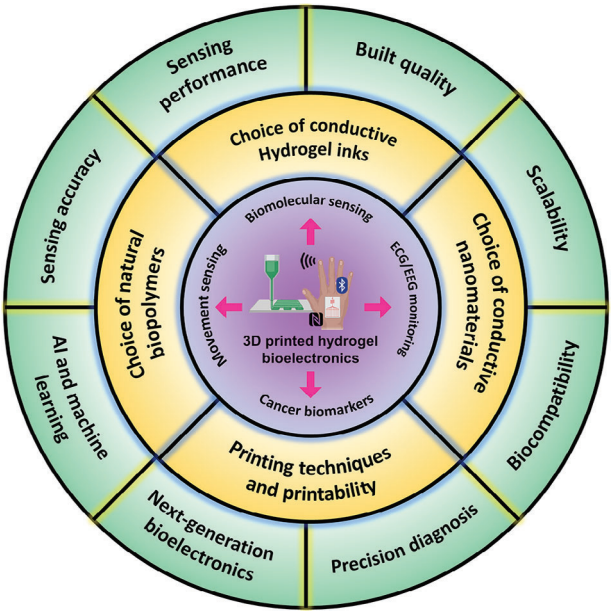

Scheme 1. Schematic overview of the design strategies and applications of the 3D printable wearable bioelectronics for precision medicine.

electronics; and 6) minimum energy for operating the touch/pressure sensors. An ideal patch with all the above features could be recognized as an "E-skin" patch that completely biomimic the human skin.[2,29–31]

With the advent of advanced biofabrication tools, the wearable bioelectronics sector is increasing rapidly in biomedical engineering. Additive manufacturing, commonly known as 3D printing, is an ultramodern nano/biofabrication tool enabling the rapid prototyping of a computer-aided model (CAD) into a 3D structure.[32,33] The 3D printing technology allows precise patterning of a hydrogel ink with sufficient details, which could be used for the fabrication of various bioelectronics devices, such as electrodes,[34–36] circuits,[37–39] sensors,[40,41] and microchips/needles.[42–44] Traditional bioelectronics primarily relies on conventional fabrication techniques, such as patterning, screen printing, drop casting, or spray coating, which is sometimes inappropriate for large-scale manufacturing of bioelectronics owing to high price tags and complicated fabrication processes.[45,46] One significant challenge with conventional bioelectronics is their bulky structure and noisy artifacts when attached to the skin surface. The bulky structure with complicated electronic interfaces often leads to unwanted noise, loss of skin adhesion, faulty readings, and difficulty carrying with body parts as it tends to fall during active motion or bending of body parts. Thus, traditional bioelectronics often showed inaccurate data with faulty diagnostic advice, which is practically inappropriate for clinical application. Besides, 3D printing offers a wide range of conductive hydrogel inks into a single place that can be accurately printed and transported to the patient's body parts wireless to monitor various pathophysiological conditions without distortion or dislocation.[47] **Scheme 1** schematically shows the present status and future prospects of wearable bioelectronics for healthcare and medicine. It is well-documented that most commercially available bioelectronics already in clinical trials are not additively manufactured. A few reports are available in the existing literature about the successful translation of research and development (R&D) into clinics, rest assured still in the research stage. For example, the first 3D printed bioelectronic chip was developed by ActiPatch Corporation for diagnosis of chronic and post-operative wound care and musculo-skeletal pain recording. Later on, An implantable bioelectronic device was also demonstrated by SetPoint medical company, California, for the treatment of rheumatoid arthritis and associated inflammatory disorders.[48,49] Following that, 3D printed conductive surgical patch was used in clinical trials for studying spinal cord injury.[50] In recent years, most of the 3D printed bioelectronic devices with high precision and high accuracy are in the research phase and need more extensive collaboration with biomedical engineering to move towards precision diagnosis for healthcare and medicine.

This review article aimed to document the present state-of-the-art wearable bioelectronics fabricated through 3D printing technology for human body sensing and disease diagnosis applications. Many review articles recently demonstrated the use of various conductive biopolymers to fabricate wearable bioelectronics.[51–54] Conductive biopolymers, combined with various carbon-based or non-carbon-based nanofillers, have been shown to enhance electrical conductivity and superior sensing ability and, therefore, used for conductive electrode fabrication. A reader should read the cited literature for more details about the role of conductive nanofillers.[45] Yuk et al. previously reported using soft hydrogel bioelectronics for sensing applications.[32] This article mainly focused on the fundamentals of skin-electrode interface with a particular focus on rational designs for hydrogel (e.g., conductive polymer composites, in situ polymerized hydrogels, and inner-penetrating network hydrogel) bioelectronics fabrication. However, this report does not include the fabrication strategies for stretchable bioelectronics and their uses. In another study, Ge et al. reported the design strategies of 3D-printed stretchable inotropic hydrogels for multi-faceted applications.[55] At a glance, this study provides an overview of the various printing techniques (e.g., extrusion printing, light-based printing, embedded printing, and ink-based printing) for fabricating flexible sensors, actuators, electroluminescent devices, and soft hydrogel robots. Despite of many outstanding reports in bioelectronics, there is no single report integrating in-depth knowledge for design strategies of 3D printable soft and stretchable hydrogel bioelectronics and biosensors for health monitoring and disease diagnosis application. In this review, we first introduced the potential of various conductive biopolymers derived from natural resources or chemical processing. Then, we summarize the necessity of 3D printing and other 3D micro/nanotechnologies for the fabrication of bioelectronics in light of material design, printability, post-processing, and further improvement of various multi-material hydrogel inks. Then, we presented an in-depth literature survey on the present status of various printed sensors (e.g., tactile, piezoelectric, piezoresistive, and triboelectric) and their sensing performances. Next, we briefly introduced the application of various 3D-printed hydrogel bioelectronics and chips for human health monitoring and disease diagnosis, with a special focus on cancer diagnosis. Finally, we presented the ongoing research direction on printable bioelectronics and provided an expert opinion on 3D printed bioelectronics development in terms of future

perspectives, such as scalability, biodegradation and eco-friendly management, printability, and durability, improving shelf-life, multi-modal strategy, and the use of artificial intelligence (AI) and machine learning towards precision medicine.

2. Nanocomposite Hydrogels as Smart "E-Skin" Patch

2.1. Biopolymer and Its Nanocomposites

Naturally derived biopolymers have been shown to exhibit good biological compatibility, excellent biodegradability, and exhibit desirable mechanical properties, which could be used as a platform for the fabrication of soft and flexible sensors. Naturally-derived biopolymers that are frequently used for skin electronics fabrication are either polysaccharides (e.g., cellulose/nanocellulose, chitin/chitosan, alginate) or protein-based (e.g., gelatin and silk fibroin) biopolymers and their nanocomposites, which are non-toxic to the human body. Those biopolymers are also used for 3D printing applications owing to their unique structure and availability of various surface functional groups, which can be tailored via acid, base, or alkali treatment to obtain the desired functionality. Conductive hydrogel fabrication may vary based on the biopolymer composition, the type of nanomaterials embedded inside, and the cross-linking techniques. For instance, Wang and co-workers reported a recent article emphasizing on the fabrication and application of naturally sourced conductive hydrogels for sensing applications.[54] To gain insight into conductive hydrogel fabrication and its application in 3D printing, a reader is recommended to read the cited literature.[56–60] In this section, we discussed the role of commonly used biopolymers, nanocomposite hydrogels, and their potential in 3D printing for skin bioelectronics fabrication.

2.1.1. Cellulose/Nanocellulose and Its Nanocomposites

Cellulose is one of the most abundant biopolymers used to fabricate conductive hydrogels. Cellulose is a long-chain polysaccharide containing repetitive β−1,4-linked glucose (=D-glucan) units. Cellulose is the primary component of the plant cell wall, which provides structural rigidity and provides sufficient mechanical strength for survival.[57,61] Cellulose can be extracted from the plant biomass by removing the lignin and hemicellulose moieties.[62–64] However, pure cellulose is not water-soluble owing to the high crystallinity index and the presence of strong inter- and intra-molecular hydrogen bonds.[61] However, surface modification of cellulose (e.g., methyl-, carboxymethyl-, hydroxypropyl methyl groups) may give rise to a water-soluble form, which can be used easily for hydrogel fabrication.[65–67] Cellulose can be transformed into nanocellulose (cellulose nanocrystals, cellulose nanofibrils, bacterial nanocellulose) via bottom-up methods (e.g., bacterial synthesis) or top-down methods (e.g., acid hydrolysis, peroxidation, or enzymatic hydrolysis), which are highly crystalline and conductive[68–71] (**Figure 1a**). The molecular structure of cellulose exhibits a flat rope-like structure with two-fold helical symmetry, where the hydroxyl (-OH) groups align mainly on the flat surface of the rope. Each cellulose chain is connected to each other by O3...O6 intermolecular hydrogel bonds, whereas the intramolecular hydrogen bond is mainly found in between O2 and O3 —OH groups of the cellulose Iα (110) and Iβ (100) allomorphs.[72] The inter- and intramolecular hydrogen bond participation makes it a more stable and stoichiometrically two-fold symmetrical structure with a high degree of crystallinity (Figure 1b).

Cellulose/nanocellulose, in combination with various polymers, can be used as a printable hydrogel ink with high electrical conductivity for strain sensors. Recently, Heidarian et al. fabricated a printable hydrogel based on iron (Fe^{3+})-catalyzed cellulose nanofibrils/chitosan/tannic acid (*Ox*-CNF/CMCS/TA) for strain sensing application.[73] The as-fabricated hydrogel demonstrated superior self-healing, adhesive, and conductive properties with a gauge factor (GF) of 2.69 (Figure 1c). Similarly, Patel et al.,[74] reported using spherical nanocellulose/methacrylated chitosan (s-CNC/CSM)-based conductive and printable hydrogels for strain and temperature sensing applications. Incorporating s-CNCs improved the viscoelasticity, mechanical strength, and, subsequently, the printability of the CSM hydrogel with unique sensing properties.

Due to its unique molecular structure, nanocellulose has been utilized as a semiconductor, triboelectric generator, and energy harvester. Koga et al.,[75] reported that by controlling the drying process and selective pyrolysis under certain chemical reactions, bulk CNF can be transformed into nano/micro CNPs (Figure 1d(i)). Selective pyrolysis can be used to enhance the insulating property (10^{12} Ω cm) to the quasimetallic property (10^{-2} Ω cm) of the CNF, which could be used as an ideal sensing platform. This group also demonstrated that pyrolysis (≈600 °C) with controlled embossing generated micro/nano architectures than the conventional drying technique (Figure 1d(ii–ix)), which usually creates a porous matrix. The embossed CNP is moldable and foldable to develop various kinds of "origami" or "kirigami" structures (Figure 1d(x,xi)). Moreover, the authors demonstrated that the pyrolyzed CNP "origami" or "kirigami" structure, when attached to the surgical mask or wrist, efficiently monitored the breathing pattern or wrist movement (Figure 1d(xii–xv)). The high-temperature carbonization of the native CNFs allowed better conductivity (carrier charge mobility = 0.235–2.59 $cm^2\ V^{-1}\ s^{-1}$) owing to the presence of Sp^3-conjugated C—C bonds and flexibility for wearable sensing. In another study, Liu et al.[76] fabricated a CNF/methylsilane-based conductive paper for multifunctional sensing applications (Figure 1e). Nanocellulose reinforcement improves the conductivity and mechanical strength and enhances the printability and filament stability during 3D printing. Surface-modified nanocellulose, for example, cationic CNCs (CCNCs), could be used for reinforcing bulk polymers to improve the printing performance and viscoelasticity of the nanocomposite hydrogels for wearable sensing (Figure 1f).[77] These examples envisioned the exceptional conductive and sensing behavior of the cellulose/nanocellulose-based biopolymers. Several reports suggest that nanocellulose in combination with other conductive materials (*e.g.*, carbon nanotubes/CNTs, graphene oxide/GO, metals) may synergistically improve the conductivity and charge-carrier mobility,[78,79] which could be utilized for the development of stretchable skin bioelectrode fabrication.

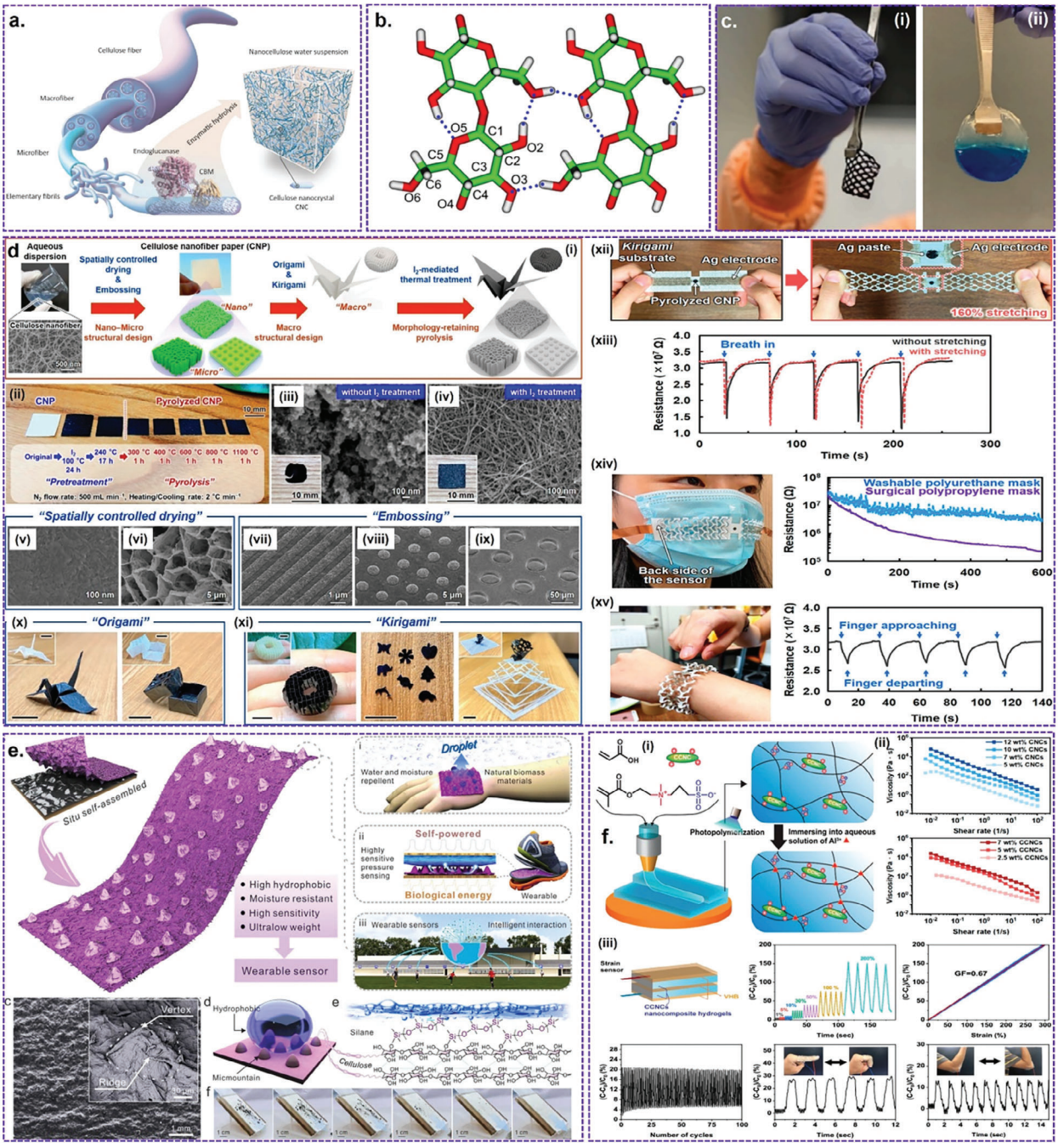

Figure 1. a) Schematic illustration of the hierarchical structure of cellulose and its derivatives.[68] Copyright 2020, Springer Nature. b) Representative ball and stick model of cellulose showing the intra- and intermolecular hydrogen bonds.[72] Copyright 2018, American Chemical Society. c) Fabrication of nanocellulose-based printable hydrogels for strain sensing. i) Digital photographs of the printed hydrogel containing Ox-CNF/CMCS/TA hydrogel, ii) Self-healing property, and iii) Digital photographs with real-time strain sensing of the printed hydrogel attached to the finger showing the change in relative resistance.[73] Copyright 2022, Elsevier. d) Demonstration of a nano/micro-fabricated cellulose paper for wearable sensing. i) Schematic illustration of cellulose nanofibers (CNPs) functionalization. ii-iv) Digital photographs and SEM images of the unmodified and modified CNPs. v, vi) SEM images of pyrolyzed CNPs with spatially controlled drying technique. vii-ix) SEM images of the pyrolyzed but microembossing of the CNPs. x) Demonstration of shape-morphing "*origami*" and "*kirigami*" structures prepared using the pyrolyzed CNPs. xii, xiii) Demonstration of the sensing performance of the flexible and wearable CNPs and "*kirigami*" paper during stretching experiment. xiv, xv) Demonstration of the sensing behavior of the device attached to the surgical mask for exhalation-derived moisture sensing. Scale bar: 100 nm, 500 nm, 1 μm, 5 μm, and 10 mm.[75] Copyright 2022, American Chemical Society. e) Schematic illustration of cellulose/silane-based stretchable and wearable triboelectric nanogenerators for pressure sensing. Scale bar: 30 μm and 1 mm.[76] Copyright 2023, Elsevier. f) Illustration of a cationic nanocellulose (CCNC)-based printable and photo-cross-linkable hydrogel for biosensing application. i) Mechanisms of hydrogel fabrication. ii) Shear-thinning curve of the different weight ratio CNCs and CCNCs showing the printability. iii) Demonstration of the strain sensing performance of the CCNC-based hydrogels in terms of conductance.[77] Copyright 2021, MDPI.

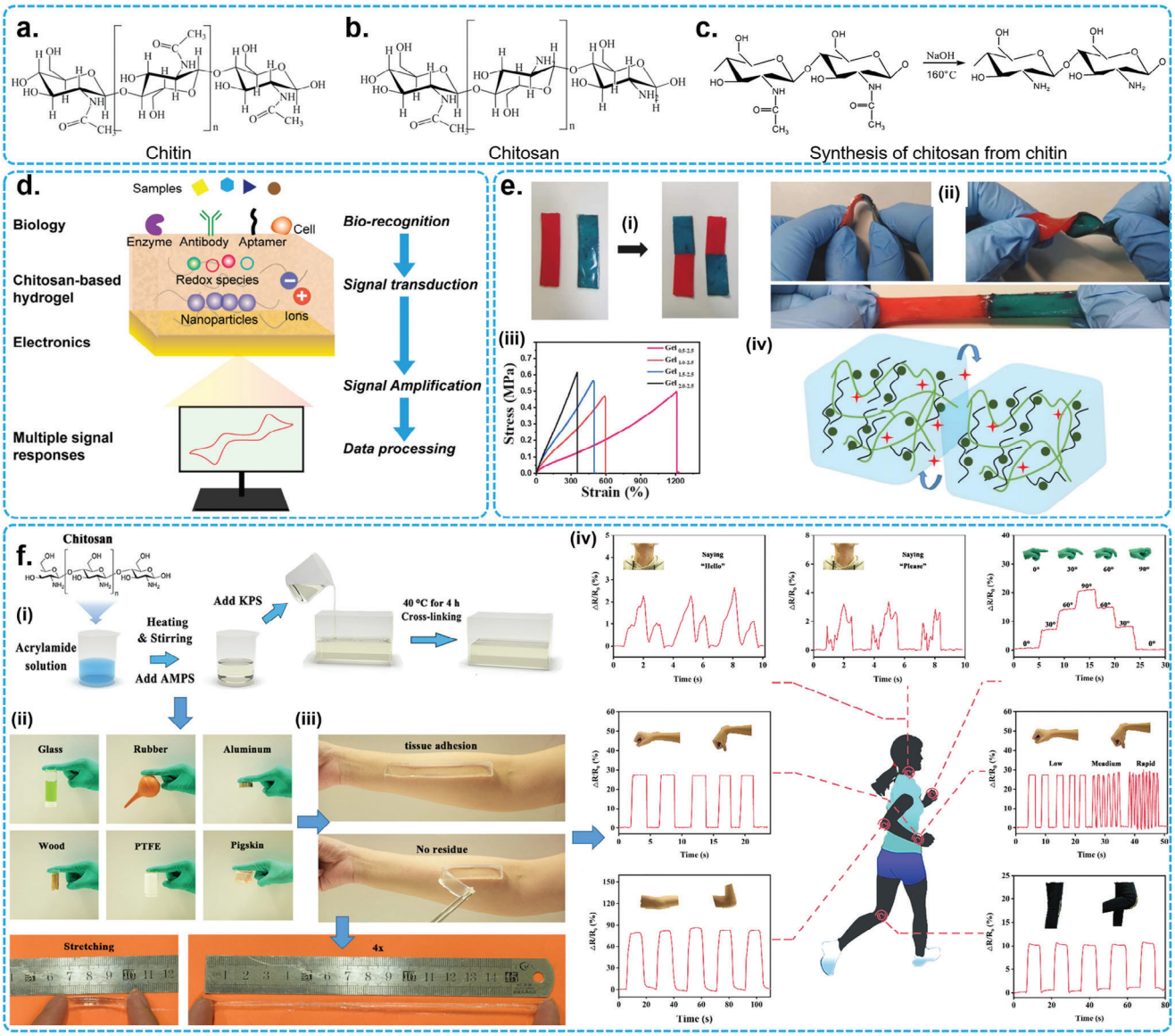

Figure 2. Chitin/chitosan-based conductive hydrogels as stretchable bioelectronics. Chemical structure of a) chitin and b) chitosan.[81] Copyright 2017, Springer Nature. c) Synthesis of chitosan from chitin.[81] Copyright 2017, Springer Nature. d) Signal perception mechanism of chitosan-based hydrogels for biomolecular sensing.[83] Copyright 2023, MDPI. e) Fabrication of chitosan/polyacrylic acid-based flexible hydrogels for strain sensing. Digital photographs of the hydrogels showing i) self-healing ability and ii) excellent stretchability at room temperature. The representative iii) stress-strain curve and iv) mechanism of self-healing ability of the hydrogels.[84] Copyright 2021, Elsevier. f) Fabrication of chitosan/acrylamide-based adhesive and stretchable hydrogels for human body sensing. i) Schematic illustration of the hydrogel fabrication, ii) multiple adhesion test, iii) skin adhesion test, and stretchability property of the chitosan/acrylamide hydrogels. iv) demonstration of the chitosan/acrylamide hydrogels for wearable sensing with strain sensitivity. The hydrogel efficiently detected the voice, finger, wrist, elbow, and knee bending, which was obtained via recording in the relative resistance.[85] Copyright 2021, Elsevier.

2.1.2. Chitin/Chitosan and Its Nanocomposites

Chitin is another important amine-based polysaccharide used extensively in tissue engineering and regenerative medicine. Chitin mainly comprises 2-acetamido-2-deoxy-β-D-glucose linked through β−1,4 glycoside linkage (**Figure 2a**). Chitosan is the deacetylated (mainly *N*-acetylated) product of chitin (Figure 2b). Unlike cellulose, chitin and chitosan comprise ~9% of nitrogen.[80] In chitosan, nitrogen is present as a primary aliphatic amine group exhibiting strong antimicrobial activity. Chitosan can be derived from chitin via oxidation reaction with sodium periodate ($NaIO_4$) at high temperature or by treatment with chitin deacetylase (Figure 2c), which is widely used as a hydrogel due to its non-toxicity.[81] The physicochemical properties, such as biodegradability, biocompatibility, adhesive, hemostatic, analgesic, antimicrobial, and antioxidant property, chiefly depends on the degree of deacetylation, molecular weight, viscosity of the bulk chitosan.[81,82] Owing to the presence of

reactive groups in the chitosan backbone, it is widely explored as a hydrogel matrix for bioelectronics fabrication and biosensing applications. Chitosan and chitosan-based nanocomposites act as an electronic bridge between tissue and analytes (Figure 2d), thereby enabling the identification or recognition of several ionic species, such as aptamer and nucleic acids.[83] A study conducted by Liang et al.,[84] reported the use of chitosan/polyacrylic acid with superior anti-freezing and ultra-stretchable properties for multi-modal biosensing. Incorporating chitosan with polyacrylic acid led to the development of adhesive properties with fast self-healing and showed excellent mechanical strength required for skin adhesion (Figure 2e). In another study, Jin and co-workers developed a chitosan/acrylamide-based skin adhesive hydrogel with multi-modal human body sensing.[85] Using chitosan with acrylamide demonstrated a tougher hydrogel network with extreme adhesive ability. The hydrogel can be molded and obtained as a transparent film easily attached to human skin, fingers, wrists, elbows, and knees to record the electrical signals (Figure 2f). These examples clearly suggest that chitosan-based hydrogels hold tremendous potential in hydrogel bioelectronics, especially for preparing the adhesive layer of a sensory element with good electrical conductivity.

2.1.3. Alginate and Its Nanocomposites

Alginate, or sodium alginate, is derived from brown sea algae.[86] The sodium alginate can be obtained from the dried sea algae via mineral acid and bicarbonate treatment (**Figure 3a**). The raw algal mass is converted into sodium alginate by the treatment with sodium carbonate. Alginate is a type of marine polysaccharide composed of irregular blocks of α-glucuronic acid (G) and β-D-mannuronic acid (M), linked together via 1,4-glycosidic linkage.[87,88] Alginate is usually water-soluble, and the building blocks are found either in homogenous form (Poly-G or Poly-M) or heterogeneous form (mixture of G/M) (Figure 3b). Due to carboxylic acid groups in the alginate backbone, it is easily cross-linkable with divalent cations, such as calcium (Ca^{2+}) or magnesium (Mg^{2+}), giving rise to an "egg-box" structure. Crosslinked alginate (i.e., calcium alginate) is highly stable, conductive, and generally used for making various tissue-engineering scaffolds.[87] Apart from ionic cross-linking, calcium alginate exhibits poor mechanical properties and printing performance. Therefore, alginate is frequently mixed with other biopolymers to enhance the mechanical and printing properties. Dutta et al.[86] showed that the introduction of gelatin into the alginate matrix enhanced the printing performance of the alginate due to both physical and ionic cross-linking occurring between gelatin and alginate (Figure 3c).

Alginate can be functionalized with various chemical moieties to increase the cross-linking ability, conductivity, and bio-adhesive properties. For example, pyrrole (Py)-modified alginate has good electrical conductivity with Young's modulus ranging from 20 to 200 kPa, ideal for soft tissue regeneration.[89] Moreover, surface oxidation of alginate with $NaIO_4$ enhanced the cross-linking of alginate with gelatin owing to adding aldehyde groups in the alginate backbone, giving rise to amide bonding. In some cases, the oxidized alginate reacts with cationic biopolymers/cations through Schiff base reaction, allowing double-network hydrogel formation.[90,91] Alginate can also be functionalized by catecholamine, acrylate, and RGD (Arginine-Glycine-Aspartic acid) peptides to improve the antimicrobial and bio-adhesive properties.[92] Next, regarding biocompatibility, it has been reported that alginate-based hydrogels are extremely biocompatible, which can support the growth and proliferation of various stem cells (Figure 3d). Incorporation of various conductive metal nanofillers with double-network alginate hydrogel may improve stretchability, ionic conductivity, and cytocompatibility. For example, the silver nanoparticle decorated polyacrylamide/alginate hydrogel developed by Ohm et al. shows an electrical conductivity of $\approx$350 S cm^{-1} with remarkable mechanical properties (elastic modulus $\approx$10 kPa) for soft tissue engineering.[93] The as-fabricated hydrogel with homogenously dispersed silver nanoflakes improved the physico-chemical properties of the bulk hydrogel and enhanced the sensing ability toward neuromuscular tissue (Figure 3e). When attached to the hand, the fabricated hydrogel effectively recorded the muscle stimuli through a wireless device, demonstrating excellent sensing behavior. In another study, 3D-printed stretchable, self-healing, and ionically conductive polyvinyl alcohol/alginate hydrogel was demonstrated as a motion sensor (Figure 3f).[94] Taken together, alginate-based hydrogels and their nanocomposites hold much promise toward stretchable and flexible sensor fabrication in wearable bioelectronics.

2.1.4. Silk Fibroin and Its Nanocomposites

Silk fibroin can be used as a promising material for conductive hydrogel fabrication. Silk fibroin is a protein with a structure resembling spider silk, and it offers several advantages as a material for soft polymeric hydrogel preparation. Two methods for producing silk fibroin hydrogels are physical cross-linking and chemical cross-linking. In the physical cross-linking method, silk fibroin molecules are combined through non-covalent bonds to form hydrogels using physical interactions such as hydrogen bonding, hydrophobic interaction, electrostatic interaction, ionic interaction, and chain winding. The methods used for physical cross-linking include ultrasonication, shear-induced deformation/reformation, electric field, temperature change, pH adjustment, organic solvents, and surfactant application (**Figure 4ac**).[96] In chemical cross-linking, silk fibroin molecular chains are linked through covalent bonds, making them a more stable 3D network structure. Chemically cross-linked silk fibroin hydrogels typically demonstrate enhanced physical stability and mechanical strength compared to physically cross-linked silk hydrogels. Chemical cross-linking methods include photopolymerization, gamma irradiation, or enzymatic cross-linking (Figure 4d–g).[96] Silk fibroin hydrogels are conductive and printable with slightly high concentrations. Silk fibroin is known for its biocompatibility, meaning it is safe to interact with the human body and does not cause immune reactions.[97] Also, silk fibroin possesses a remarkable balance of strength and flexibility.[98] The unique temperature-responsive behavior of silk fibroin has been utilized as a promising material for 3D printing, which displayed conductive properties and superior biocompatibility.[99] Thus, silk fibroin's outstanding

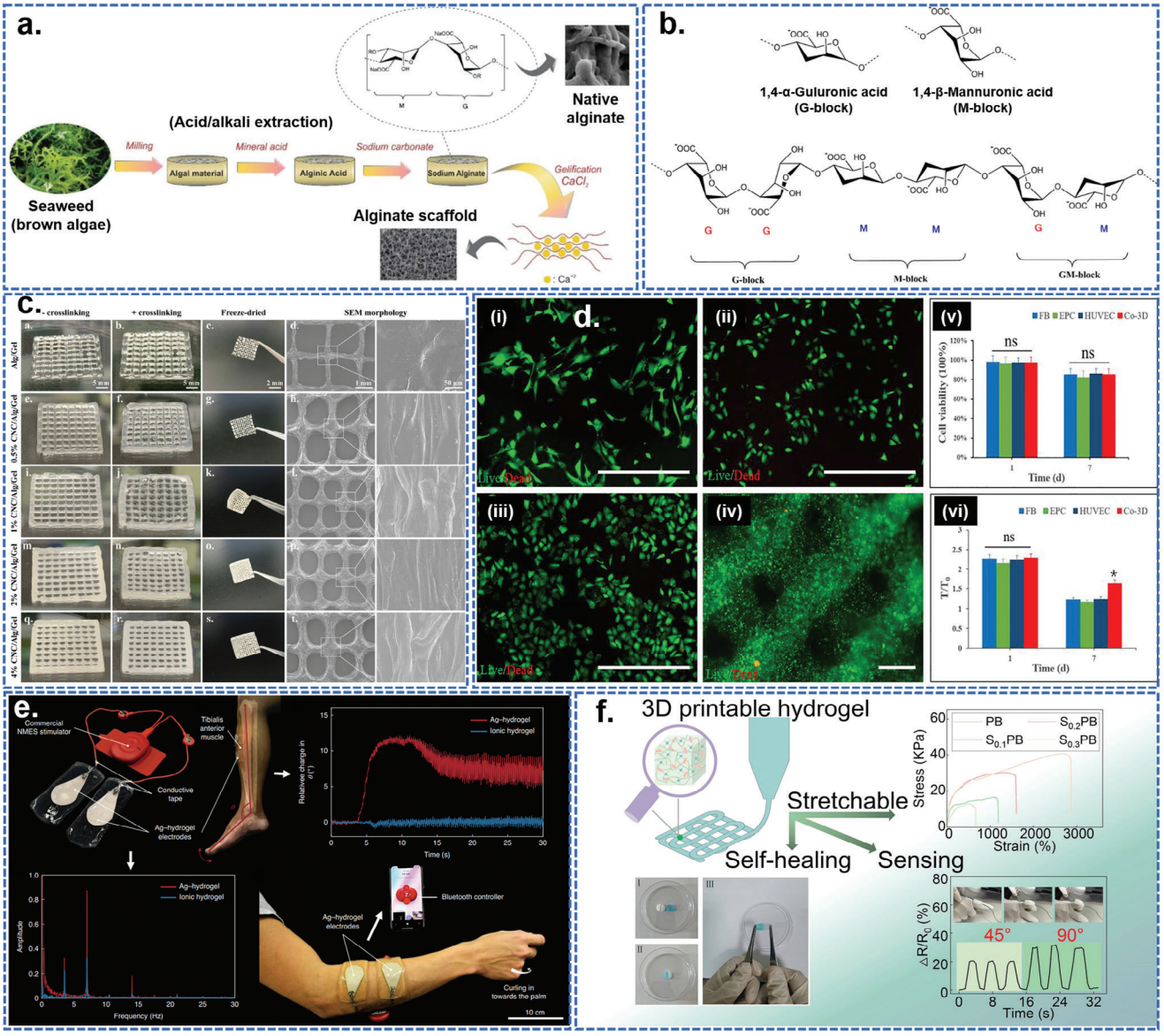

Figure 3. Structure and function of alginate as a conductive hydrogel base. a) Schematic illustration of sodium alginate preparation and purification from sea weed (algae).[88] Copyright 2020, Springer Nature. b) Chemical structure of the alginate showing the repetitive units of glucouronic acid (G), mannuronic acid (M), or a mixture of G/M.[88] Copyright 2020, Springer Nature. c) Demonstration of 3D printing of high-resolution structures using alginate/gelatin/CNCs, where alginate is used as a supporting and semi-IPN network hydrogel. Scale bar: 1 μm; 1, 2, and 5 mm.[86] Copyright 2021, Elsevier B.V. d) Biocompatibility of human skin cells onto the 3D printed alginate-based hydrogels showing excellent cytocompatibility. Live/dead assays and cell viability assays of fibroblast cells at indicated time points. Scale bar: 500 μm.[95] Copyright 2023, Elsevier. e) Neuromuscular electrical stimulation of Ag/polyacrylamide/Alginate hydrogels shows excellent sensing ability.[93] Copyright 2021, Springer Nature. f) Schematic illustration of the 3D printable PVA/SA-based hydrogels for human motion sensing.[94] Copyright 2022, Elsevier.

structural and functional properties make it an ideal candidate for hydrogel electronics, especially for soft hydrogel electrode fabrication.

2.1.5. Gelatin and Its Nanocomposites

Gelatin, a frequently employed polymer, is a hydrolytic product of collagen and is widely used as a polymer matrix for encapsulating drugs and biomolecules (**Figure 5**a). Nonetheless, its exclusive application is curtailed by drawbacks like rapid degradation and lesser mechanical robustness.[107] Gelatin methacryloyl, or GelMA, stands out as a remarkable gelatin derivative. GelMA, a modified hydrogel capable of photocross-linking, is obtained through the reaction of gelatin with methacrylic anhydride (MA). Owing to the unique temperature-dependent gelation properties, gelatin, and GelMA are widely used for 3D printing applications. For GelMA, by introducing and regulating photoinitiators and employing light exposure (such as UV light, blue light, or white light), the methacrylamide and methacrylate

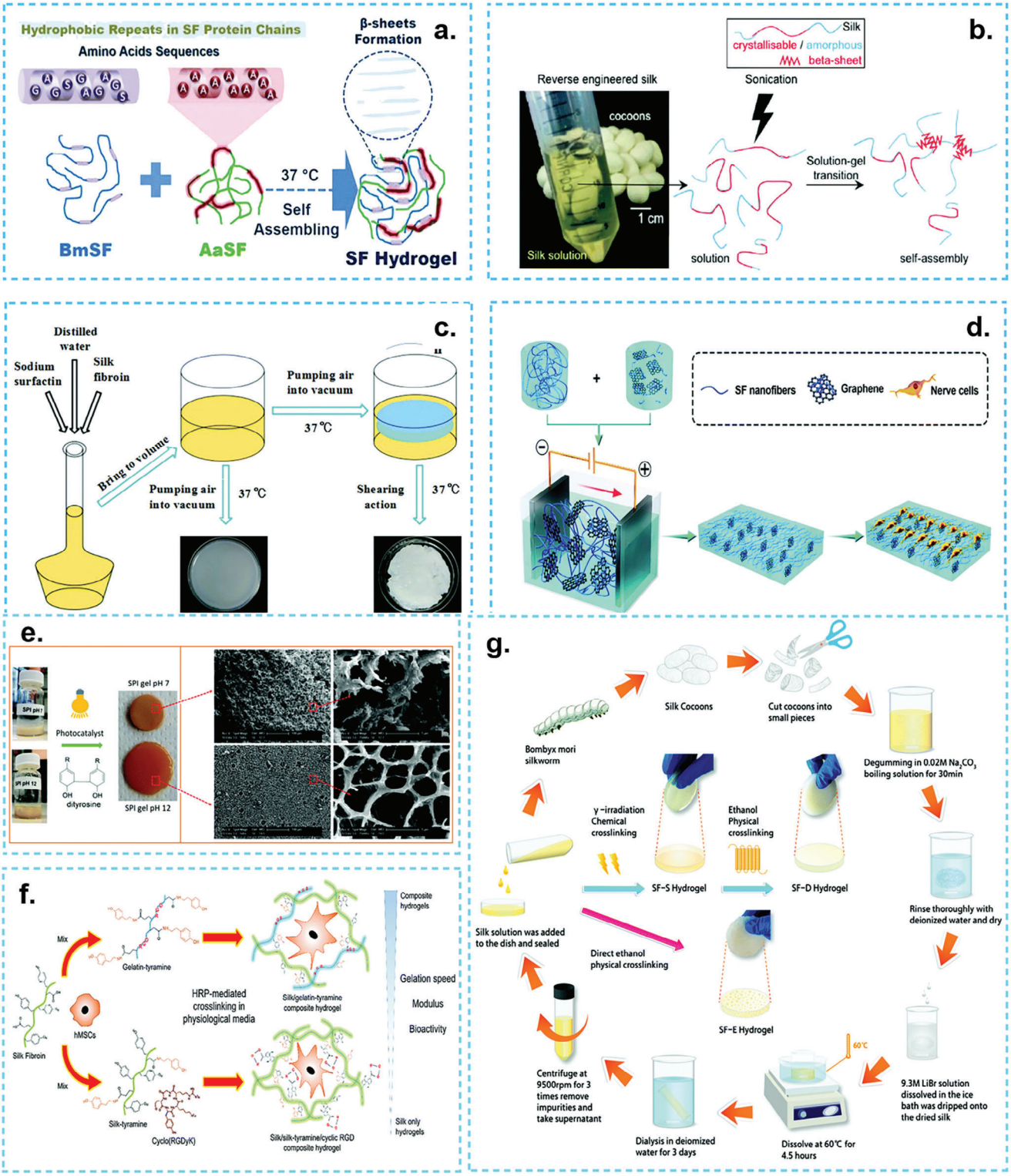

Figure 4. Structure and function of silk fibroin-based hydrogels. a-c) Examples of physical cross-linking strategies for silk fibroin hydrogel fabrication.[100–102] Copyright 2018, Wiley-VCH; Copyright 2018, American Chemical Society; Copyright 2018, Wiley-VCH. d) Fabrication of graphene/silk fibroin-based conductive hydrogels under electric field stimulation.[103] Copyright 2018, Wiley-VCH. e-g) Examples of chemical cross-linking strategies for silk fibroin hydrogel fabrication.[104–106] Copyright 2019, American Chemical Society; Copyright 2020, Elsevier.

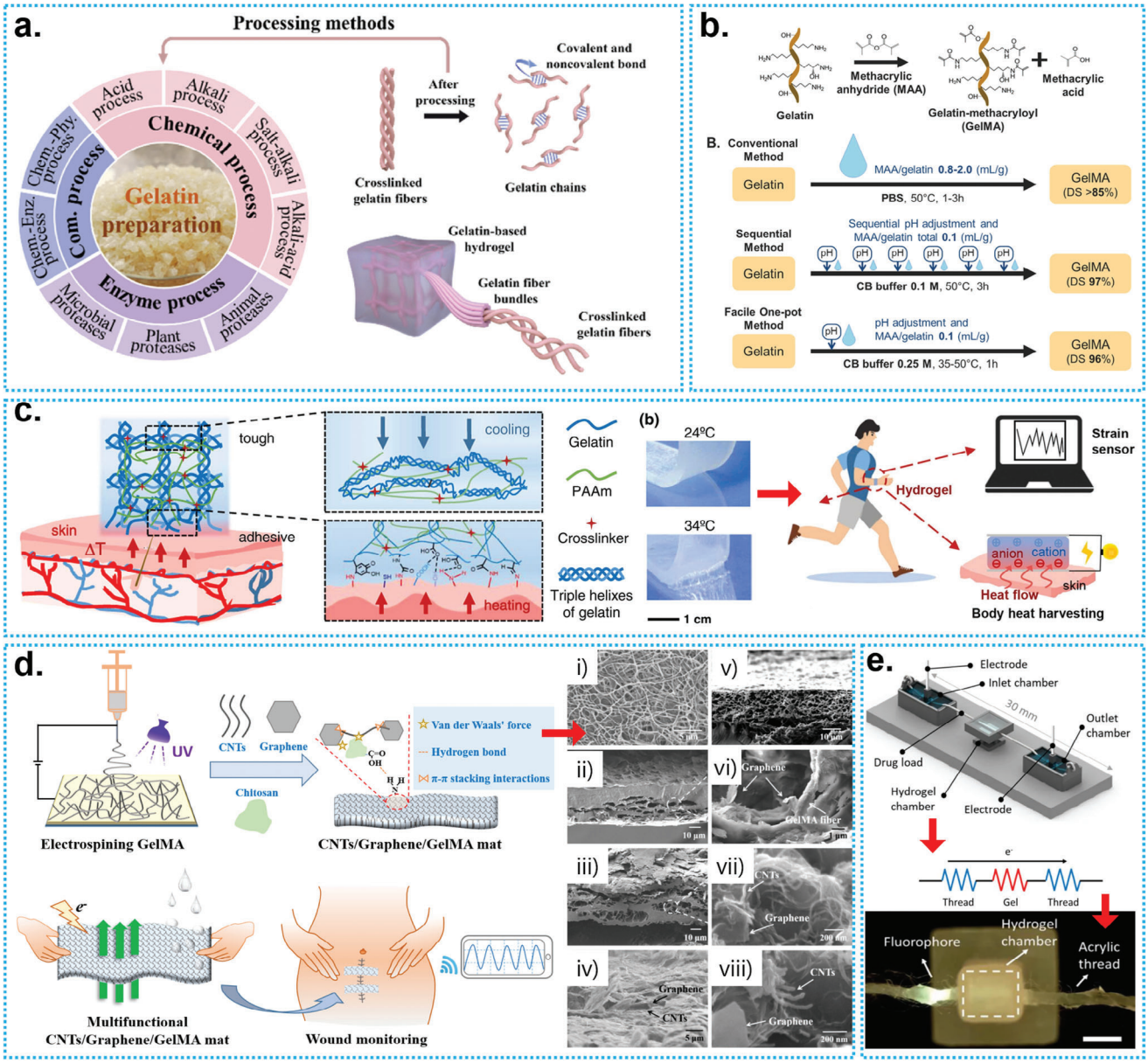

Figure 5. Properties of gelatin for biosensing applications. a) Schematic illustration of the extraction process of gelatin from collagen fibers.[110] Copyright 2022, Elsevier. b) Synthesis strategies of GelMA for gelatin.[112] Copyright 2016, Springer Nature. c) Demonstration of gelatin/polyacrylamide-based stretchable and conductive hydrogel sensors.[113] Copyright 2022, Elsevier. d) Example of GelMA/CNT/graphene-based conductive electrospun scaffold for wound biosensing application. FE-SEM images of the fabricated nanofibers show CNTs and graphene's presence in the GelMA fibers.[111] Scale bar: 5, 10 µm, and 200 nm. Copyright 2022, Elsevier. e) Demonstration of a gelatin/polyethylene glycol-based soft and conductive hydrogel sutures for drug delivery application. Scale bar: 2 mm.[114] Copyright 2020, Springer Nature.

functional groups within the gelatin chain can be photopolymerized to create a stable, interconnected hydrogel network with higher mechanical properties.[108] The degree of substitution (DS) of GelMA can be tuned *by* changing the pH and the concentration of MA (Figure 5b). Gelatin is frequently employed with alginate to improve printing and mechanical properties. Nevertheless, the amalgamation of alginate and gelatin has demonstrated the ability to promote substantial cell adhesion, diffusion, expansion, migration, and proliferation. This combination also ensures accelerated self-renewal of stem cells.[109]

Apart from alginate, gelatin is frequently combined with hyaluronic acid and other biopolymers. Gelatin, in combination with metals (e.g., gold and silver nanoparticles) and/or carbonaceous materials (e.g., GO, CNT, and nanodiamond), has been shown to exhibit excellent conductive properties with good sensing abilities. Also, gelatin, combined with various conductive biopolymers, is frequently used for achieving desirable conductivity and mechanical properties. These biopolymers include various ionic and electronic-ionic hydrogel composites.[110] For example, gelatin/polyacrylamide hydrogel has been shown to

demonstrate good stretchability with desirable conductive properties for wearable sensing applications (Figure 5c). The above-mentioned composition is highly temperature-responsive and could be an ideal adhesive material for biological applications. Gelatin and its derivatives can be electrospuned to achieve 3D scaffolds for electrical stimulation and biosensing applications. A combination of GelMA with CNT and graphene has been shown to improve the conductivity (Figure 5d) owing to the formation of reticulate biomimetic structure (e.g., development of soft and biodegradable surgical sutures), which is ideal for skin tissue engineering and wound pH sensing applications.[111] Similarly, soft gelatin-based electrodes can be used for the electrical stimulation of stem cells and drug delivery applications (Figure 5e). The gelatin and its derivatives hold tremendous potential in soft bioelectronics fabrication due to its easy availability, cheap, versatile functionality, and rapid prototyping nature.

2.1.6. Keratin and Its Nanocomposites

Keratin is another least explored biomaterial for tissue engineering and regenerative medicine. Keratin comprises cysteine-rich protein units assembled to form a sizeable intermediate filament, one of the chief constituents of hair, thorns, nails, fish scales, feathers, and fur/wool.[115–117] Keratin can be classified into soft and hard keratin based on its sulfur content. The hard keratin has good mechanical properties and is thus used as a bulk polymer for fabricating various hydrogels. The soft keratin with low sulfur content is secreted by the keratinocyte cells of the epidermis and is mainly associated with ECM remodeling.[115] Approximately 50 genes are involved in the keratinocytes to produce keratins (**Figure 6a**). To date, there are 28 different types of Keratin-I (acidic cytokeratin) proteins and 26 types of keratin-II (basic cytokeratin) proteins secreted by keratinocyte cells.[116] The 3D structure of the native keratin protein is shown in Figure 6b. Keratin can be extracted from different sources through chemical treatment, enzymatic methods, steaming, and microwave irradiation. The most commonly exploited chemical extraction includes reduction (thioglycolic acid, sodium hydroxide, sodium dodecyl sulfate, 2-mercaptoethanol/urea),[118–121] oxidation (peracetic acid/HCl),[122] hydrolysis,[122] and ionic liquids.[123] From the past few decades, keratin is not well-explored for bioelectronics fabrication. Combined with other conductive nanomaterials, keratin may exhibit good electrical conductivity and sensing performances.[124,125] For example, Zhu et al.,[126] recently demonstrated the use of wool keratin/polyacrylamide/CNTs for the fabrication of stretchable strain sensors (Figure 6c). The developed biosensor exhibited desirable mechanical strength and flexibility for human skin nano-bio interfaces toward EEG electrode fabrication.

2.1.7. Glycoproteins-Based Nanocomposites

Glycoproteins are the proteins where the polypeptide chains are linked with either N- or O-types (polyamines or poly/oligosaccharides) of glycosylation. Glycosylation results from post-translational modification of cellular proteins, usually secreted as extracellular matrix (ECM) and associated with various physicochemical processes.[127,128] For example, mucin, a well-known glycosylated protein secreted by the epithelial tissues of animals, could be used as an ideal biomaterial for conductive hydrogel fabrication. Yang et al. demonstrated the modification of mucin via oxidation of side chains (addition of aldehyde groups) and methacrylation, which produces cross-linked mucin hydrogel with good electrical conductivity for soft bioelectronics fabrication.[129] Tissue-derived decellularized extracellular matrix (d-ECM) also comprises various kinds of glycosylated proteins (e.g., glycosaminoglycans or GAGs), which are proton-conductive and behave as conductive biopolymers when stimulated with specific electric fields.[130] A study conducted by Tsui et al. reported that cardiac tissue-derived d-ECM in combination with rGO exhibited superior electrical conductivity (≈3.5 S m^{-1}) upon the addition of sodium borohydride ($NaBH_4$).[131] The $NABH_4$ acts as a proton carrier on the surface of d-ECM, helping it to cross-link with rGO and maintain electrical conductivity. These examples suggest that glycoprotein and its conjugates can be molded into soft hydrogels and used as a biomaterial for soft bioelectronics fabrication.

2.2. Chemically Derived Biopolymer and Its Nanocomposite Hydrogels

Like naturally derived conductive polymers, various chemically derived biopolymers are frequently employed for bioelectronics fabrication. These biopolymers have been reported as biologically safe and extensively used for stretchable hydrogel fabrication. A schematic illustration of some commonly used chemical biopolymers and their synthesis route is shown in **Figure 7**. This section briefly discusses the most important and widely used chemically derived biopolymers (polyaniline, polypyrrole, and PEDOT:PSS) for wearable bioelectronics.

2.2.1. Polyaniline and Its Nanocomposites

Polyaniline, commonly known as PANI, is a frequently used conductive biopolymer and has gained significant attention owing to its cost-effectiveness, excellent thermostability stability, quick oxidation-reaction potential, and high energy density.[134] PANI is widely used in various sectors, including biosensing, biocatalysts, and electrode manufacturing.[135–137] PANI can be synthesized in several ways, including heterophase polymerization, solution polymerization, interfacial polymerization, seeding polymerization, metathesis polymerization, self-assembling polymerization, sonochemical synthesis of polyaniline, electrochemical synthesis of polyaniline, enzymatic synthesis of polyaniline, photo-induced polymerization, and plasma polymerization.[134] The most common method of PANI synthesis includes either an oxidation reaction, which directly leads to the formation of PANI, or a reduction method, which leads to the formation of a PANI derivative known as leukoemraldine. Besides, PANI is also widely used in electromagnetic interference shielding, solar cells, anticorrosion devices, biological and chemical sensors, and organic light-emitting diodes because of its excellent optical and electrical properties and decent anticorrosion properties.[138] PANI, combined with other biopolymers, is an

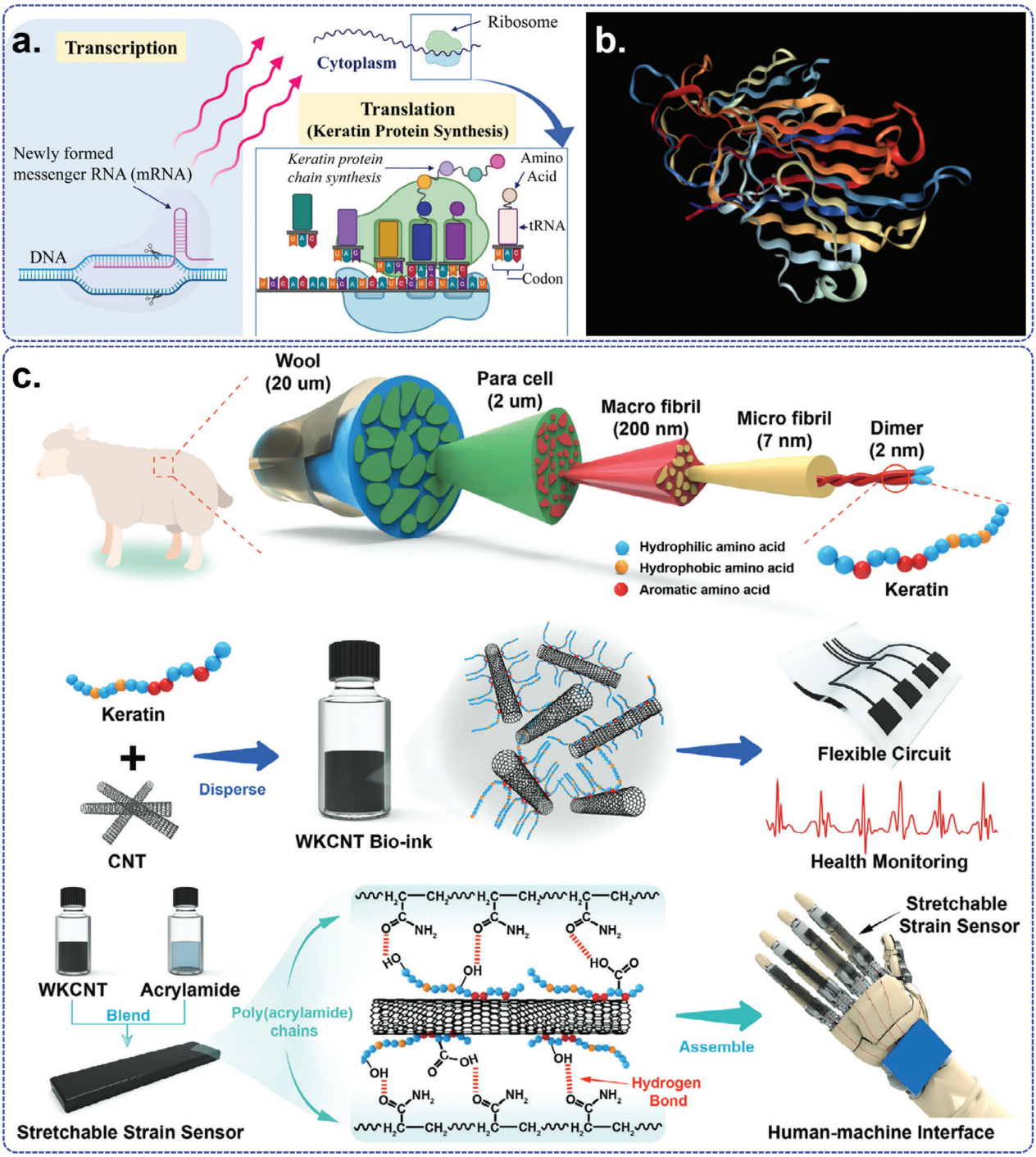

Figure 6. a) Synthesis of keratin protein by keratinocyte cells.[116] b) Representative 3D structure of the keratin protein.[116] Copyright 2022, Elsevier. c) Demonstration of keratin/CNT-based conductive, flexible, and stretchable bioelectronics for EEG monitoring and human-machine interfaces.[126] Copyright 2023, Wiley-VCH.

ideal candidate for 3D printing, especially for fabricating conductive "E-skin" patches.[139] For example, Sani et al. reported using a stretchable multiplex sensor for wireless wound healing applications.[140] The 3D printed pH sensor was fabricated using a PANI/Au ink, which can selectively measure the pH of the wound during chronic wound healing (**Figure 8**). Similarly, Montaina et al. demonstrated using photopolymerized PEGDA/PANI hydrogels via SLS printing with unprecedented electrical and electrochemical performances for real-time electrocardiograph (ECG) recording.[141] The as-fabricated hydrogel was soft, flexible, and displayed stress resistance properties, which is helpful for soft electrode fabrication. Apart from the

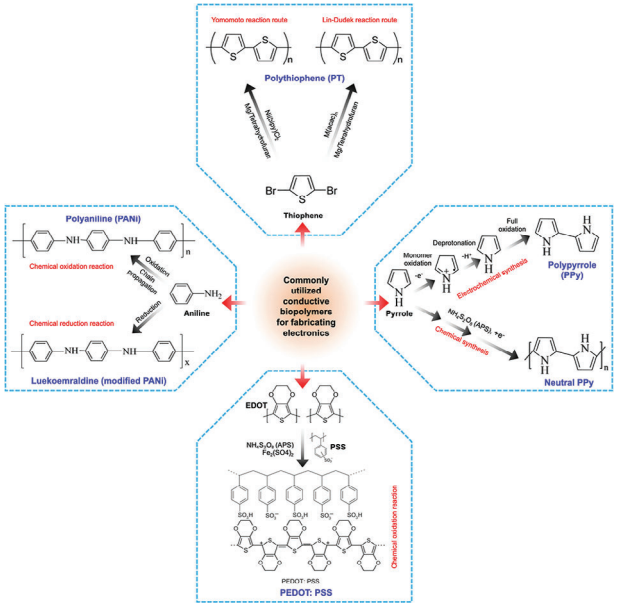

Figure 7. Schematic illustration of some commonly used chemical biopolymers and their synthesis route for biosensing applications.[132,133] Copyright 2019 and 2021, Royal Society of Chemistry.

exceptional conductivity, PANI is difficult to synthesize as it is highly insoluble in water and sometimes causes stiffness in the hydrogel matrix, thereby restricting its commercial application.[142] To resolve this issue, the PANI can be modified with various functional groups (e.g., incorporating various polar groups onto the polymer backbone) to improve its solubility and mechanical properties.[143] Moreover, thermoplastic molding of PANI and its composites has shown better performances than conventional hydrogel fabrication.[144]

2.2.2. Polypyrrole and Its Nanocomposites

Polypyrrole (PPy), another essential biopolymer, can be electrosynthesized directly onto metallic implants.[145,146] PPy can also be synthesized using a chemical oxidation technique using ammonium persulfate (APS) to give rise to neutral PPy. PPy is highly biocompatible,[145] promoting cell adhesion and proliferation,[147,148] and has been reported to combat against pathogenic bacteria.[147] Thus, PPy in combination with bioactive coatings, such as SH porous Ti substrates, could be beneficial for tuning mechanical properties (corrosion resistance and bone ingrowth, for instance) with enhanced antibacterial properties, which is especially helpful for restoring electrical conductivity of body tissues and infection-impaired healings.[149] Additive manufacturing of PPy and its composite hydrogels is highly conductive and biocompatible for sensing applications. For instance, Dutta et al. demonstrated the use of a triple cross-linking strategy for the fabrication of GelMA/PPy bioink for electrical stimulation of stem cells toward bone regeneration[150] (**Figure 9a**). The as-fabricated hydrogel can be thermo-photo-chemo responsive and display an electrical conductivity of ≈12.8 mS cm^{-1}, similar to the bone endogenous electric field. Incorporating PPy into the GelMA matrix and Fe^{3+} cross-linking improved the conductivity and enhanced the hydrogels' stability under physiological conditions (Figure 9b-d). In another study, Yamada et al. reported the use of a printable PPy/Nafion sheets using Ti/sapphire (λ_{ex} = 850 nm)-based femtosecond laser (multi-photon polymerization) using ruthenium (Ru^{3+}) photochemistry.[151] The application of Tris(2,2′-bipyridyl) ruthenium enhanced the photopolymerization and rapid prototyping of sodium *p*-toluenesulfonate/poly pyrrole with nearly 0.8 µm fine architectures with an electrical conductivity of ≈4.1×10^3 S m^{-1}. Similarly, Keirouz et al. demonstrated the fabrication of a conductive microneedle (MN) patch (Figure 9e,f) based on stereolithographically fabricated structures with PPy coatings via in situ polymerization of Py.[152] The oxidative coating of PPy onto the MN resulted in excellent electrical conductivity (resistivity = 8 ± 1 kΩ sq^{-1}) with higher biocompatibility of human skin cells (Figure 9g–i). These reports envisioned that functionalization of PPy with various polymers may result in highly conductive and flexible composites for bioelectronics fabrication.

2.2.3. PEDOT:PSS and Its Nanocomposites

Among many conductive biopolymers, poly(3,4-ethylene dioxythiophene):poly (styrene sulfonate) (PEDOT:PSS) serves as one of the versatile electronic and ionic conductors, making it an ideal candidate for soft bioelectronics fabrication. PEDOT:PSS is an extensively studied biomedical biopolymer due to its exceptional conductivity and superior cytocompatibility.[153] Usually, PEDOT:PSS-based hydrogels are prepared via direct in situ polymerization or mixing with other non-conductive polymers to form a semi-inner-penetrating polymer network (semi-IPN) hydrogel, which is moldable and printable.[154–157] Various physicochemical properties of PEDOT:PSS are schematically demonstrated in **Figure 10a**. The use of non-conducting biopolymers having good hydrogel formation ability may reduce the conductivity of the PEDOT:PSS because the non-conducting biopolymers sometimes act as insulators (conductivity <1.0 S cm^{-1}) and thus reduce the ionic conductivity of the PEDOT:PSS. Although it is possible to use the bulk PEDOT:PSS as a hydrogel, pure PEDOT:PSS polymer lacks the desirable conductivity, stability, self-healing, and stretchability owing to the absence of supporting polymer matrix.[153] To overcome this issue, PEDOT:PSS is frequently mixed with carbon-based (e.g., GO, CNTs, and MXene) and non-carbon-based metal (e.g., metal nanoparticles and nanowires) nanofillers to enhance the conductivity. In this context, recent studies indicate the use of naturally-derived conductive biopolymers, such as γ-polyglutamic acid (γ-PGA) in combination with PEDOT:PSS improves the biocompatibility, adhesiveness, conductivity (~12.5 S m^{-1}), self-healing (healing time 2 s), stretchability (up to ≈300%) and flexibility (>300 kPa stress, ≈650% strain) towards wearable bioelectronics fabrication.[158] Similarly, many recent studies demonstrated that the use of chitosan,[159] alginate,[160–163] gelatin,[164–168] and cellulose[169–173] with PEDOT:PSS improved the conductivity and biocompatibility of the composites.

Self-assembly of monomers during hydrogel formation is critical in enhancing PEDOT:PSS hydrogels' conductivity and physicochemical properties. For instance, several active bonds and chemical interactions (e.g., protonation/deprotonation,

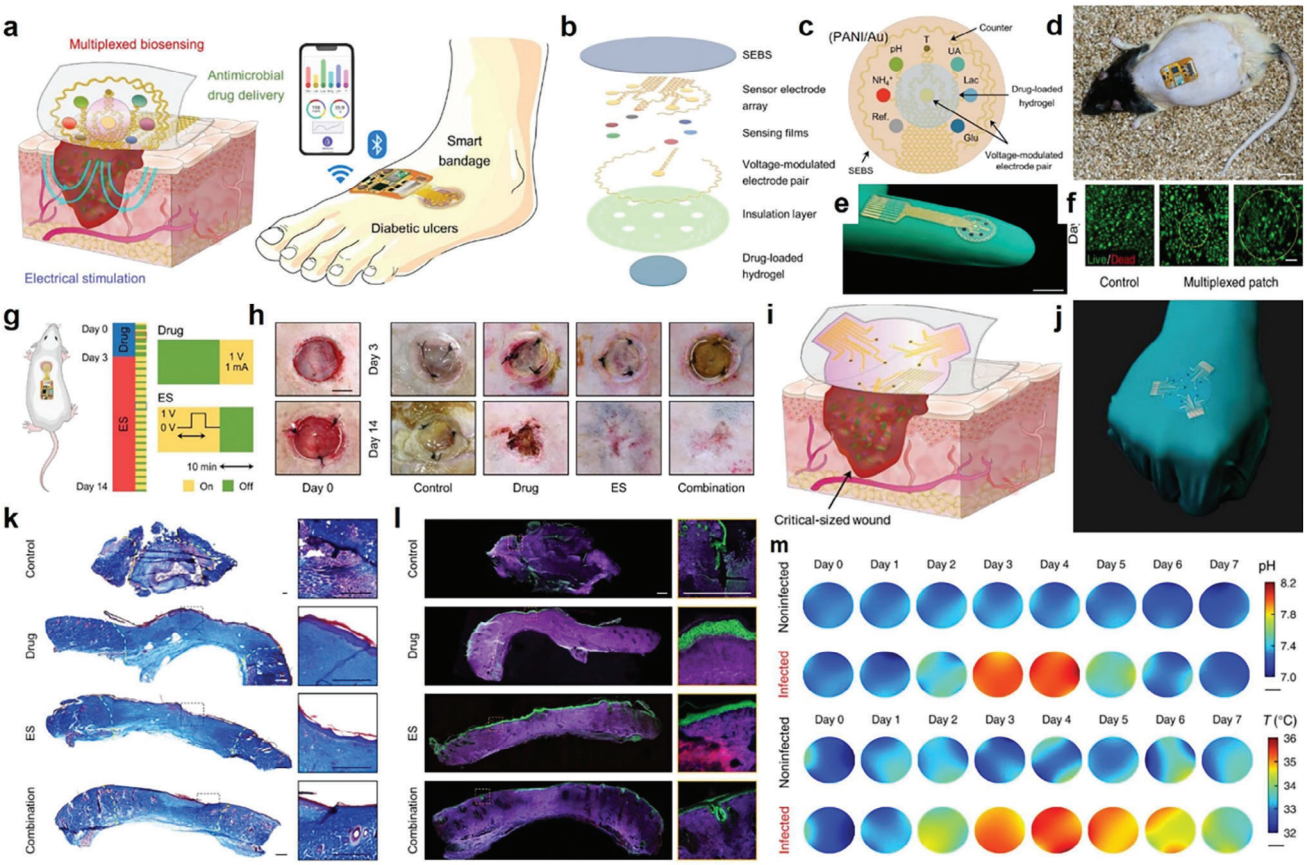

Figure 8. Fabrication of a multiplex wearable wound biosensing platform based on polyaniline (PANI) electrodes. a) Schematics of the biosensing chip. b) The segments of the biosensing chip. c–f) Demonstration and application of the multiplex biosensing chip for in vitro and in vivo wound pH monitoring during chronic wound healing. g,h) Demonstration of the electrical stimulation assisted-advanced wound healing. The digital photographs show the macroscopic wound closure after electrical stimulation. i,j) Demonstration of the sensing bandage applied to the wound area. k,l) Trichrome and fluorescence staining of the wound area showing the epidermis development in vivo. m) Heatmaps show the relative change in pH and temperature after implantation of the multiplex chip.[140] Copyright 2023, American Association for the Advancement of Science.

hydrogen bonding, hydrophobic interaction, and host-guest interaction) are responsible for PEDOT:PSS self-assembly. For example, high-temperature and sulfuric acid treatment of PEDOT:PSS allows the PEDOT particles to self-assemble during hydrogel formation owing to the π–π stacking and hydrophobic interactions,[174] which displays higher electrical conductivity (≈46 S m^{-1}) and water retention capacity (~99 wt%) than room temperature PEDOT:PSS hydrogels.[175] Owing to good hydrogel formation ability, pristine PEDOT:PSS hydrogel made in DMSO is viscoelastic, printable, and exhibited drying-induced self-assembly behavior, which showed desirable conductivity unlike bulk hydrogels, ideal for soft bioelectronic fabrication.[33,153,155] In other studies, dynamic hydrogen bonds, host-guest interactions, and incorporated nanomaterials exhibited tougher and biocompatible PEDOT:PSS hydrogels for multifaceted applications.[175–178] The PEDOT:PSS-based electrodes are conductive in both dry and wet conditions. Zhao et al.,[179] reported the use of a highly conductive (≈142 S cm^{-1}) and ultra-thin (≈100 nm) dry electrode made up of PEDOT:PSS/graphene for electrophysiological studies (Figure 10b). Incorporating graphene into PEDOT:PSS matrix improves the conductivity and charge carrier mobility through PEDOT:PSS via π–π interactions. Moreover, the fabricated electrode displayed good adhesive properties on the skin surface and showed an extremely higher muscular signal-to-noise ratio (SNR) of ~23 ± 0.7 dB, much higher than commercial Ag/AgCl electrodes (≈19 ± 0.5 dB). In another study, an MXene/PEDOT:PSS integrated polyacrylamide hydrogel was fabricated for strain sensing.[180] In the quinoid phase, the MXene and PEDOT:PSS formed dynamic hydrogen bonds, further stabilized by polyacrylamide (Figure 10c(i–iii)). Interestingly, the composite hydrogel, when stretched, showed a dynamic change in electrical conductivity owing to the increase or decrease of resistance (Figure 10c(iv)). Furthermore, the composite hydrogel displayed a strain-dependent change in gauge factor (3.98 at 100% to 9.93 at 500% strain) with real-time sensing ability within 30–85% strain rate and a frequency range of 0.039–0.316 Hz (Figure 10c(v)). Besides, the composite hydrogel maintained the sensing ability under an aqueous environment even after 300 loading-unloading cycles with a maximum strain of 100%. These examples indicate that PEDOT:PSS is ionically conductive and shows tailorable sensing ability with a combination of suitable dopants, which could be an ideal candidate for soft electrode fabrication.

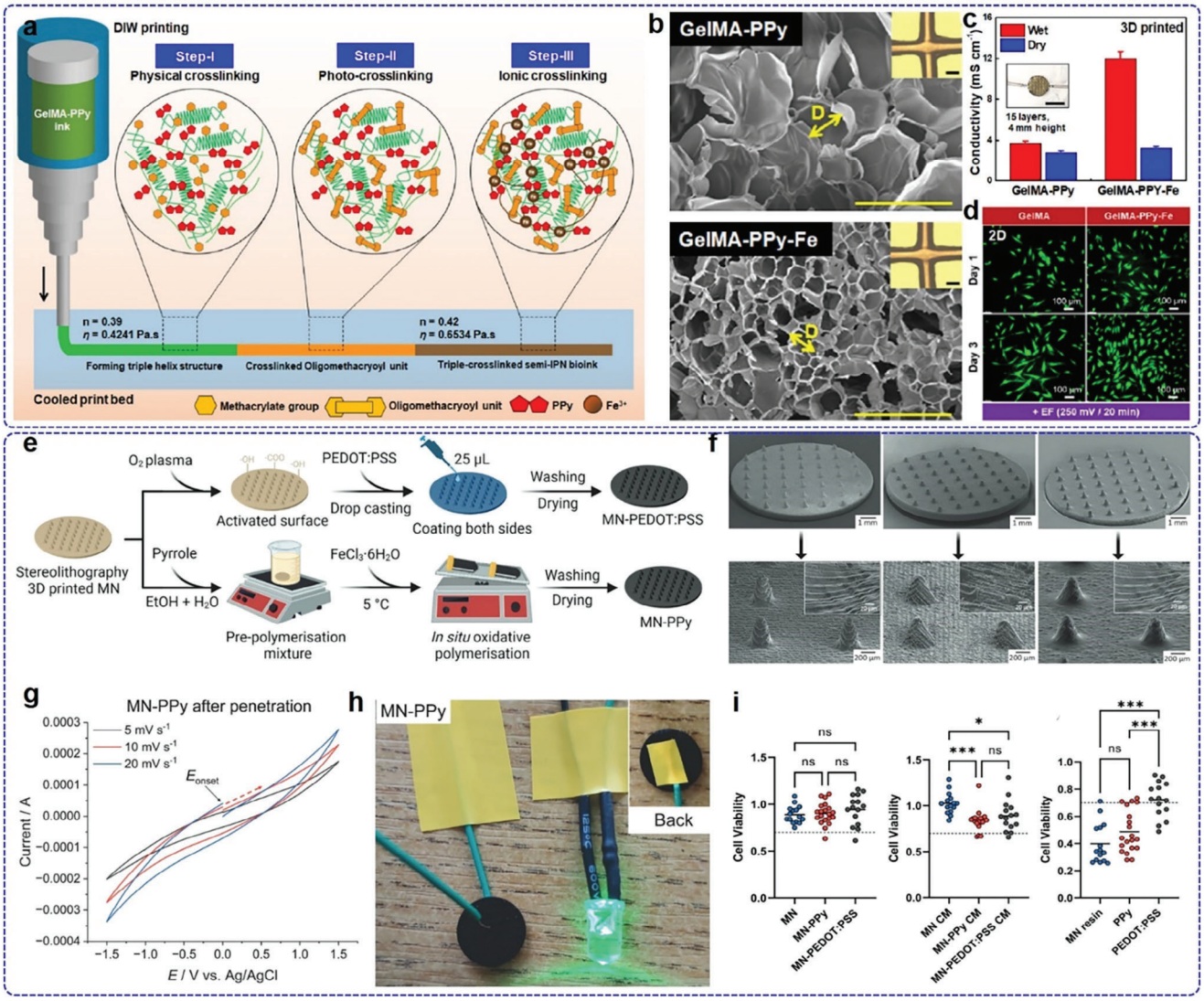

Figure 9. Demonstration of polypyrrole (PPy)-based conductive hydrogels for biological application. a) Schematic illustration of GelMA-PPy-based conductive hydrogel fabrication for tissue engineering. b) FE-SEM images of the pristine GelMA-PPy and Fe-catalyzed GelMA-PPy scaffolds. Scale bar: 50 µm. c) Comparison of electrical conductivity of the GelMA-PPy and GelMA-PPy-Fe hydrogels. d) Biocompatibility assessment of hBMSCs using the GelMA-PPy hydrogels.[150] Copyright 2023, Elsevier. e) Illustration of the synthesis procedure of PPy and PEDOT:PSS-coated microneedle (MN) patches for skin bioelectronics. f) FE-SEM images of the uncoated MNs (left), PPy-coated (middle), and PEDT:PSS coated (right) surfaces. Scale bar: 200 µm and 1 mm. g,h) Cyclic voltammetry and conductivity test of the PPy-coated MNs showing good electrical conductivity. i) Cell viability assay of human skin cells in the presence of various MNs.[152] Copyright 2023, Wiley-VCH.

3. Advantages of 3D Printing in Soft Bioelectronics

3.1. Necessity of 3D Printing for Bioelectronics

To date, various fabrication techniques are available to develop stretchable bioelectronics. For example, the conductive hydrogels can be molded to form a hydrogel thin film or can be used directly as a material for screen printing.[181,182] In some cases, the hydrogel polymers are directly drop-casted onto the surface of conductive electrodes[183] or spray-coated to improve the conductivity.[184] These conventional techniques are relatively simple, cost-effective, and require minimum time to fabricate the electrodes, films, and chips. With that, the spray coating or drop-casting may enhance the conductivity of the electrode material significantly higher than the screen printing or hydrogel molding techniques; however, over-drying or over-curing of sprayable materials may cause damage to the electrodes.[184] However, one potential disadvantage of this technique is the spatial control over the shape and geometry of the developed conductive materials. Besides, 3D printing technology offers a wide range of biofabrication with precisely controlled 3D structures which can be programmed for multi-faceted applications with minimal errors. For example, the printable hydrogels can be programmed according to the CAD models, allowing the researchers or manufacturers

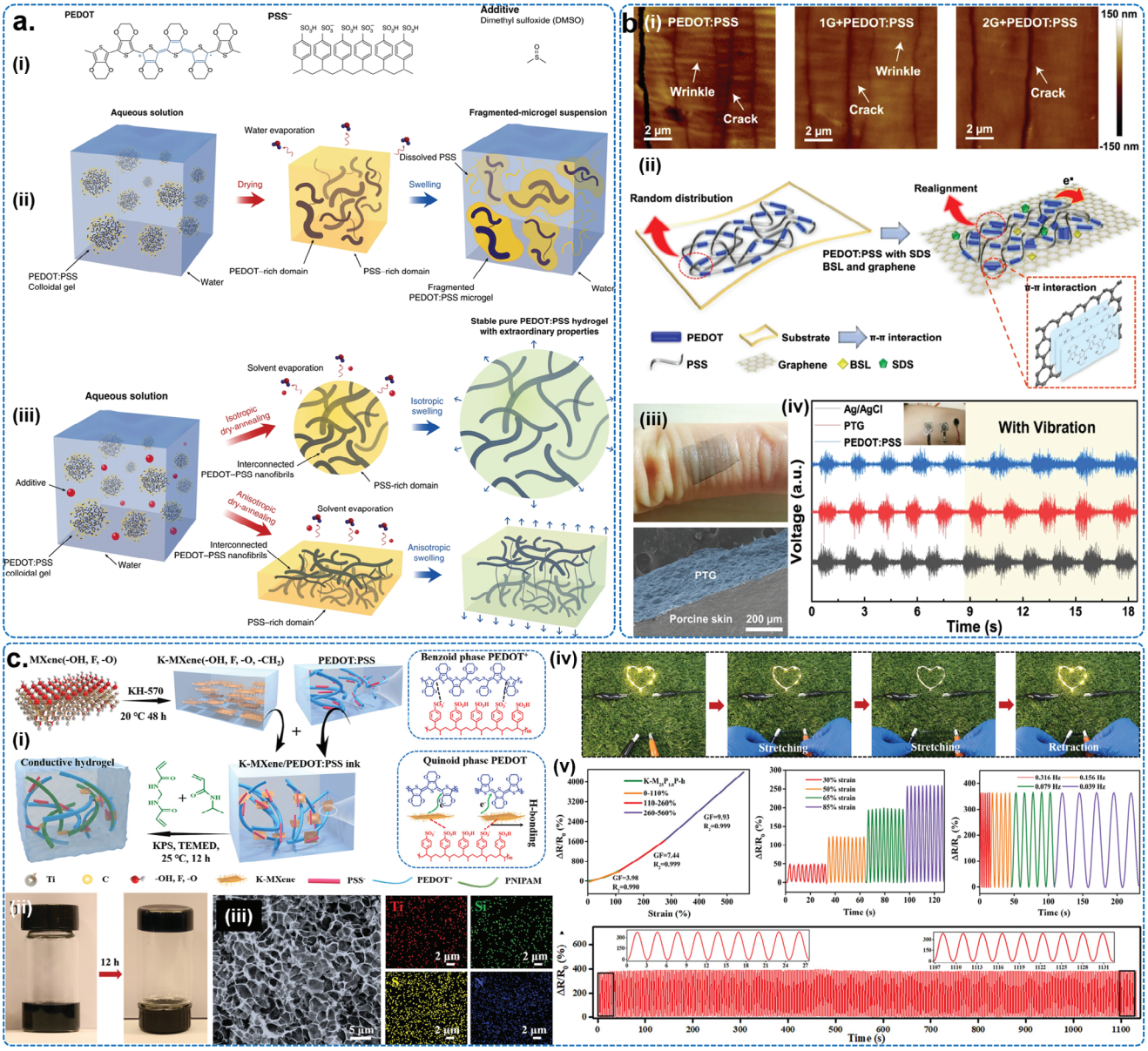

Figure 10. Fabrication of PEDOT:PSS-based conductive hydrogels for tissue engineering and biosensing. a) The schematic diagram for the fabrication strategies of PEDOT:PSS-based hydrogels. Chemical structure of PEDOT and PSS (i); strategies for microgel fabrication (ii), and anisotropic PEDOT:PSS hydrogel fabrication (iii).[153] Copyright 2019, Springer Nature. b) Demonstration of graphene-decorated PEDOT:PSS hydrogels for real-time EEG monitoring. The AFM phase images of the nanocomposites (i), mechanism of self-assembly (ii), adhesion test of the hydrogel onto porcine skin (iii), and EEG sensing performance of the hydrogel (iv). Scale bar: 2 and 200 μm.[179] Copyright 2021, Springer Nature. c) Fabrication of MXene-based biocompatible hydrogels for human motion sensing applications. Schematic illustration of the hydrogel fabrication (i), physical appearance of the hydrogel (ii), and FE-SEM with EDS map showing the presence of MXene (iii). Demonstration of the electrical conductivity of the composite hydrogel and change in resistance ($\Delta R/R_0$) under varying strain (iv, v). Scale bar: 2 and 5 μm.[180] Copyright 2023, Wiley-VCH.

to understand their exact needs. An overview of various conventional techniques versus 3D printing is schematically represented in **Figure 11**.

Direct Ink Writing (DIW) 3D printing is a versatile additive manufacturing technique that has gained significant attention in fabricating stretchable bioelectronics. Unlike traditional 3D printing methods, DIW utilizes specialized ink or bioink extruded through a nozzle to create intricate structures layer by layer.[57,185] This method allows for the precise deposition of materials, integrating multiple materials with varying mechanical properties to produce stretchable and flexible bioelectronic devices (**Figure 12a**). The DIW process offers several advantages for stretchable bioelectronics. First, it allows for the incorporation of conductive materials, such as conductive polymers, nanoparticles, or even liquid metal inks, which are crucial for the functionality of bioelectronic sensors and circuits. Secondly, DIW can be combined with biocompatible and stretchable materials like hydrogels or elastomers to create bioelectronic devices that can

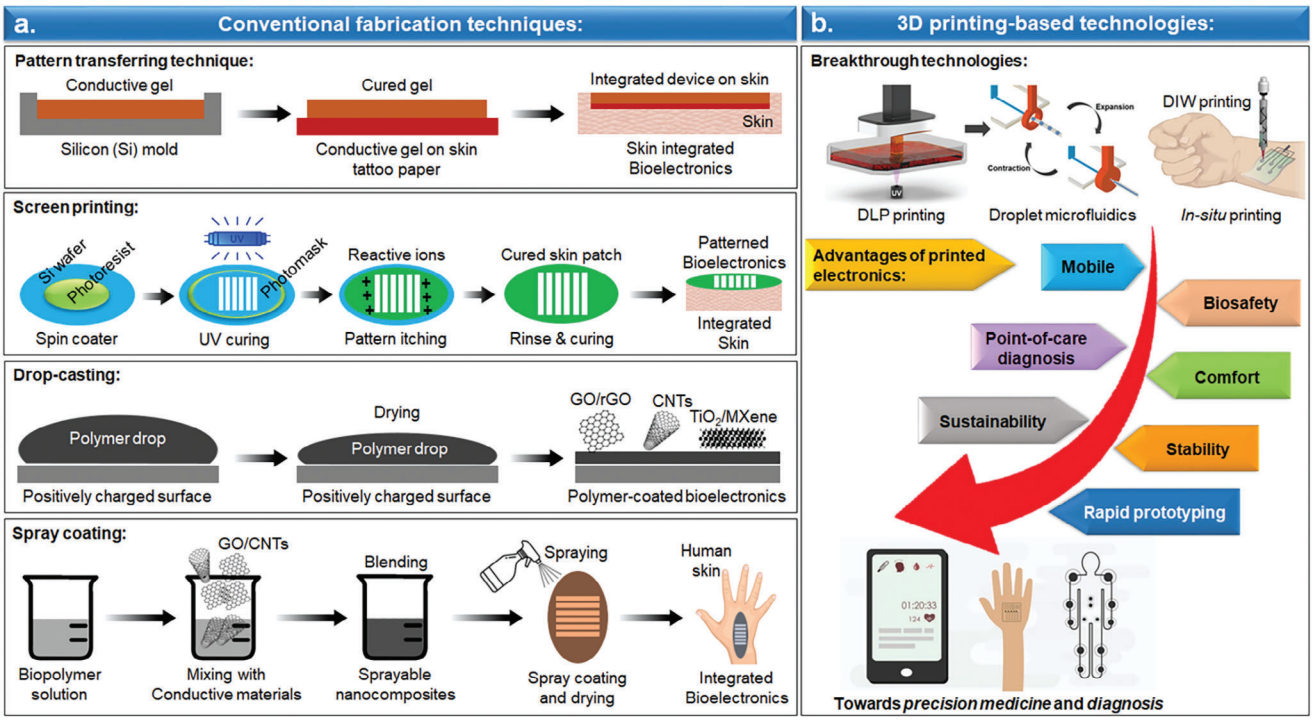

Figure 11. An overview of conventional and modern fabrication techniques for skin bioelectronics. a) Conventional techniques of bioelectronics fabrication include pattern transferring, screen printing, solution drop-casting, and spray coating. The recent technology, such as b) "additive manufacturing" or "3D printing", may serve as promising alternatives for bioelectronics fabrication owing to the superior printability, biosafety, stability, sustainability, and rapid diagnostic performance. The 3D printing technology offers various fabrication methods, such as digital light processing (DLP) printing, droplet printing, and *in-situ* printing, allowing precision measurement for healthcare and medicine.

withstand mechanical deformation and interface with biological tissues without causing damage or discomfort.[185] One of the key aspects of DIW for stretchable bioelectronics is the ability to print complex, 3D structures with high resolution. This feature is crucial for fabricating customized and patient-specific bioelectronic devices, such as wearable sensors, soft implants, and electronic skins. Several research studies have demonstrated the potential of DIW for stretchable bioelectronics. Hinton et al. introduced a novel approach for DIW using a hydrophilic support bath, enabling the 3D printing of polydimethylsiloxane (PDMS) elastomers, a popular material for stretchable bioelectronics.[186] Tumbleston et al. highlight the development of continuous liquid interface production (CLIP) 3D printing (Figure 12b), a DIW variant capable of producing high precision and mechanically robust structures, particularly for stretchable bioelectronics.[187] As research progresses, we can expect further innovations in materials, printing techniques, and applications, making DIW an indispensable tool for the future of stretchable bioelectronic devices.

Stereolithography (SLA) and digital light processing (DLP) are the types of vat polymerization techniques where the liquid resin is solidified layer-by-layer in the presence of laser or UV light, allowing for the creation of intricate and high-resolution 3D structures (Figure 12c,d). Achieving high-resolution printing makes SLA suitable for producing stretchable bioelectronics with complex geometries and precise features.[188,189] SLA can also be used for the 3D printing of intrinsically conductive polymers (ICPs). For example, Takenouchi et al. reported using a blue light-assisted microlithography technique to fabricate stretchable PEDOT:PSS-based polymers with a conductivity of ≈16 S cm^{-1}.[190] Fused deposition molding (FDM) is another type of extrusion 3D printing like DIW (Figure 12e), where a conductive nanocomposite filament is extruded from a heated metal nozzle and immediately cooled when deposited onto the platform.[144] Besides, inkjet printing utilizes a piezoelectric nozzle where the ink is deposited onto the platform via droplet generation. For successful 3D printing, various factors, such as ink viscosity, density, printability, and post-processing, should be considered while printing high-resolution structures. Selective laser sintering (SLS) is an approach for fabricating 3D structures by successively fusing and sintering polymer or ceramic grains using a controlled laser beam (Figure 12f). SLS uses a laser to selectively fuse powdered materials, typically polymers, to create 3D objects. It is a process used to manufacture various types of flexible bioelectronics. SLS builds sophisticated 3D structures by layering powdered materials like thermoplastics or biocompatible polymers with a high-powered laser.[191] Flexible bioelectronics can use this technology to construct complex devices with electric functionality. SLS 3D printing's ability to create complicated geometries and structures without supporting elements is a significant advantage. Another advantage of this technique is a wide range of printable materials, high utilization (unsintered powder may be removed and reused), and overhanging structures that can be printed without support.[192] **Table 1** depicts the advantages and disadvantages of various printing techniques for hydrogel bioelectronics.

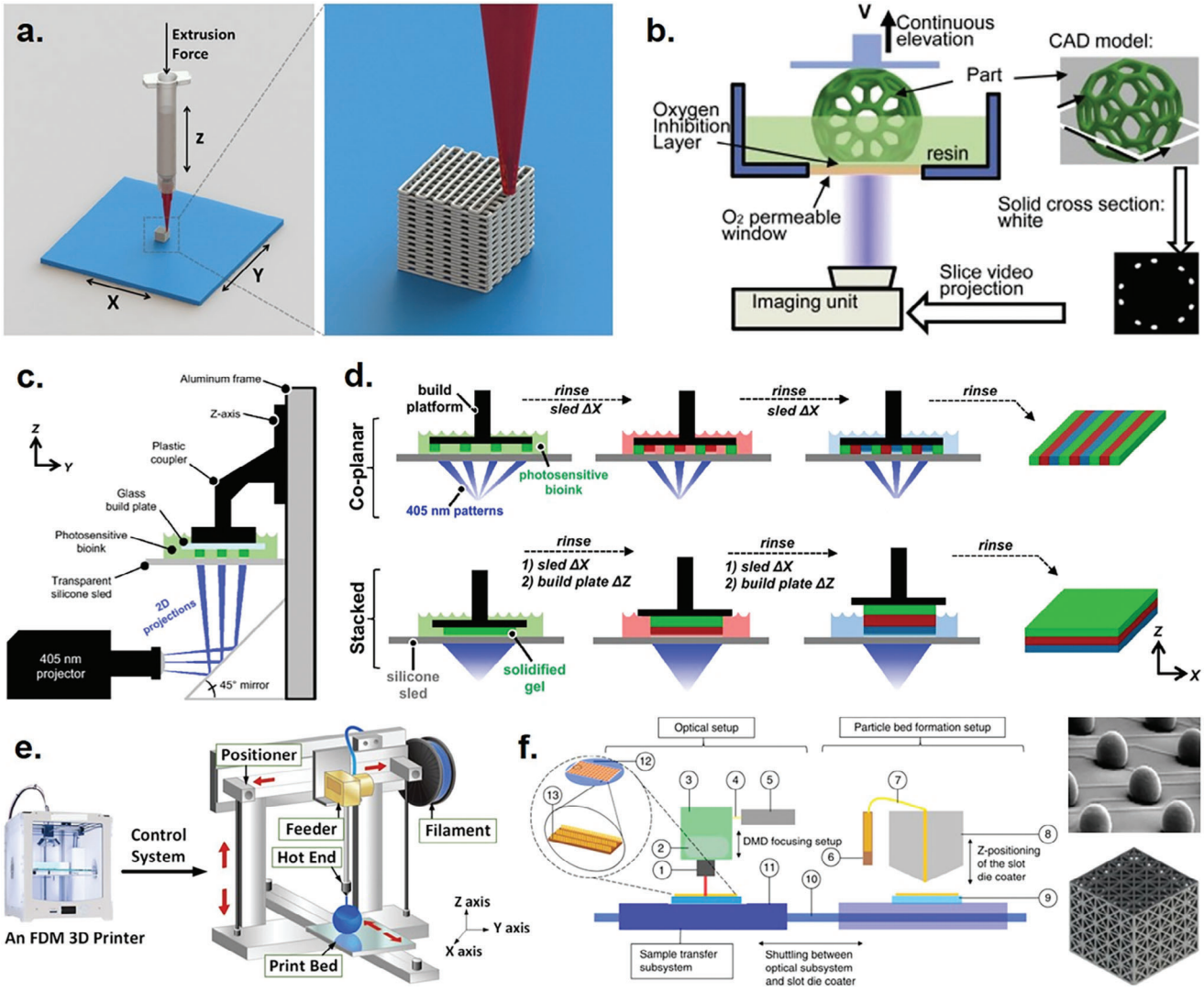

Figure 12. Various types of 3D printing technology for the fabrication of hydrogel bioelectronics. a) Demonstration of direct ink writing (DIW) 3D printing. DIW uses a pneumatic air pressure to extrude hydrogel inks.[193] Copyright 2021, Elsevier. b) Continuous liquid interface production (CLIP) printing.[194] Copyright 2019, Elsevier. c,d) Vat polymerization-based 3D printing (stereolithography and digital light processing) and its working principle.[195] Copyright 2021, Springer Nature. e) Fused deposition molding (FDM) 3D printing.[196] Copyright 2018, ACM Digital Library. f) Selective laser sintering (SLS)-based 3D printing with demonstrated 3D structures showing unique geometry.[197] Copyright 2019, Springer Nature.

3.2. Design Parameters for 3D-Printed Bioelectronics

Hydrogel inks can be used directly for 3D printing to obtain various shapes and geometries. Several review articles have emphasized the state-of-the-art techniques for optimizing 3D printing for multi-faceted applications in the past few years. Generally, there are two key approaches for designing soft hydrogel bioelectronics (**Figure 13**). The "top-down" approach involves the fabrication of various biocompatible and conductive hydrogels in a bulk volume, which is the first step of sensor fabrication.[46] The next step involves the fabrication, which is 3D printing (e.g., inkjet, DIW, microlithography, and many others) of hydrogel inks. After that, the hydrogel ink undergoes various cross-linking to achieve a stable geometry, followed by post-processing. The hydrogel inks are usually analyzed through rheology to understand the viscoelasticity and shear-thinning nature, which is crucial for 3D printing. The final step of the top-down approach involves the application, which includes various characterization, such as conductivity test, stretchability test, and self-healing analysis, followed by the sensing application. Besides, the "bottom-up" approach involves understanding the fundamental principle of application strategy and focuses on fabricating small-scale or miniature constructs.[46,216] In this approach, the biomimetic structures are first visualized. It involves the design of various biomimetic structures, such as anisotropic models, isotropic models, bioinspired mimetics, and many others. After that, the necessity of the bioelectronic device was determined. This can be done by analyzing a predetermined database or consulting medical doctors. The next part involves 3D printing, which is performed according to patients' needs. The 3D printing process can be

Table 1. Advantages and disadvantages of 3D printing technologies for bioelectronics fabrication.

Printing technology	Advantages	Disadvantages	Cost	References
Fused deposition molding (FDM)	Fast, simple, accurate, environmentally friendly, one-step fabrication offers a wide range of materials and good flexibility without post-processing.	Limited materials, quality issues, low-resolution printing, Restricted to thermoplastic materials	Low-cost	[198–201]
Stereolithography (SLA)	Fast, high-precision printing with complex geometries, ideal for electrode/microelectrode fabrication	Not environmentally friendly, only printing of light reactive materials	High-cost	[202–206]
Direct metal laser sintering (DMLS)	Fast, ability to print high viscosity inks, higher reproducibility, laser-induced sintering	Small build volume, only printing of light reactive materials	High-cost	[70, 207, 208]
Inkjet	Fast, high precision, bulk printing	Poor mechanical property	Low-cost	[202, 209, 210]
Polyjet	Fast, accurate, and high precision, it offers multi-material printing	Poor mechanical property	High-cost	[211, 212]
Molding	Fast, rapid prototyping for mass production	Limited materials, Required melted materials	Low-cost	[204]
Bioprinting	Fast, multi-material printing	Small build volume	High-cost	[150, 213–215]

accomplished by either self-assembly (e.g., template-directed or direct self-assembly) of hydrogels or by the development of microfluidic devices (e.g., aligned fibers or self-assembled hydrogel beads through multi-flow capillary chip).[46] After 3D printing, the hydrogel electronics were implanted into the patient's skin and allowed to diagnose the target molecule in the human body. Based on the sensing data, the patients are subsequently prescribed medication. The "bottom-up" strategy is more convenient to design hydrogel bioelectronics for precision medicine.

Print geometry is crucial for developing 3D constructs. Various CAD have been employed for the 3D printing application. Based on the primary shape and mesh structure, the hydrogel ink was extruded through the printing nozzle to mimic the CAD model in actual shape and size. In this context, infill density is an

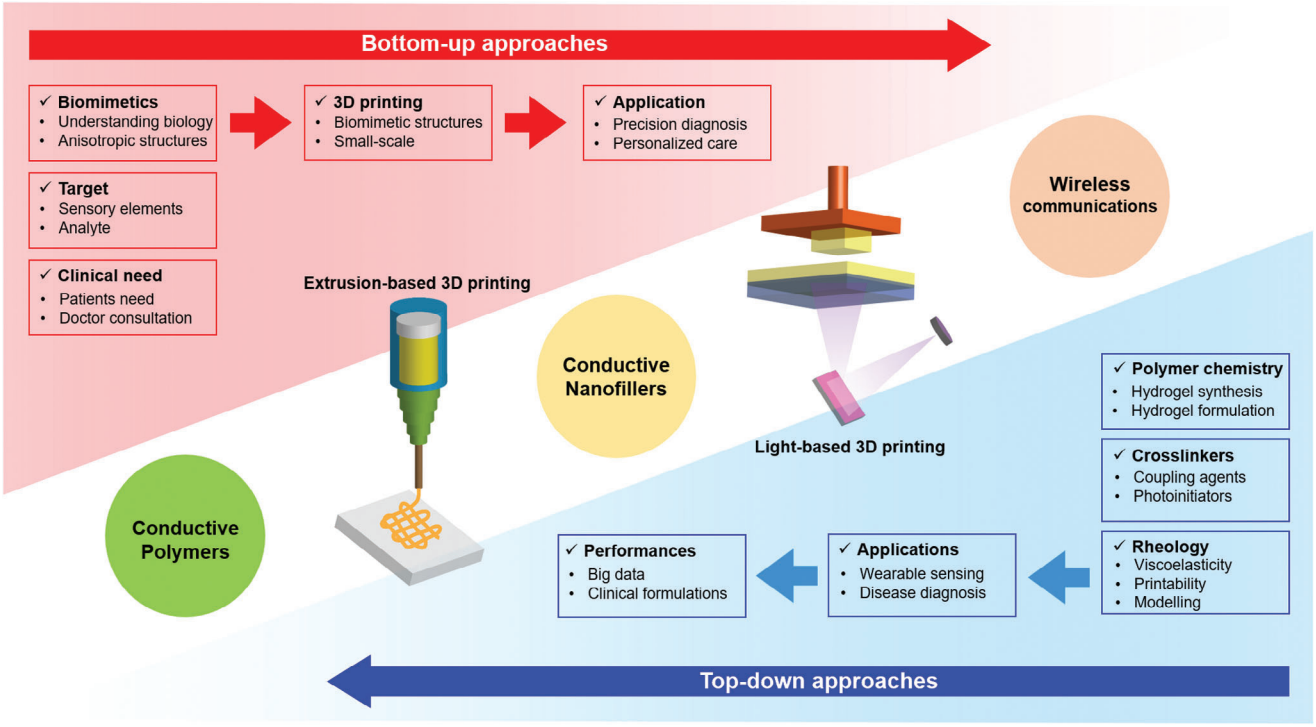

Figure 13. "*Top-down*" and "*bottom-up*" approaches for 3D printing wearable bioelectronics for precision medicine.

important parameter to consider. 3D objects can be designed with a porous inner articulation and a solid outer shell. Infill density is usually created to decrease the printed parts' bulk weight and stabilize the printed strands during 3D printing.[217] Porous geometry is ideal for soft tissue engineering, whereas less infill may give rise to high-weight 3DP structures, which are often suitable for load-bearing applications. Thus, any printed structures with an infill density are commonly represented as smooth outer surface layer with interconnecting struts. In the case of conductive bioinks, the filaments can be extruded with proper infill density to create high-resolution 3D structures.

Another crucial parameter for 3D printing is the choice of conductive biopolymers and their physicochemical properties. Homogeneous biopolymers and conductive inks require a higher cross-linking degree (mostly chemical cross-linking) and often display poor printability and conductivity (<100 S cm^{-1}).[218] Besides, heterogeneous biopolymers and inks display good printability owing to both physical and chemical cross-linking, and the incorporation of conductive nanomaterials enhanced the printing as well as conductive behavior (>200 S cm^{-1}) of the final product.[219] For skin bioelectronics, the adhesive property of an electrode is also a demanding factor. Printable hydrogels with significantly higher self-healing and adhesive property may not be suitable for 3D printing as it tends to be over-sticky onto the built platform and hinder the detachment. On the other hand, hydrogel inks with optimal self-healing and adhesive property during 3D printing may give rise to high-resolution printed structures with good structural stability.

3.3. Role of Conductive Nanofillers in 3D Printing

Nanofillers play a significant role in tuning the physicochemical properties of a bulk hydrogel. Particularly, using a suitable conductive nanofiller, its concentration, and biocompatible biopolymers may result in good electrical conductivity, mechanical property, and biocompatibility, which is crucial for fabricating soft bioelectronics. In this section, we briefly discussed some of the aspects of conductive nanofillers and their role in the 3D printing of stretchable bioelectronics. The first step of 3D printing involves the choice of proper nanofillers (**Figure 14a**). Various types of carbon (e.g., graphene, carbon nanofibers, CNTs, and nanodiamond), modified-carbon (e.g., MXene, carbon nitrides, and carbon dots), and metal (*e.g.*, AgNPs, AuNPs, CuNPs, ZnO NPs, and many others)-based nanofillers has been demonstrated in the literature to enhanced the cross-linking ability, tuning the mechanical, electrical, and biological properties, suggesting that the concentration and conductivity of nanofiller is important for hydrogel fabrication. The next step involves optimizing and understanding nanofillers' role in 3D printing. This includes the study of rheological parameters (e.g., viscoelasticity, shear thinning, and elastic modulus) and hydrogel formation ability, which is important for sensing application (Figure 14b). Although 3D printing can be performed by using various conductive biopolymers, the advanced and multi-stimuli assisted nanocomposite hydrogels could be achieved by choosing a combination of conductive biopolymers with nanofillers, which will synergistically enhance the conductively, stretchability, fatigue resistance, and durability. Figure 14c diagrammatically represents the possible advantages and disadvantages of conventional 3D printing and advanced nanocomposite-based 3D printing.

Another remarkable consideration is the interaction and self-assembly behavior of the conductive nanofillers in the polymer matrix, which is also critical for bioelectronics fabrication. Studies have shown that conventional hydrogel molding after hydrogel fabrication is not an ideal technique for biosensor development. This can be explained by understanding some basic facts of hydrogel fabrication, where the key dominating factor is nanofiller concentration (Figure 14d). It was observed that a low concentration of nanofiller in a polymer matrix shows good gelatin and conductivity with compromised mechanical properties. Besides, the moderate concentration of nanofiller displays higher conductivity with gauge factor owing to the homogeneous mixture and proper interaction with the polymer chains with desirable mechanical properties. High nanofiller concentration often leads to crack formation or deformation due to particle aggregation and higher mechanical stiffness, which is practically inappropriate for biosensor fabrication. Inversely, 3D printing holds tremendous promise for bioelectronics fabrication. During 3D printing, the nanofillers assemble towards the printing direction due to the temporary deformation in the polymer matrix generated through extrusion pressure (shear stress). Thus, the self-assembly of nanofillers in the polymer matrix generates anisotropic morphology with higher electrical conductivity and mechanical properties. Therefore, the proper knowledge of nanomaterials, their functionalization, and design is crucial for 3D printing applications.

4. Transmission Mechanism of Bioelectrical Signals

Wearable biosensors are usually integrated with a portable electronic circuit system that acts as a signal transmitter (Personal Area Networks or PANs) and able to collect the human body signals wirelessly. The human body creates a transmission channel when the individual wearing the transmitter contacts the receiver's electrode. In this scenario, the recipient acknowledges the user's identification and has the ability to customize it. The advantage of this technology lies in the fact that data is sent via everyday physical interactions, such as a simple touch on the receiver. The electromagnetic wave produced by the device, which is ultimately connected to the human body via electrodes, is used in the near field area for this communication system.[220] Therefore, the configuration of electrodes is a crucial factor for biosensing. **Figure 15** describes the transmission procedure of bioelectrical signals through hydrogel-based biosensors based on the sensing mechanisms. The biological signals can be obtained by changing pressure, temperature, use of external magnetic fields, ultrasound, optoelectric stimuli, and electrochemical reaction with the electrodes. When the analyte comes into contact with these sensing components, they transform the energy shift into electrical signals. This technique enables the quantitative determination of physiological data, including temperature, pulse, glucose, heart rate, and many others.[221]

Blood pressure, heart rate, and other mechanical variables have all been measured using *pressure-sensitive* sensors. Typically, they consist of an intermediate conductor that is enclosed inside a flexible support matrix.[222] Temperature is an important human

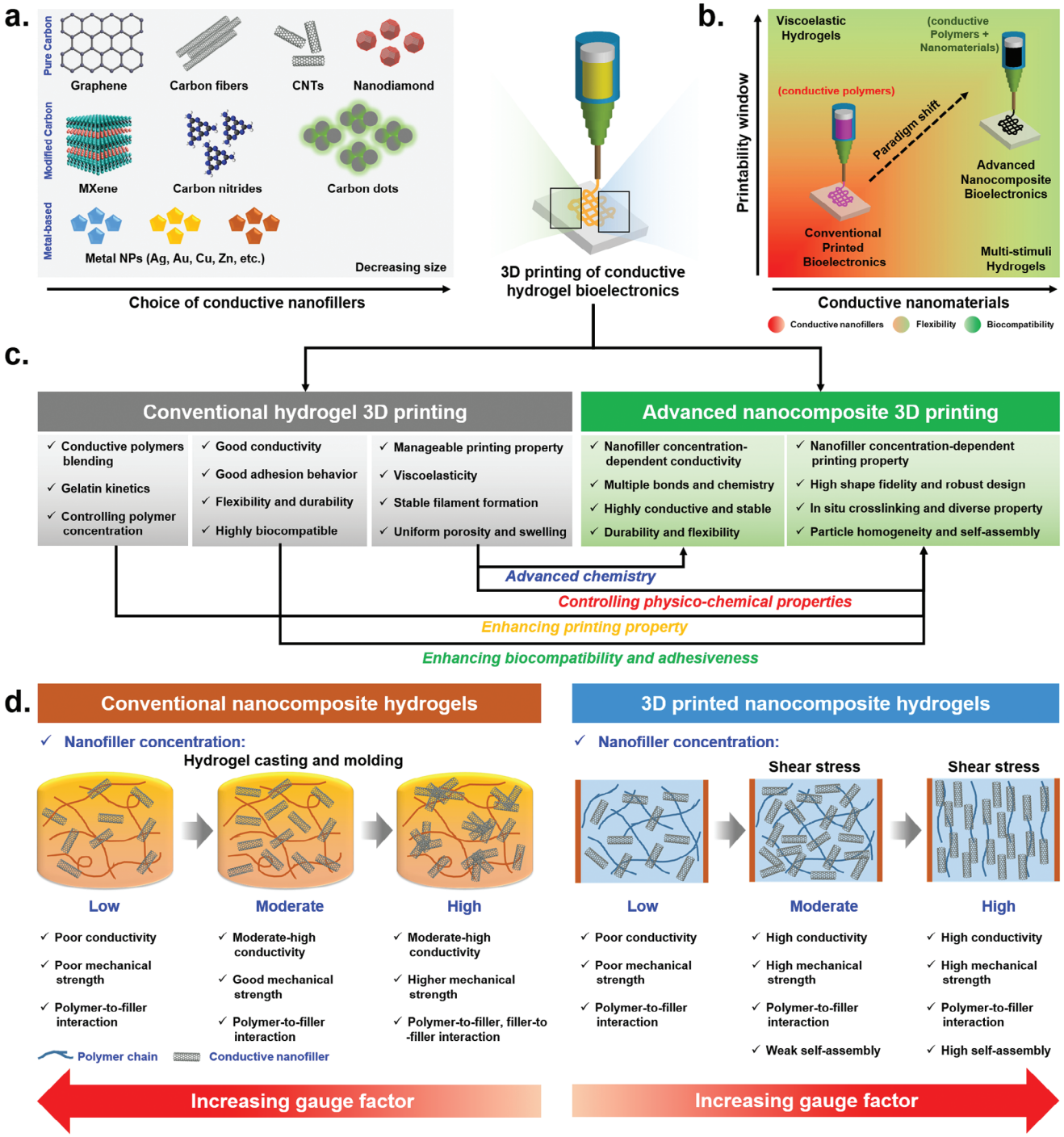

Figure 14. Schematic illustration of the role of various conductive nanofillers in improving printability and shape-fidelity for bioelectronics development.

body indicator that provides an immediate diagnosis of fever and hypothermia. The intricate metabolic alterations in the human body result in a fluctuation in temperature, which may be quantified using a thermopile or thermistor and seamlessly incorporated into flexible circuits for monitoring the temperature of the body using wearable devices.[221]

Magnetic or electromagnetic sensors provide autonomous sensing signals by capturing mechanical energy. Voltage is produced by the magnetic coupling between coils and permanent magnets when mechanical disturbances cause changes in the distribution of the magnetic field. Such sensors can resist a range of humidity and temperature conditions, resulting in a longer service life and improved durability. The electromagnetic core components are normally mechanically isolated to avoid direct contact and wear. These electromagnetic sensors may be used in abundance to perform sensing in numerous locations for

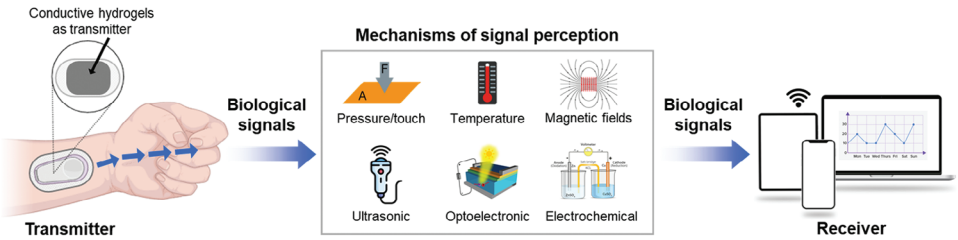

Figure 15. Schematic illustration showing the transmission system of a soft hydrogel-based biosensor with corresponding signal perception mechanisms.

health applications, namely in areas like rehabilitation and voice assistance.[221]

Ultrasonic sensors use body acoustic waves or surface acoustic waves to find changes in the piezoelectric effect, mass density, electrical conductivity, viscoelasticity, and other physical or chemical properties.[223] The interaction between biometric parts (like hemoglobin) and the target analyte (like oxygen) changes the optical properties, which is what optoelectronic sensors use. These changes may appear as variations in absorption, fluorescence, reflectance, emission, or interference patterns. Key vital indicators, including heart rate, breathing rate, and blood oxygen level, may be detected using photodetectors, which measure changes in the concentration or shape of molecules and translate those measurements into electrical impulses.[221]

5. Types of 3D-Printed Wearable Sensors

The human body constitutes various receptors that create diverse signals, such as biophysical (e.g., temperature, pressure, motion) and biochemical (e.g., metabolites and electrolytes secretion) signals. Skin is one of the essential multicellular organs that can be used for sensing various biological signals generated from internal organs, blood vessels, and muscles.[8,23,31,224–227] The skin serves as a medium for the concurrent detection of external stimuli and the representation of internal bodily data. These stimuli include physical attributes like pressure and stretching, chemical factors such as sweat, and physiological indicators like temperature, respiration, and pulse.[228] In bioelectronics, "E-skin" emerges as a promising alternative to human skin to capture external signals from the surrounding environment and internal data from individuals. The acquisition of data from the patient throughout the rehabilitation process, particularly pertaining to strain and pressure, may provide the therapist with immediate insights on the precision of movement and the physiological condition.[229] **Table 2** shows the human skin's and E skin's key sensing features. Highly sensitive, flexible, and adhesive wearable sensors are gaining enormous attention in the bioelectronics field due to their ability to attach to human skin, biomimicking the properties of skin, or integrate with textiles to monitor the physiological responses of the human body. Motion sensing is a biosensing technique where humans and robots cross-talk via touch sensors.[230–232] In this section, we briefly demonstrated the types of various wearable sensors fabricated through 3D printing technology.

5.1. Tactile Sensors

Tactile sensors are widely used to analyze human tactile perception, such as shear, pressure, bend, torsion, strain, and vibrational signals within a pressure range of 5–100 kPa and a vibrational frequency within 400 Hz.[23,233] During signal perception, tactile sensors are subjected to exogenous stress, and as a result of that, mechanical signals are converted into electrical signals. External wireless devices, such as cell phones or IoT gadgets, then analyze the electrical signals. To mimic the actual functionality of human skin, an ideal tactile sensor must have the following features: 1) high flexibility and stretchability so that it can be easily attachable and wearable; 2) high sensitivity, i.e., the minimum amount of pressure, stress, strain, and torsion can be detected; 3) wide pressure range and excellent linear input-output characteristics; 4) completely safe and biocompatible, i.e., it will not harm the skin tissue or cells; and 5) fast and reliable for monitoring physiological parameters.[23,234] Thus, 3D-printed wearable patches are emerging nowadays with a tremendous advantage over conventional fabrication techniques due to the ability to create a computer-generated 3D pattern from raw materials and bioinks.[235–239] Recently, the 3D printing technique also offers a wide range of flexibility in material selection, suitable for tactile device fabrication. A study by Guo et al. demonstrated the potential applications of 3D-printed AgNPs/silicon nanocomposite scaffolds for tactile pressure sensing.[232] In this study, the authors have prepared a sinter-free ink with tunable viscosities and electrical conductivities (**Figure 16**). The scaffold was fabricated via four independent ink cartridges, including the base layer (cartridge 1), a sensor layer (cartridge 2), two electrode layers (cartridge 3), an isolating layer, and a topmost pressure-force sensitive layer (cartridge 4) as indicated in Figure 16a–d. To enhance the conductivity and stretchability of the scaffold,

Table 2. Representative sensing features of human skin and an *E-skin*.[228]

Surface	Pressure sensitivity	Thickness	Temperature sensitivity	Mechanical property	Response time
Human skin	0.078-0.018 kPa	1 mm	20 mk	Stretchable up to 30%	15 ms
E-skin	0.01-200 kPa	50 μm-5 mm	0.01°C^{-1} to 2410 ppm°C^{-1}	Flexible and stretchable up to 800%	9–32 ms

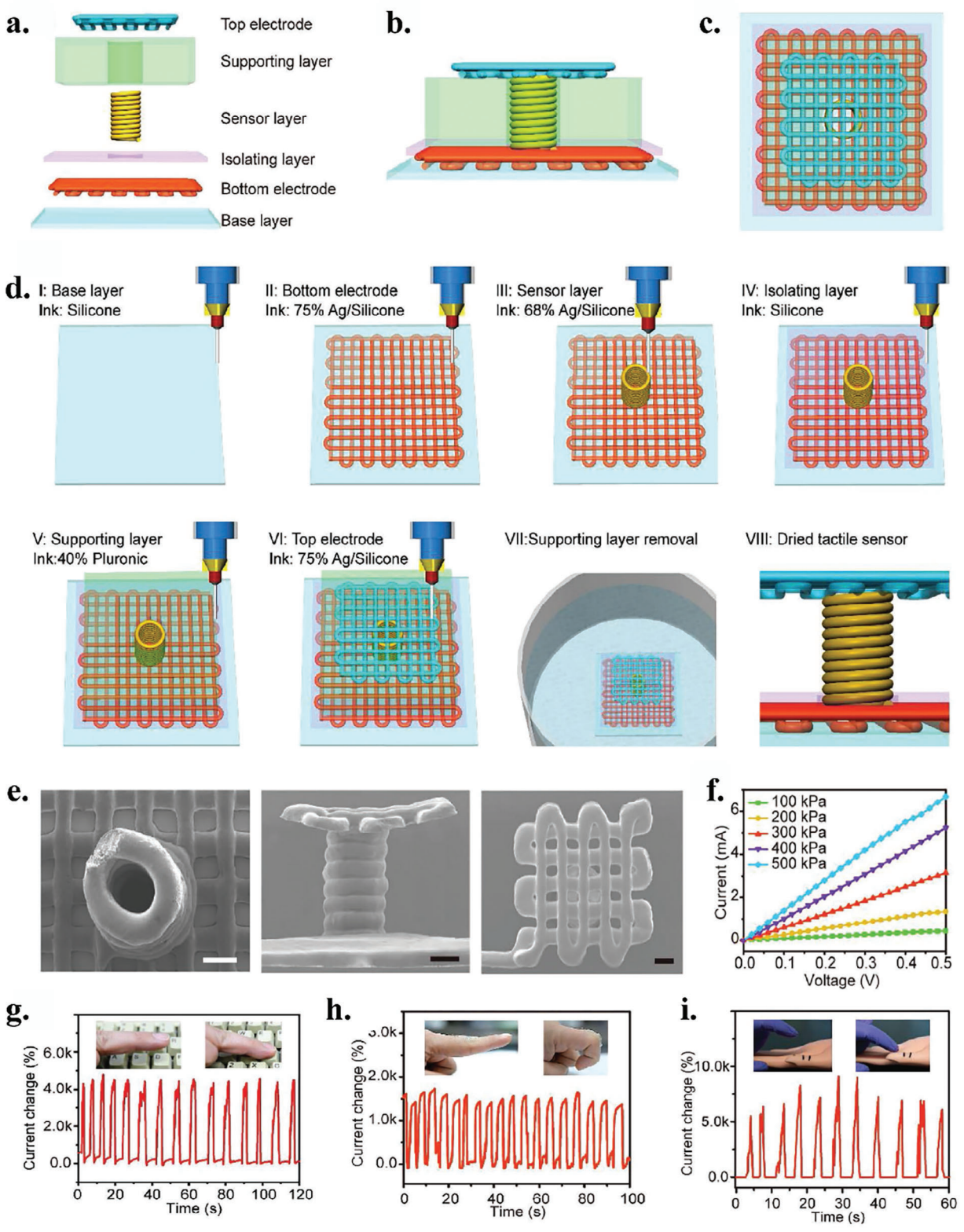

Figure 16. Design and fabrication of 3D printed tactile sensor. a) Schematic illustration of tactile sensor consisting of a base layer, top, and bottom electrodes with an isolating layer, a sensor layer, and a supporting layer. b,c) Side view and top view of the sensor. d) The 3D printing process of the tactile sensor. e) SEM morphology of the printed sensor indicating the structure of the top and side view (from left to right). Scale bar: 200 μm. f) Current-voltage characteristics of the sensor under varying pressure conditions. g,h) Current change signals respond to dynamic loading and unloading during pressing and bending of human fingers. i) Current change of the 3D printed device during 100 pressing cycles with a pressure of 100 kPa at 0.25 Hz frequency.[232] Copyright 2017, Wiley-VCH.

Table 3. Piezoelectric natural and organic biopolymers for wearable electronics.

Biomaterials	Type of material	Piezoelectric coefficients (d)	References
β-Glycine	Anisotropic, β-crystal	$d_{16} = 195$ pm V^{-1}	[255]
Collagen	Anisotropic, randomly-oriented	$d_{14} = 0.1$ pm V^{-1}	[256]
Silk	Anisotropic, semi-crystalline	$d_{14} = -1.5$ pC/N	[257]
Peptide nanotubes	Self-assembly crystals of diphenylalanine	$d_{14} = 60$ pm V^{-1}	[258, 259]
PVDF	Anisotropic, polymeric	$d_{33} = -33$ pC N^{-1}; $d_{31} = 23$ pC N^{-1}	[260]
PLLA	Anisotropic or transversely isotropic, polymeric	$d_{14} = 6$–12 pC N^{-1}	[261]
Graphene	Single-layer	$d_{33} = 1.4$ nm N^{-1}	[262]

PVDF; Polyvinylidene fluoride, PLLA; Poly-L-lactic acid, pm V^{-1}; Picometer/unit of applied voltage, pc N^{-1}; Picocoulombs/Newton, nm N^{-1}; Nanometer/Newton.

sub-micrometer-sized AgNPs were dispersed into the stretchable silicone elastomer. The incorporation of AgNPs into silicon yields linear I–V curves when the applied pressure was between 100 and 500 kPa with decreased resistance Figure 16f. Moreover, the fabricated sensor was able to generate a specific amount of currents depending on the physiological conditions, such as straight or bending motion (Figure 16g–i). Dynamic pressure sensing can be achieved through different sensing techniques. Previously, it was demonstrated that silicon-metal oxide semiconductor-based sensors have the potential to measure accurately with high sensitivity.[234,240] However, silicon-based nanomaterials display many problems due to low adhesive properties. A new sensing mechanism was proposed to address these shortcomings, i.e., organic field-effect transistor (OFET) for preparing stretchable sensors.[23,241–243]

5.2. Piezoelectric Sensors

Piezoelectricity is the property of materials by which a transient voltage is generated in response to mechanical stress (**Figure 17a**). Both organic (mainly polymers and biomaterials) and inorganic materials can create a substantial amount of electricity due to specific mechanical stress.[244–246] The piezoelectric behavior of materials can be defined by using the following two equations:[23,246]

$$\delta = \frac{\sigma}{Y} + dE \tag{1}$$

$$D = \epsilon E + d\sigma \tag{2}$$

where δ, σ, and Y represents the strain, stress, and Young's modulus of elasticity. The d is the piezoelectric coefficient, and D is the charge density for piezoelectricity. Besides, the ϵ and E represent the piezoelectric material's dielectric constant and electric field. Since most of the piezoelectric material shows anisotropic behavior, different subscripts (e.g., ij) are used to distinguish the orientation of polarization (i) and the applied force (j). For example, an indication of d_{31} and d_{33} means that the applied electric field is either perpendicular or parallel to the input strain direction (Figure 17b). Most wearable biosensors follow the d_{31} mode of piezoelectricity.[244,246–249]

When an external force is applied to the piezoelectric material, the internal polarization changes linearly, creating an electric field at the material boundary. In the case of organic polymers, such as biomaterials, the piezoelectric effect is profoundly affected by the molecular structure and its orientation in the polymer matrix.[244,245,250] Also, polyethylene terephthalate (PET)/paper-based flexible biosensors utilize the piezoelectricity for sensing (Figure 17c,d). The piezoelectric effect is also found in some human tissues (e.g., bone tissue, muscle, ligaments, and tendons) and biomacromolecules (α-keratin and collagen). **Table 3** depicts some naturally derived and organic biopolymers with different piezoelectricity. Organic biopolymer-based piezoelectric sensors are emerging due to their extreme flexibility and high sensitivity.[251,252] Recently, polyvinylidene fluoride (PVDF) and polyvinylidene fluoride-trifluoroethylene (PVDF-TrFE)-based piezoelectric polymers have been used in biosensors due to their flexibility, mechanically stable, and cytocompatibility. PVDF-based polymers can be printed directly by direct-ink writing (DIW) printing to obtain thin PVDF micropatterns. Such 3D-printed PVDF micropatterns can bear an extended range of dynamic stress ranging from 5N to 45N for 50 cycles (Figure 17e).[253,254]

5.3. Piezoresistive Sensors

In piezoresistive sensors, a highly sensitive upper layer of piezoresistive materials transfers the mechanical stimuli into resistive or conductive stimuli. The conductive stimuli are measured by an external circuit.[23] The piezoresistivity is generated by the external stress that creates a band gap, which alters the charge carriers' mobility. The relative change of resistance (R) is given by the following equation:[254,263]

$$R = \frac{\rho L}{A} \tag{3}$$

where R denotes the resistance, ρ is the resistivity, L is the length, and A denotes the cross-sectional area of the conductor. Therefore, the material's resistance depends on the shape, geometry, and resistivity, as shown in **Figure 18a**. Stretchable and soft electronics are principally dependent on this kind of sensor due to its flexibility, low energy consumption, easy-to-analyze, broad pressure range, and scalable fabrication processes via 3D printing.[236,263–272] Despite many advantages, most of the piezoresistive sensors made nowadays use planar elastomer composites with various conductive materials, such as reduced graphene oxide (rGO), carbon nanotubes (CNTs), and

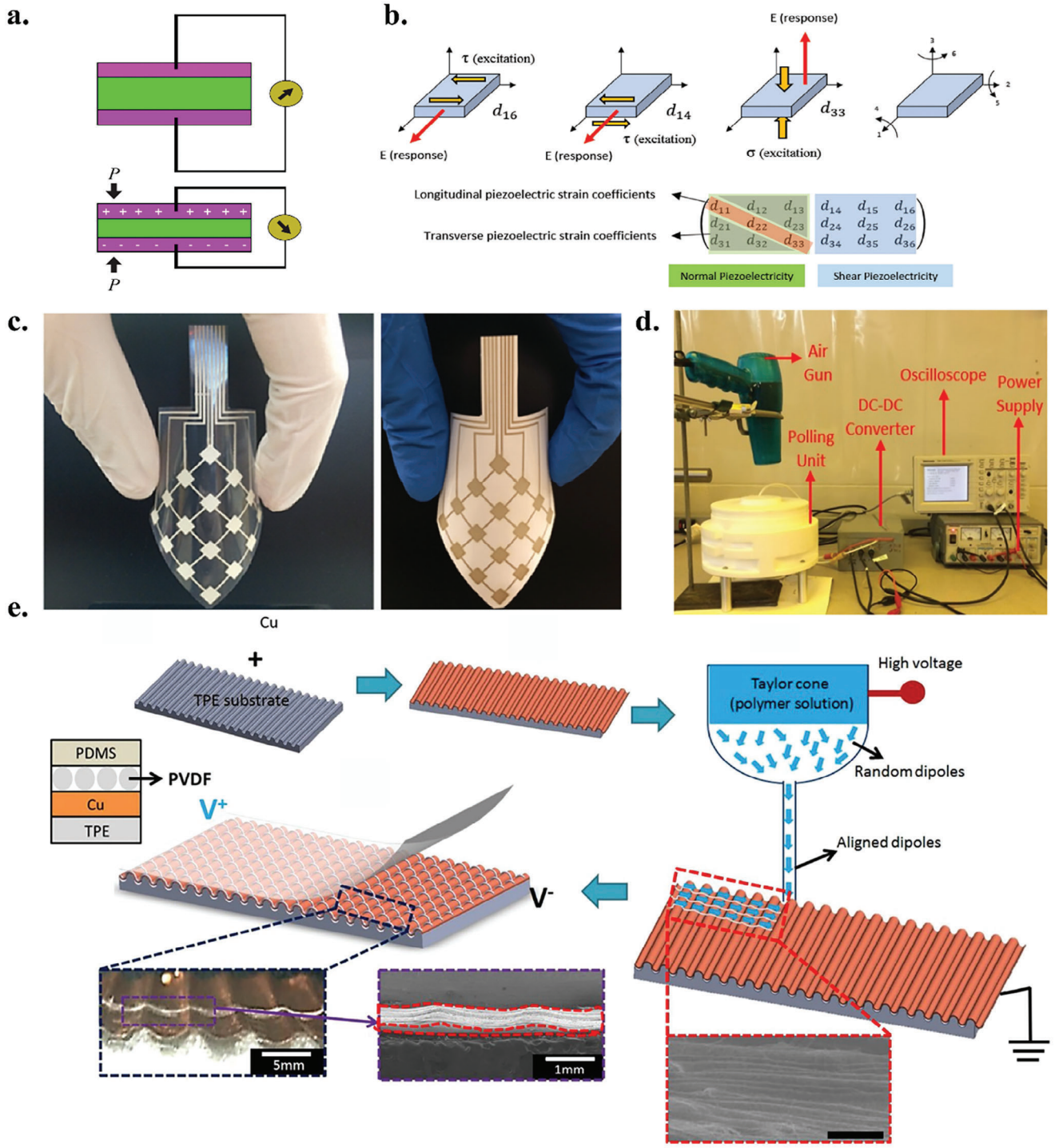

Figure 17. a) The piezoelectric sensing technique. Indication of normal (σ) and shear (τ) stress with corresponding electric field (E). b) Illustration of piezoelectric-based 3D printed touch sensor.[244] Copyright 2019, Wiley-VCH. c) Digital photograph of polyethylene terephthalate (left)-based and paper-based (right) 3D flexible touch sensors.[246] Copyright 2017, Elsevier. d) Heat-induced polarization of 3D printed electronics. The piezoelectricity was generated by applying an electric field across the printed layer, measured by an oscilloscope.[246] Copyright 2017, Elsevier. e) Fabrication of polyvinylidene fluoride (PVDF) fibers by direct-ink writing (DIW)-based printing onto a wavy copper surface as a piezoelectric sensor.[253] Copyright 2017, Springer Nature.

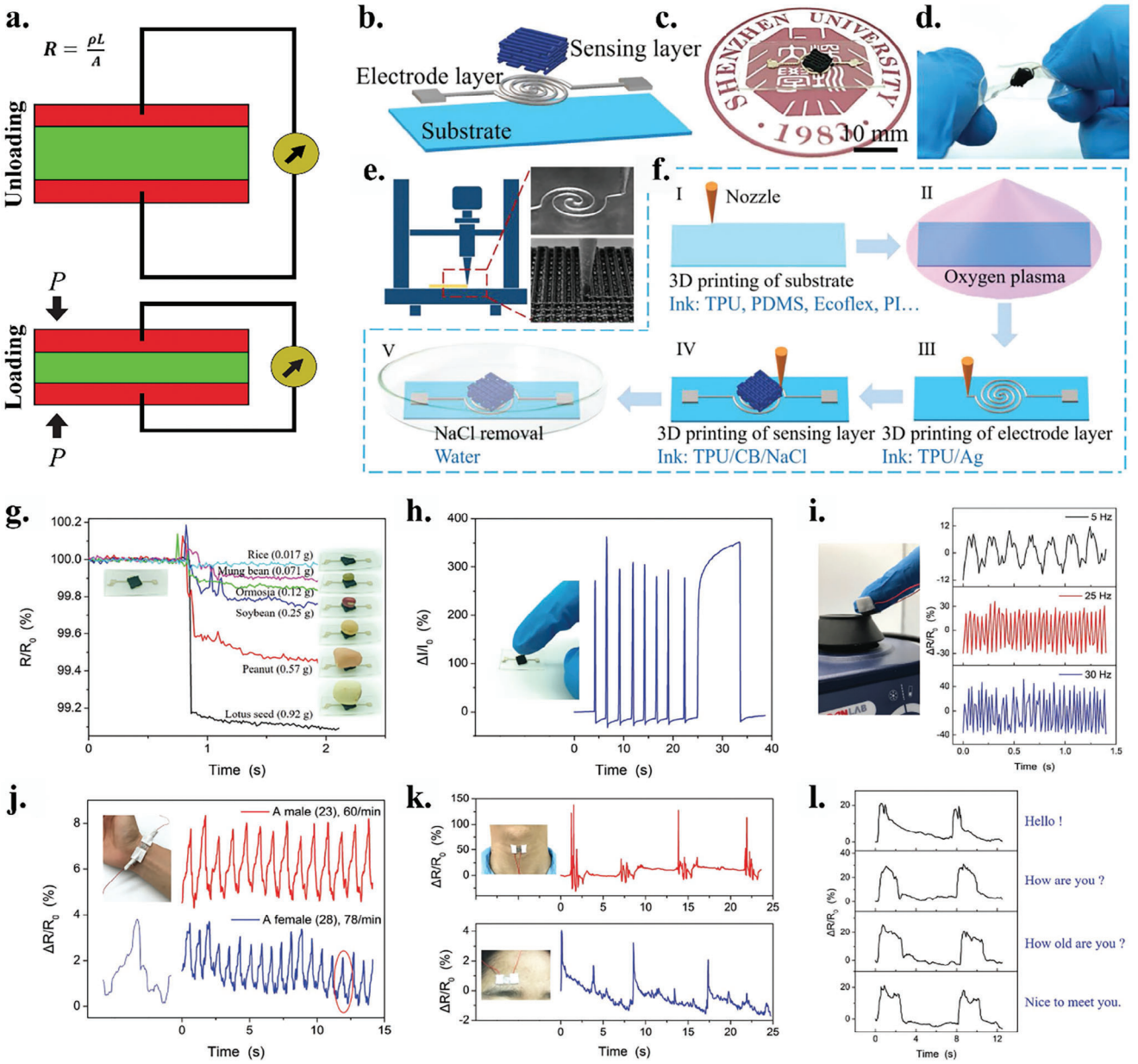

Figure 18. a) Schematic illustration of Piezoresistive sensing mechanism. b) Fabrication and demonstration of a stretchable Piezoresistive sensor (SPS) by 3D printing. c,d) Digital photograph of the SPS in its original and twisting state. e,f) Demonstration of direct-ink writing (DIW)-based printing of SPS. g–i) Applications of the 3D printed SPS as tactile biosensors. Different sensing modes include weighing grains (e.g., rice, bean, soybean, peanut, and lotus seed), tapping motion of the human finger, dynamic vibration of the machine, pulse monitoring, swallowing, and eye blinking.[264] Copyright 2019, Wiley-VCH.

metal nanoparticles as an upper sensitive layer. However, these composite materials often suffer from unsatisfactory or very low detection ranges because the pressure sensitivity is very low.[23,227,273–275] Therefore, the conventional piezoresistive sensors are unsuitable for multifunctional applications. To overcome this problem, developing novel nanomaterials with tunable sensitivity is required to produce highly conductive and stretchable sensors. Recently, gold (Au) and silver (Ag)-based nanowires have gained remarkable attention due to their superior conductivity and sensitivity.[276–278]

The piezoresistivity of conductive polymer nanocomposites differs from those of pure metals (e.g., silicone, CNTs, rGO) in such a way that nanocomposite materials increase their sensitivity for biosensing applications when combined with the pure metals. A study by Wang et al.,[264] demonstrated a low-cost and facile fabrication of a stretchable piezoresistive sensor (SPS) by DIW-based 3D printing. For this, the NaCl was premixed into a polyurethane (PU) matrix composing carbon black (CB) for achieving a hierarchically porous structure. The presence of CB in the PU matrix enhanced the sensitivity and the

sensor's measurement range, respectively. The assembled sensor comprises a basal elastomer substrate, an integrated electrode layer, and a highly precise and resilient piezoresistive sensory layer (Figure 18b-f). To test the device initially, lightweight substances, such as rice grain (0.017 g), mung bean (0.071 g), soybean (0.25 g), peanut (0.57 g), and lotus seed (0.92) were introduced (Figure 18g). Interestingly, the $\Delta R/R_0$ value was found to be significantly higher (>300%) when the device was exposed to repeated tapping through a human finger (Figure 18h). Similarly, the device was able to monitor the dynamic vibrational frequencies (5 Hz, 25 Hz, and 30 Hz) when patched onto the fingertip, as shown in Figure 18i). Moreover, the device efficiently monitored the physiological parameters, such as pulse response, swallowing, and blinking motions (Figure 18j-l). Thus, the CB-based 3D printed biosensors are excellent piezoresistive sensors with multifunctional applications.

In another study, a highly stretchable and piezoresistive skin patch was developed by parallelly aligned microtransistors.[266] The core of the transistor array is made up of intrinsically stretchable materials that act as semiconductive, dielectric, and conductive, respectively (**Figure 19**a,b). The fundamental principle of this array is simple and highly sensitive. Initially, a dextran-coated Si/SiO_2 wafer was prepared, and a stretchable dielectric material was spin-coated over the wafer surface, followed by photopatterning. Next, a semiconductive and conductive layer (CNTs) was deposited over the photo-patterned coating. Finally, a stretchable substrate (SEBS) is laminated, and gate electrodes are deposited to complete the array (Figure 19c). After completion, the array is photo-cross-linked and subjected to inkjet printing as an additive patterning process for stretchable film (Figure 19d). Incorporating tri-layer conductive material made the transistor array more flexible, stretchable, and highly conductive for monitoring the physiological conditions of human skin. A transistor array with 347 transistors cm^{-2} has an average charge-carrier mobility compared to amorphous silicon.

5.4. Triboelectric Sensors

Triboelectric sensors (TESs) and/or nanogenerators (TENGs) are the next generation and are self-powered electronic systems. TESs have gained remarkable attention for their superior ability to convert mechanical energy to electrical energy, based on a concept known as triboelectrification and electrostatic induction.[254,279–287] When two different triboelectric materials are rubbed with each other, the mechanical energy is transferred into electrical energy and stored on the material surface (**Figure 20**a). The polarities between the two materials profoundly affect the electrical energy generated on the material surface. During mechanical deformation, the two surfaces of the materials come in contact, and opposite charges are formed on the surface. The two surfaces separated automatically once the mechanical deformation was restored.[254,284] This type of sensor is often found in mechanical energy harvesters (Figure 20b).

Recently, 3D printing technology has mainly been exploited to produce triboelectric sources to fulfill the increasing demand for wireless biosensors,[279,284,288–290] implantable biomedical devices,[291–293] and IoT devices[286,294–297] with the hope of on-demand and point-of-care diagnostics. Figure 20c depicts an overview of 3D-printed triboelectric nanogenerators for multifaceted applications. However, the fabrication of 3D triboelectric sensors remains challenging because the 3D ink preparation for energy harvesters is unfavorable for conventional types. A 3D triboelectric nanoprinting technology could help eliminate the shortcomings of developing novel sensors-based energy generators. **Table 4** summarizes various 3D printed sensors (piezoelectric, piezoresistive, and triboelectric) and their fabrication procedure w.r.t. printing technology for skin bioelectronics.

6. Biomedical Applications

6.1. 3D-Printed Biosensors and Chips for Motion Sensing

Various types of 3D-printed wearable biosensors have been reported in the literature in the past few years. The 3D-printed microfluidic biosensors and chips gained enormous attention due to their ability to manipulate and analyze cellular physiology, biomolecules, and other organic molecules on a precision scale. Soft hydrogel-based printed electronics with self-adhesive properties have also emerged rapidly for human skin-based biosensing applications. These body/organ-on-chip models provide a better tissue/organ-mimicking platform for next-generation disease diagnosis.[315,316] The flexible biosensors have a wide range of applications in the biomedical sector, including blood glucose, cholesterol, pH, electrolytes, heartbeat, electrocardiogram/electroencephalogram (ECG/EEG), and even mobile catheters.[315] For example, a study conducted by Kim et al. reported the use of a printed wearable skin patch (**Figure 21**a) for in situ sweat biosensing.[317] For this, the printable electrode layer was fabricated using a sacrificial layer (Figure 21a(i)) composed of polyvinyl alcohol (PVA) and polydimethylsiloxane (PDMS). After that, the silver-based elastomeric ink was printed onto the surface of the sacrificial layer to fabricate the working and reference electrodes (Figure 21a(ii,iii)). The printed, electronic device was made in such a way that it can sense various electrolytes (e.g., Na^+, K^+, and Ca^{2+} ions). As a result, the fabricated device could sense selective electrolytes when integrated into the skin under static current stimulation (Figure 21a(iv–vii)). The reported sensitivity of the device for Na^+, K^+, and Ca^{2+} ions were 41.1, 37.5, and 31.7 mV dec^{-1} with a limit of the detection value of ≈100, ≈92, and ≈0.5 mM, respectively. In another study, a lightweight and conductive scaffold was prepared using sugar/silicon elastomer via powder bed fusion printing (Figure 21b(i,ii)) with CNT and rGO to enhance the sensing performance.[318] Adding SWCNT and rGO inside the polymer network enhanced the electrical conductivity and improved the flexibility and rigidity of wireless applications. The 3D-printed electrodes can easily be connected with a portable kit that can monitor the movement of the hand muscle (biceps brachii). The portable kit selectively monitors the electromyogram (EMG) when the hand is positioned upward or downward (Figure 21b(iii–v)). The authors also reported that the sugar/elastomer patch sensor efficiently measures brain wave patterns through EEG. The printed patch can be used as a head-mount or over-the-ear setup to monitor the EEG (Figure 21b(vi)). The sensor patch comprises two forehead electrodes (ground and positive electrode) and one earlobe electrode (ground electrode). The authors demonstrated that the dry EEG electrodes were efficient in detecting the brain wave patterns during non-rapid eye

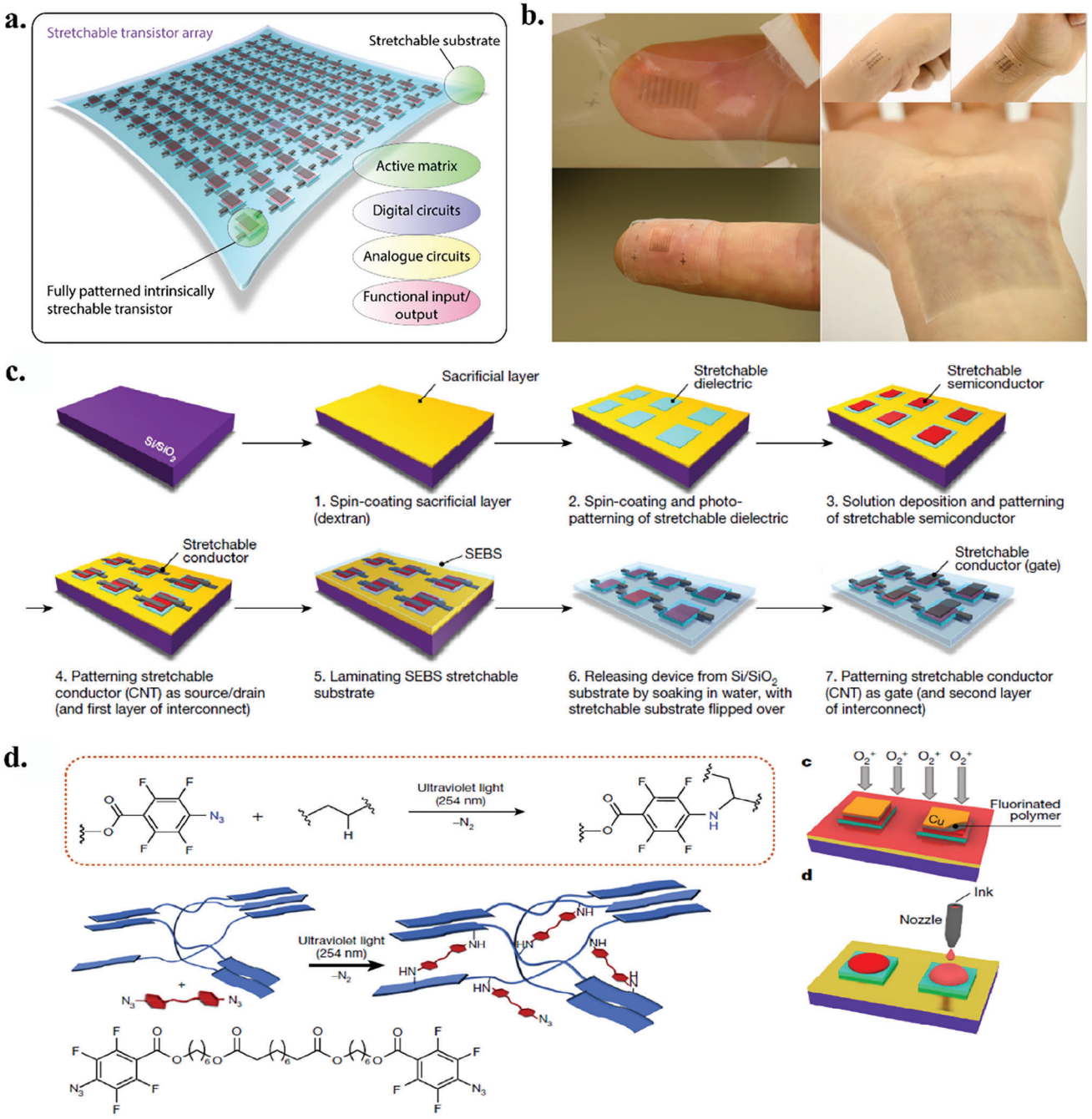

Figure 19. Design and fabrication of a piezoresistive stretchable transistor array as a core platform for functional skin electronics. a) 3D model of the intrinsically stretchable transistor array. b) An array of stretchable transistors for the fingertip (347 transistors cm^{-2}), straight wrist (6300 transistors cm^{-2}), and bending wrist (108 transistors cm^{-2}). c,d) The workflow for the fabrication of intrinsically stretchable transistor array and inkjet printing.[266] Copyright 2018, Springer Nature.

movement (non-REM or sleep phase), REM (paradoxical sleep), and resting phase (comfortable phase) (Figure 21b(vii)). Therefore, using a printed EEG device, the human brain physiology can easily be monitored wirelessly.

Apart from metal-based biosensors, 3D-printed conductive hydrogel composites are also emerging rapidly owing to their flexibility, excellent biocompatibility, and good adhesive properties.[319–321] Biological tissue exhibits moderate electrical conductivity due to mobile electrolytes inside the cells and the dissolved ions in the cell culture media.[32,33,322] The electrical conductivity of biological tissue usually ranges from 0.1 to 1 S m^{-1}; the phenomenon is illustrated in **Figure 22a**. Since culture media does not have free electrons, the electrical potential between cells mainly relies on the change of ion flux. Soft

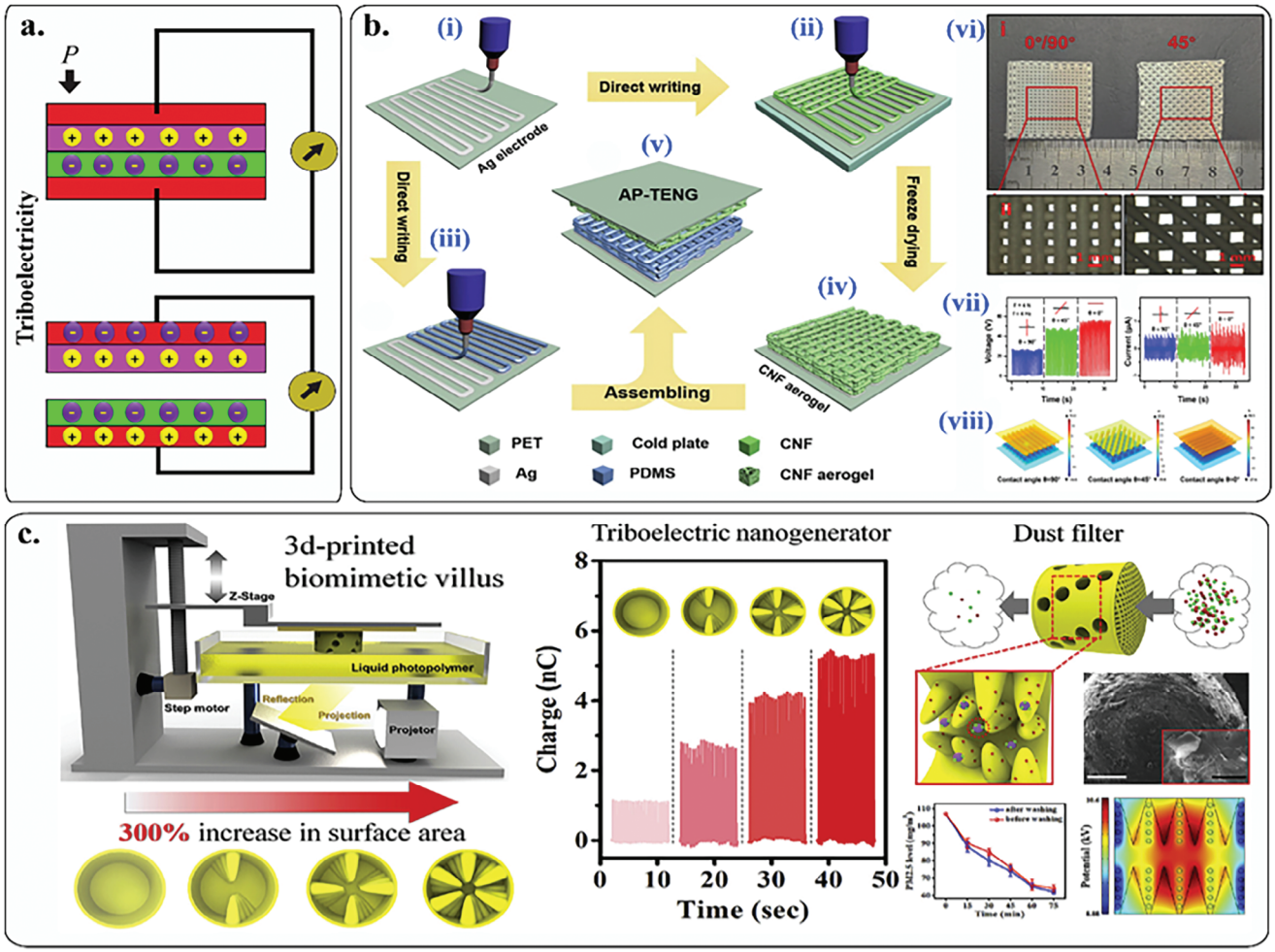

Figure 20. a) 3D printed triboelectric generator (TEG). b) Schematic illustration of the fabrication of all-printed TEGs (AP-TEGs) using cellulose nanofibrils (CNF) and Ag/PET composites (i-v); (vi) digital photograph of the 3D printed Ag/PET-CNF nanocomposites; (vii) Voltage-current output of the printed Ag/PET-CNF composites at different angle (90°, 45°, and 0°) loaded with a 4N pressure gauge at 4 Hz frequency; (viii) Corresponding CFD simulation model of voltage output of AP-TEGs of different angle.[287] Copyright 2019, Elsevier. c) Biomimetic-villus like DLP-based 3D printed nanogenerators (BV-TEG) by commercially available photopolymer-ABS resin and Ag paste.[286] Copyright 2019, Elsevier.

bioelectronics hydrogels bridge cell and culture media, commonly known as tissue-electrode interface (Figure 22b). For example, the transmembrane potential of a neuronal cell is generally negative and varies from −60 to 70 mV during the resting phase. An external electric field creates a transient oscillation of electrical potential across the neuronal cell membrane.[32] Next, the critical parameter is the distance between the hydrogel electrode and cells, which profoundly affects the physiological behavior of the neuronal cells. At a certain distance (<100 μm or even 100 nm scale), the electrode potential activates the free electrons in the culture media via interacting with various ions, maintaining the stable current flow between tissue and hydrogels. When neuronal cells are excited with a bioelectronics device/hydrogel, the cell membrane depolarizes and activates various types of ion channels (*e.g.*, voltage-gated Na^+ or K^+ channels) (Figure 22c). Two key phenomena are observed at the tissue-hydrogel interface: faradic charge injection and capacitive change injection, which primarily responds to the electrical impulse generation in tissue/cells (Figure 22d). The faradic charge injection involves surface-confined electrochemical reactions, whereas the capacitive charge injection relies on the printed hydrogel layer's simultaneous charge/discharge mechanism without any electrochemical reaction.[32]

Many biopolymers and their nanocomposites are used to fabricate printable electrodes for wearable biosensors. **Table 5** demonstrates various types of polymeric hydrogel inks for wearable biosensing applications. Xiong et al. reported a supramolecular hydrogel composed of acrylated β-cyclodextrin (β-CD), polyethylene glycol (PEG), and bile acid to achieve a rapid polymerizable pseudorotaxane (PR) hydrogel using DLP 3D printing with excellent electrical conductivity.[323] The as-fabricated hydrogel was reported to monitor human motion precisely during the running or resting phase (**Figure 23a**). The PR hydrogel was highly stretchable and had a gauge factor of 8.52 to 8.26 (≈400–500% strain range) after several use cycles. In another study, Pal et al. fabricated a 3D printable zirconia (Zr)-based metal-organic framework (MOF) ionogel for wearable sensor and colorimetric biosensing applications.[324] The printable ionogel comprised

Table 4. Various printing techniques are commonly employed to fabricate stretchable skin electronic sensors.

Sensing mechanism	Type of printing/ resolution	Printed component	References
Piezoelectric sensing	Custom-made printing (IR hydrodynamic spray)	Surface sensor	[298]
	Custom-made printing (ultrasound pressure)	Helical surface sensor	[299]
	3D stereo lithography (UV assessed)	Array sensor body	[300]
	FDM printing	Sensing layer	[301]
	Inkjet printing	Sensing layer	[247]
Piezoresistive sensing	FDM printing	Sensing layer, Sensor body	[302]
	Aerosol jet printing (200 µm)	Sensing layer	[303]
	DIW printing (10 µm)	Sensing layer	[304]
	FDM printing	Sensing layer, Sensor body	[305]
	Inkjet printing	Sensor electrode	[306]
	DIW printing (60 µm)	Sensing layer	[263]
	DIW printing (60 µm)	Whole sensor	[264]
	DIW printing	Sensing layer	[307]
	FDM printing (300 µm)	Sensing layer, Sensor body	[308]
	FDM printing	Sensing layer	[309]
	Inkjet printing (100-300 µm)	Sensor body	[310]
	Inkjet printing (50-0.25 µm)	Sensor electrode	[311]
	DIW printing (30 µm)	Sensing layer, Sensor body	[232]
	DIW printing	Sensing layer	[312]
	Inkjet printing	Sensing layer	[270]
Triboelectric sensing	Inkjet printing	Sensing frame	[285]
	DIW printing	Sensing frame	[287]
	DLP printing	Whole sensor	[286]
	3D stereolithography	Sensory electrode	[297]
	3D stereolithography	Sensing frame	[313]
	Inkjet maskless lithography	Whole body	[314]

Zr-MOF, cellulose nanocrystals (CNCs), and poly(acrylamide). The as-fabricated hydrogel displayed excellent mechanical stability even after applying 100% cyclic strain at different time points (Figure 23b). The tough hydrogel network was formed probably due to the strong interaction between CNCs and Zr-MOF with the polyacrylamide backbone, resulting in a flexible sensing patch. Furthermore, the ionogel was also reported to change the color from green to red with varying concertation of acids (0.001 to 1 M HCl). Thus, 3D-printed colorimetric hydrogels can be used as a smart skin patch for monitoring sweat pH and acidity. Similarly, Peng et al.,[325] demonstrated the use of a photocurable 3D-printed soft and porous sensor (PIFS) using DLP printing (Figure 23c). The as-fabricated hydrogel showed low hysteresis and relatively high sensitivity and exhibited excellent antifreezing properties. PEG-based hydrogel showed good viscoelasticity and provided sufficient mechanical stiffness (elongation at break: 419% and Young's modulus: 0.46 MPa) required for human skin. The temperature reversible sensing property is attractive to monitor the transient change in weather when integrated with human skin. The PIFS hydrogel was found highly sensitive when the finger movement occurred within a temperature ranging from −20 to 30°C. Therefore, temperature-responsive flexible biosensors can be used in clinics or hospitals for monitoring patient's body temperature in various conditions, such as hyperthermia or pyrexia.[326–328]

Microfabricated skin patches of CNT or graphene have long been explored in tissue engineering, especially for early disease diagnosis.[343–345] For instance, various physiological parameters, such as blood pressure, wrist pulse, heart rate, and respiratory syndromes, are vital for CNT-based biosensors.[346] The CNT-based sensors have dielectric and piezoelectric properties.[189,347] For example, Yi et al. recently developed a photocurable MWCNT-based microelectrodes using 3D printing for intelligent health monitoring.[189] A supporting ink layer was fabricated using Sylgard 184 and SE1700 onto a glass surface and cured. After that, an MWCNT/PDMS nanocomposite ink was extruded onto the supporting base platform to achieve a high-resolution printed microelectrode (Figure 23d). The electrical impedance spectroscopy (EIS) revealed that a concentration of 3% MWCNT/PDMS was highly conductive owing to the homogenous distribution of MWCNTs into the PDMS matrix, followed by a desirable rheological property (elastic modulus: 0.57–3.7 MPa of 3% CNT/PDMS composite). Moreover, the fabricated biosensor was found to have dielectric properties due to the presence of CNTs. The excellent conductivity of the MWCNT/PDMS chip was found to be ideal for monitoring the

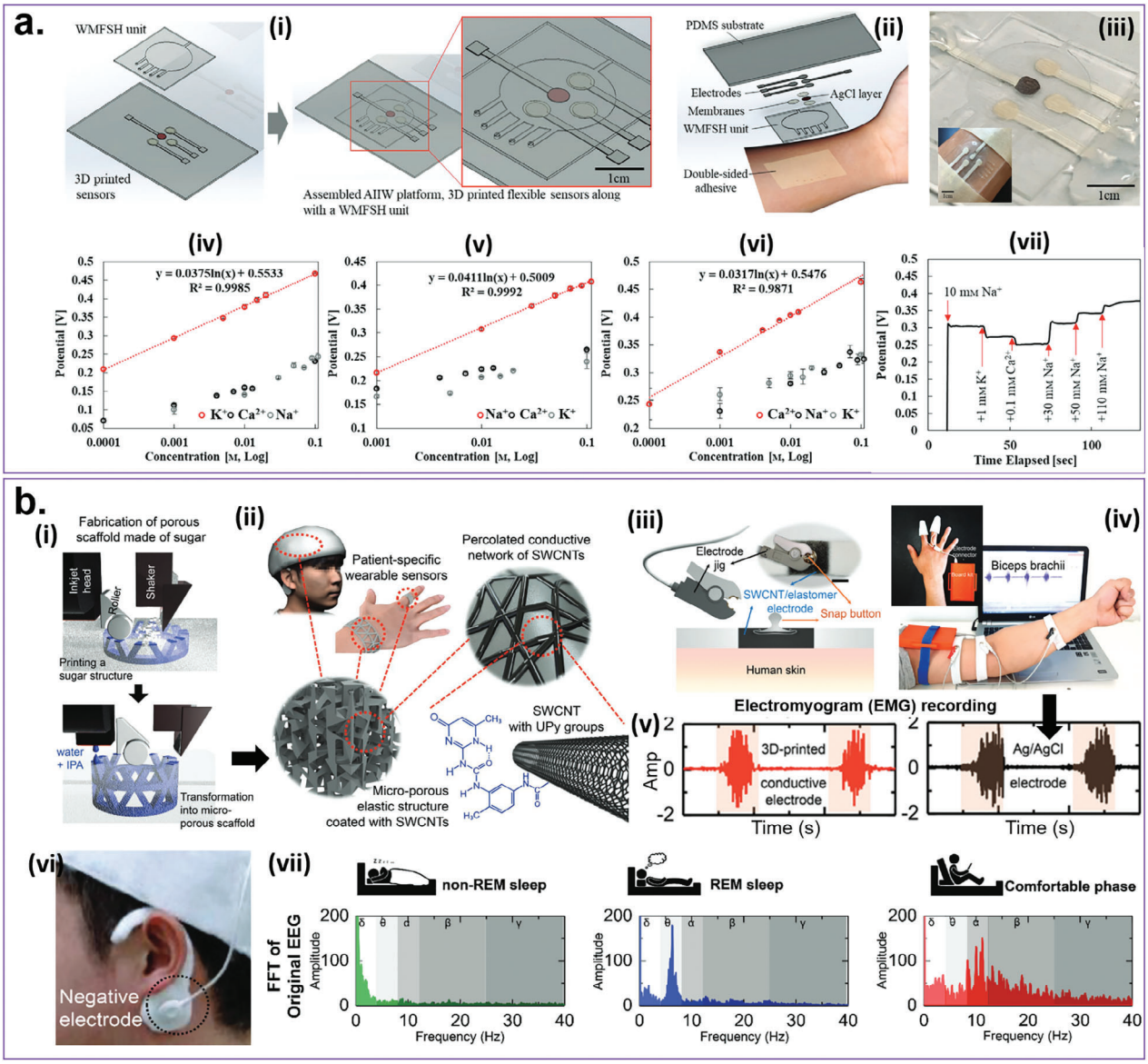

Figure 21. Examples of 3D printed conductive biosensors for wireless monitoring of human sweat and brain activity. a) Fabrication of silver-based printable biosensors for sweat electrolyte (Na^+, K^+, and Ca^{2+}) detection (i-iii). The sensing performance of the biosensor device and ion selectivity (iv-vi). Continuous off-body measurement and reproducibility (vii) of the Na^+ sensor.[317] Copyright 2021, Wiley-VCH. b) Fabrication of the sugar/elastomer/CNT/rGO nanocomposite ink for wearable biosensing (i,ii). Schematic diagram of the biosensing electrode and its possible mode of operation (iii). The continuous recording of electromyogram (EGM) using Ag/AgCl and fabricated electrode of human muscle movement (v). Demonstration of electroencephalography (EEG) using the "over-the-ear" sensing patch (vi) and its corresponding EEG results (vii).[318] Copyright 2019, Wiley-VCH.

human respiration rate (when attached to the belly) and voice (when attached to the throat), thereby conferring robust sensing ability. The use of conductive paper-based hydrogel patches is also fascinating nowadays for wireless biosensing owing to their lightweight and adhesive properties. For example, Li et al. recently developed a 3D printable conductive hydrogel-paper patch (**Figure 24**a(i–iii)) for chemical and electrophysiological biosensing applications.[329] The developed hydrogel-paper patch is made up of poly (3, 4-ethylenedioxythiophene) polystyrene sulfonate (PEDOT:PSS) hydrogel, which is self-assembled onto a paper surface (polyurethane/PtNPs thin film) via 3D printing (Figure 24a(iv)). The paper patch is also equipped with a portable battery system (3D printed circuit board) with an in-built Bluetooth device that can effectively sense and detect the body signals wirelessly (Figure 24a(v,vi)). The as-fabricated patch platform exhibited low impedance for glucose electrodes with high sensitivity (Figure 24a(vii–ix)). Moreover, the fabricated electrodes also displayed superior ECG recording ability with better precision than the commercial 12-lead ECG device, suggesting the printed hydrogel-paper patch's efficiency for health monitoring (Figure 24a(x–xii)).

Another study demonstrated versatile epifluidic skin electronics for multimodal health surveillance using semi-solid extrusion-based 3D printing.[348] The electronic chip comprises

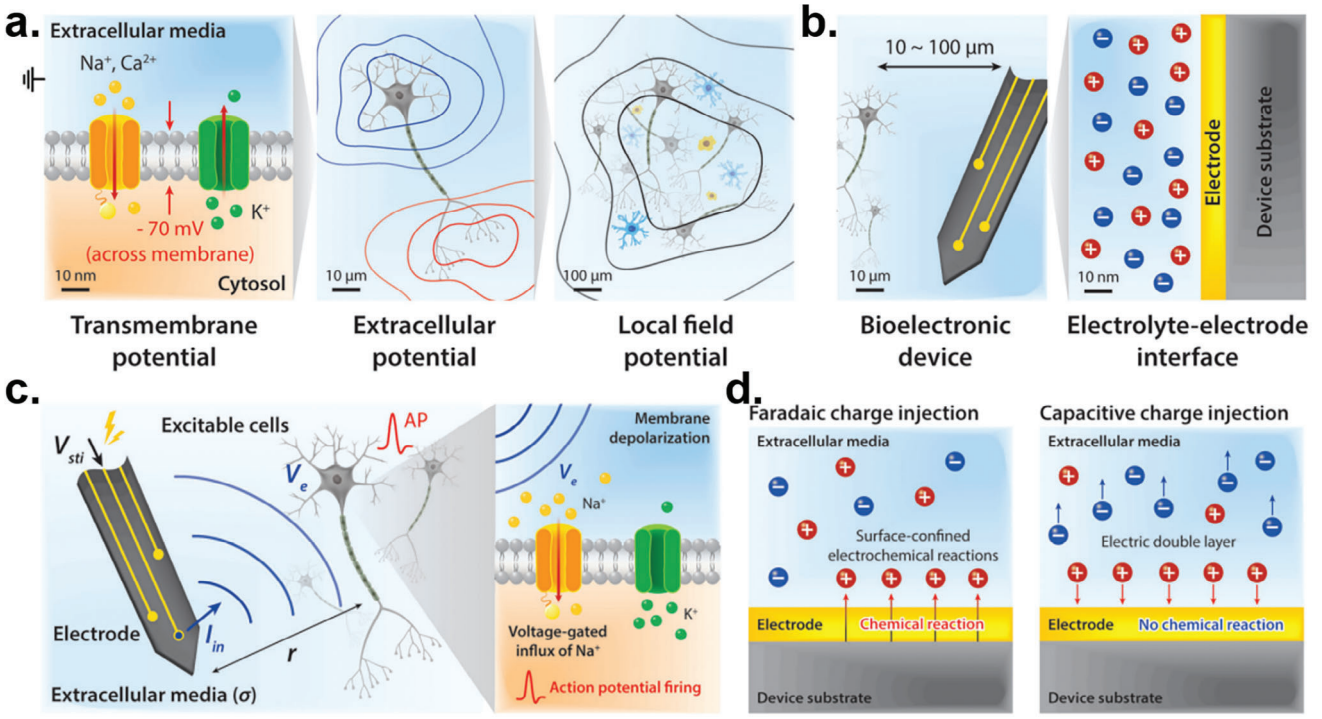

Figure 22. Illustration of the tissue-electrode interface and bioelectrical stimulation. a) The schematic diagram shows the transmembrane, extracellular, and local field potential. b) Schematic diagram showing the interaction between bioelectronics device and neuronal cell. c) The effect of electrical stimulation on neuronal cells. d) The faradic and capacitive charge injection mechanism during electrical stimulation. V_e; local field potential, V_{sti}; electrical potential of bioelectronics device, I_{in}; ionic current density at the source point (electrolyte-electrode interface), and AP; action potential of neuronal cells.[32] Copyright 2019, Royal Society of Chemistry.

four distinct layers: energy storage module, micro-supercapacitor module, biosensor module, and microfluidic module (Figure 24b(i)). The energy harvesting and micro-supercapacitor modules were fabricated using MXene-based inks for physical sensing (Figure 24b(ii)). In contrast, the biosensor module was printed using PEG/CNT nanocomposites for efficient and selective detection of various analytes, such as glucose, alcohol, and uric acid (Figure 24b(iii,iv)). The microfluidic module was printed using FD-H/MXene inks with an integrated electrode system to collect sweat from the human skin glands (Figure 24b(xiii)). The integrated device showed extreme sensitivity towards sweat pH when connected with a self-powered flexible solar device. The change in sweat volume is also reflected in the increased current density (Figure 23b(v–x)). Moreover, when the fabricated device was attached to the skin surface, it did not show any cytotoxicity to the skin cells, indicating the biocompatible nature of the hydrogel skin electronics (Figure 24b(xi,xii)). The extraordinary sensing ability of the integrated epifluidic device was due to the higher conductivity of the printed MXene hydrogel in the microfluidic module, which allows fast charge towards the detector (Figure 24b(xiv)).

Despite several advances in printable bioelectronics, the electrodes and microelectrode fabrication remain challenging due to the biomaterial inks' lack of versatile functionality.[35] Printable hydrogel electrodes must have flexibility, stretchability, and comfortability, with outstanding sensing ability, especially for electrophysiological applications. In particular, when it comes to wearing long, the hydrogel electrodes remain hydrated to maintain uniform conductivity.[349–351] Thus, printed microelectrodes must have excellent deformability and stretchability with excellent adhesive properties. Taken together, 3D printed/microfabricated electrodes and sensors have tremendous potential in biosensing, especially for human health and early disease diagnosis.

6.2. 3D-Printed Biosensors for Cancer Diagnosis

Cancer is one of the most fatal diseases of humanity, a second-leading cause of death worldwide. According to a World Health Organization (WHO) report, populations in the United States and China with cancer history during COVID-19 showed an elevated level of death (≈8.4%) than non-COVID-19 patients owing to the induction of malignancies during late 2020. Pathophysiological reports revealed an elevation of cancer biomarkers in the patient's blood samples at a higher rate than non-COVID-19 patients.[352] It has been reported that nearly 90% of cancer deaths are associated with tumor metastasis to other tissues/organs rather than the proliferation of the primary tumor.[353] The conventional diagnosis of cancer/cancer biomarker detection includes biopsies and immunogenic assays, which are expensive and time-consuming. In recent years, various nanomaterial-based platforms have been introduced, such as nanoparticle biosensors,[354] optoplasmic sensors,[355] electrochemical sensors,[356] nucleic acid sensors,[357] and many others. However, early detection of cancer biomarkers requires proper knowledge regarding the biology and prognosis of cancer, risk

Table 5. Examples of 3D printed biosensors and chips developed for human health monitoring.

Ink composition	Type of 3D printing	Applications	Reference
Poly (3, 4-ethylenedioxy thiophene) polystyrene sulfonate/polyurethane/PtNPs	Extrusion	Biomolecule and Electrophysiological sensing	[329]
MXene/styrene-based electrodes	Extrusion	Human heartbeat and pulse	[189]
Polyaniline-based hollow microneedle patch	Stereolithography	pH sensing in human skin interstitial fluid	[330]
MXene/Ecoflex/polyurethane-based smart gloves and fabrics	Extrusion	Human-machine interface	[331]
MOS_2/thiolated gelatin hydrogel	Extrusion	Human motion sensing (strain sensor)	[316]
CNT/PVB resin	Stereolithography	Real-time wound healing study	[140]
Calcium/polyacrylic acid/sodium alginate/CNT hydrogel	Extrusion	Human motion sensing (strain sensor)	[332]
2-acrylamido-2-methylpropane sulfonic acid/4-hydroxybutyl acrylate/graphene hydrogel	Extrusion	Wrist pulse and heartbeat	[333]
Ethyl-(2,4,6-trimethyl benzoyl) phenylphosphine/ polyethylene glycol dimethacrylate hydrogel	μ-stereolithography	Human motion sensing (strain sensor)	[334]
CNT/PDMS/agarose hydrogel	Hydrogel transfer printing	Human motion sensing (strain sensor)	[335]
Albumen hydrogel	Extrusion	Human motion sensing (strain sensor)	[336]
Acrylamide/*N*, *N*′-methyl bisacrylamide/LiCl hydrogel	In situ printing	Electrical impedance tomography (EIT) sensor	[337]
Poly (3, 4-ethylenedioxy thiophene) polystyrene sulfonate	Inkjet	ECG recording	[338]
N-isopropyl-acrylamide/laponite/CNT	Extrusion	Pressure sensing	[339]
Polyvinyl alcohol/borax/pectin/tannic acid hydrogel	Extrusion	Human motion sensing (strain sensor)	[340]
Ag/Polyaniline/CNT chip	μ-extrusion	Sweat pH biosensing	[341]
Poly (3, 4-ethylenedioxy thiophene) polystyrene sulfonate/polyvinyl alcohol hydrogel electrode	Direct ink writing (DIW) printing	Human motion sensing (strain sensor)	[342]

assessment, identifying tissue-specific markers, and developing accurate technology for rapid detection[358] (**Figure 25**). From the technological perspective, 3D printed micro/nano-devices play a crucial role in early biomarker detection, owing to the fast and rapid prototyping functionality.

A study conducted by Chiado et al. demonstrated using a 3D-printed microfluidic device to rapidly detect VEGF and angiopoietin-2 (Ang-2), common biomarkers found in the blood during tumor metastasis.[359] This work demonstrates the use of photocurable polymers, such as bisphenol-A-ethoxylate diacrylate (BEDA), 1,6-hexanediol diacrylate (HDDA), and poly (ethylene glycol) diacrylate (PEGDA) for the fabrication of biosensor (**Figure 26**a(i)). The device channels were immobilized with HRP-conjugated antibody, sensitive towards VEGF and Ang-2 binding (Figure 26a(ii,iii)). This work also showed how the angiogenic markers can be detected using a microfluidic device with a detection limit of 11 ng mL^{-1} (VEGF) and 0.8 ng mL^{-1} (Ang-2) for early cancer detection. In another study, an acoustic and 3D-printed electrochemical sensor was fabricated to detect S-layer proteins (rSbpA/ZZ) of liver carcinoma (HepG2) cells in real time.[360] For this, a 3D-printed gold working electrode was fabricated and modified with anti-rSbpA/ZZ antibody to capture the rSbpA/ZZ of HepG2 cells. Next, a microfluidic 3D printed structure was deposited onto the top of the electrode using an adhesive to ensure portability and flexibility (Figure 26b(i)). The electrochemical measurements showed an enhancement of frequency shift with varying times during successful anti-CD133/rSbpA/ZZ/Au binding at 37 °C. Moreover, the peak current was gradually decreased (50 → 10 μA) after addition of HepG2 cells in the Au-sensor, suggesting the binding of the HepG2 cells with the target antibody (Figure 26b(ii,iii)). This work demonstrates how the 3D printed electrochemical device can be used for the early diagnosis of liver carcinomas.

DNA methylation plays a crucial role in cancer progression and is a potential clinical research target. DNA hydroxymethylation (5hmC) is a type of epigenetic change in cancer cells, a new diagnostic target of cancer epigenetics research.[361] Bhat et al.,[362] recently developed an innovative and label-free detection of 5hmC in cancer cells using nozzle-jet printed Au@MXene-based electrochemical sensors. For this, the Au/MXene nanocomposite ink was deposited onto an Ag-printed matrix on a polyethylene terephthalate (PET) substrate (**Figure 27**a(i-iv)). The as-fabricated platform exhibited superior sensing ability towards 5hmC than 5mC, characterized by the increased current flow (≈1.8 times stronger in 5hmC than 5mC). Owing to the abundant hydroxyl groups on the surface of 5hmC,

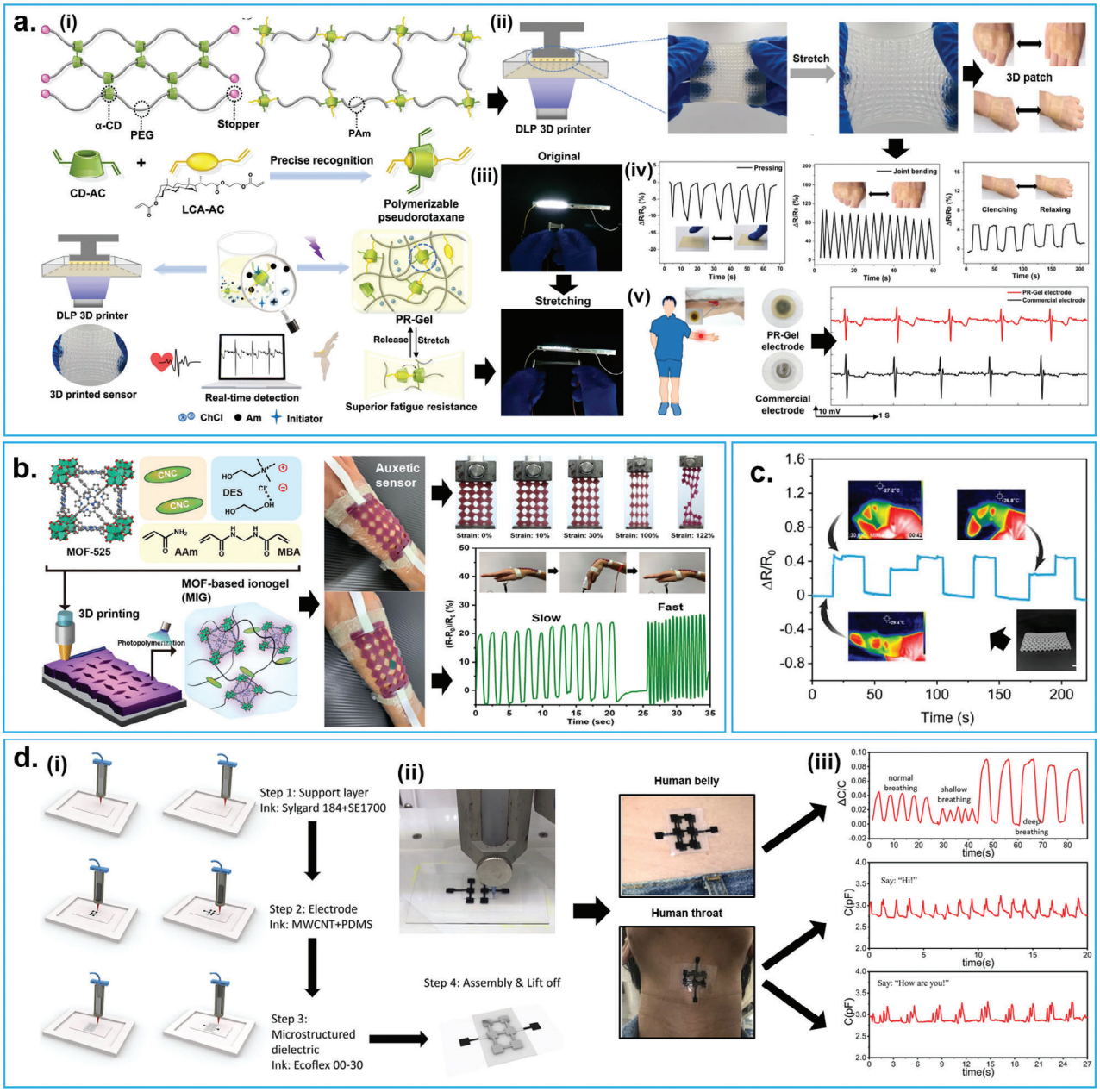

Figure 23. 3D printed conductive hydrogels for human motion sensing. a) Illustration of the supramolecular hydrogel for real-time human motion sensing. i) Schematic diagram of the printable resin preparation and DLP printing. ii) Digital photographs of the DLP-printed highly stretchable PR hydrogel. iii) Conductivity test of the hydrogel before and after stretching. iv) Test of human finger movement in terms of relative resistance during pressing, joint bending, and wrist moving. v) Real-time detection of human ECG using 40% (*w/v*) PR hydrogel electrode. ChCl; chlorine chloride, Am; acrylamide, PAm; polyacrylamide, α-CD; α-cyclodextrin, CD-AC; cyclodextrin acrylamide, and LCA-AC, ethylene glycol lithocholate acrylate.[323] Copyright 2023, Springer Nature. b) Schematic illustration of the nanocellulose/metal-organic framework (CNCs/MOF)-based ionogel preparation and its application in colorimetric biosensing.[324] Copyright 2022, American Chemical Society. c) Fabrication of a DLP 3D printed PEGDA-based flexible sensor for skin temperature detection.[325] Copyright 2022, Elsevier. d) 3D printed tactile biosensor for human health monitoring. i) Schematic diagram showing the fabrication procedure of the tactile sensor. ii) Digital photograph of the biosensor. iii) Non-contact measurement of human breathing pattern (belly) and acoustic sound measurement (throat) showing the excellent sensing ability of the biosensor.[189] Copyright 2022, Wiley-VCH.

it showed less adsorption in Au and increased the charge-transfer efficiency, resulting in higher electrocatalytic activity of MXene (Figure 27a(v)). Thus, the current response was reported higher in the presence of Au/MXene/5hmC with a detection limit of 0.632 pM (Figure 27a(vi-vii)). Therefore, it is evident that nucleic acid-based 3D printed biosensors can be used to rapidly detect cancer cells in a mixed cell population with high sensitivity and label-free manner. Similarly, cancer-derived mRNA or extracellular vesicles (EVs) can also be detected using a microfluidic 3D system. For example, Lim et al. developed a hybrid

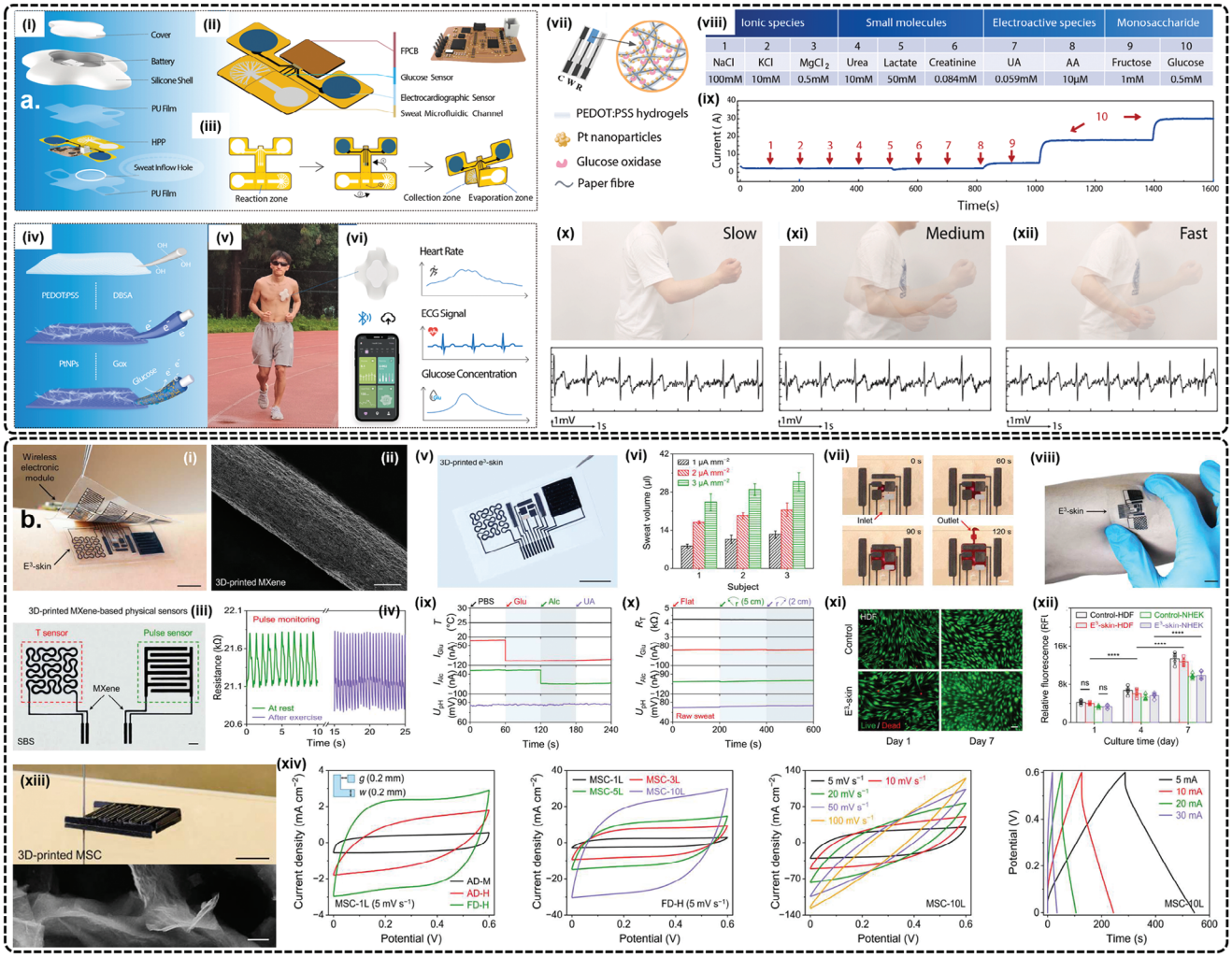

Figure 24. a) 3D printed hydrogel-paper patch platform for intelligent health monitoring. i-iii) Schematic diagram of the chip elements and fabrication process. iv) Illustration of the paper patch fabrication process and principle. v-vii) Schematic diagram showing the real-time electrocardiography (ECG) and glucose biosensing through a smartphone device. viii, ix) In vitro evaluation of the various ions (Na^+, K^+, and Mg^{2+}), small molecules (urea, lactate, and creatinine), electroactive chemicals (uric acid and amino acid), and monosaccharide (fructose and glucose) detection using the smart hydrogel-paper patch. x-xii) Real-time ECG recording (1 mV s^{-1} rate) of the human body during slow, medium, and fast walking. The paper patch was directly attached to the chest and monitored through a smartphone.[329] Copyright 2022, Elsevier. b) Fabrication and evaluation of a 3D printed epifluidic skin patch (E^3-skin) for advanced health surveillance and machine learning-based smart detection. i) Digital image of the integrated E^3-skin device. Scale bar: 1 cm. ii) SEM image of the 3D-printed MXene strand showing the unique aligned geometry. iii) Digital image of the 3D-printed MXene-based temperature and pulse sensor. iv) Real-time sensing of human pulse using the printed device. v-x) Demonstration of the 3D printed microfluidic E^3-skin patch for monitoring human sweat. xi, xii) Representative in vitro biocompatibility test of the E^3 patch using HDF cells with corresponding fluorescence intensity. Scale bar: 100 μm and 1 cm. xiii) Photographs of 3D printing of MXene-based inks with corresponding SEM images. Scale bar: 1 μm. xiv) Cyclic voltammetry test of 3D printed MXene inks with varying layers (L).[348] Copyright 2023, The American Association for the Advancement of Science.

microfluidic-3D printed nanostructured hydrogel (ExoNA chip) platform (Figure 27b(i)) for selective detection of breast cancer-derived HER2-positive exosomes using 100 μL sample volume (limit of detection: 58.3 fM).[363] PEG hydrogel was used to capture the HER2-positive exosomes inside a microfluidic device. The as-fabricated hydrogel was used to tag the probes that selectively detect the HER2 exosomes. Upon capture, the probe enters the exosome and is bound to the exosomal mRNA, which can be observed by analyzing the fluorescence signals generated by the probe. Furthermore, the authors also reported that the ExoNA chip can be used for analyzing liquid biopsy samples (150 times higher in tumor tissue than blood) obtained from in vivo tissues, demonstrating next-generation smart nanoplatforms for early tumor diagnosis (Figure 27b(ii-iv)). Thus, integrating smart hydrogel scaffolds with 3D-printed microfluidic devices, tumor-derived nucleic acids, mRNAs, or exosomes can be precisely detected in vitro and in vivo.

Methacrylated circulating DNAs (ct-DNAs) are a promising nucleic acid-based biomarker exhibiting cancer-cell-specific genetic and epigenetic information, which can be used for early cancer detection. DNA methylation is a hallmark of early carcinogenesis and is primarily detected in patients with abnormal diet,

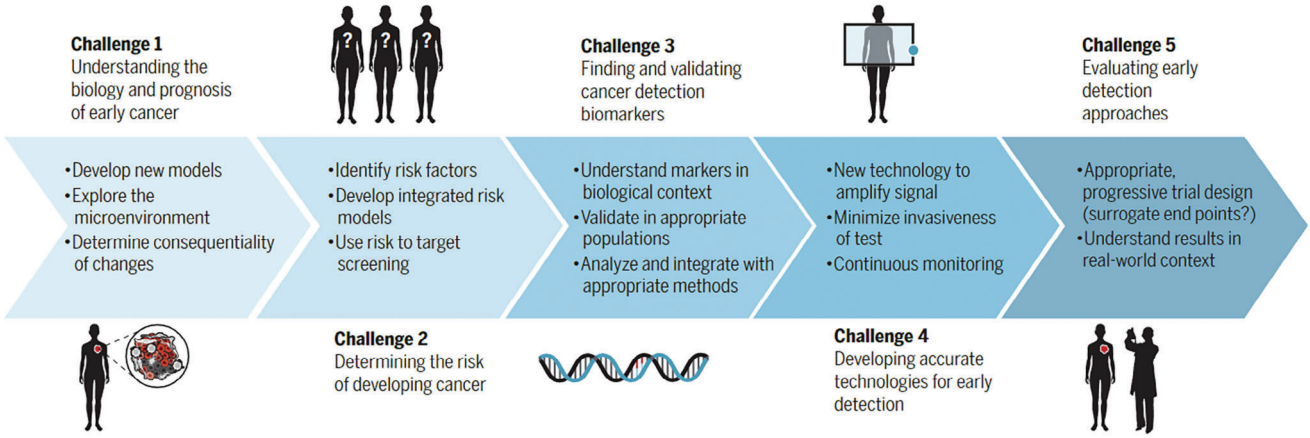

Figure 25. Present status and challenges of cancer biomarkers detection for precision oncology.[358] Copyright 2022, The American Association for the Advancement of Science.

high smoking, and alcohol consumption.[364,365] Various types of biosensors and chips, such as electrochemical sensors,[366] droplet PCR,[367] colorimetric sensors,[368] and next-generation sequencing-based techniques[369] have been developed in the past few years for precise diagnosis of ct-DNAs. In this context, 3D-printed soft hydrogel bioelectronics with rapid and accurate detection of ct-DNAs from skin exudate is highly required for personalized cancer diagnosis. For example, Fang et al. developed a self-healing, skin-attachable field effect transistor (FET)-based hydrogel bioelectronics for identification and dynamic visualization of ct-DNAs in vivo (Figure 27c).

7. Conclusions and Perspectives

7.1. Conclusions

This review systemically introduced the present status and use of various 3D printable wearable bioelectronics for biomedical applications. First, we introduced the use of various naturally-derived conductive biopolymers (e.g., cellulose, chitosan, alginate, gelatin, silk fibroin, and glycoproteins) and their potential for soft bioelectronics fabrication. Cellulose and Chitosan with intrinsic conductivity originated owing to their unique molecular

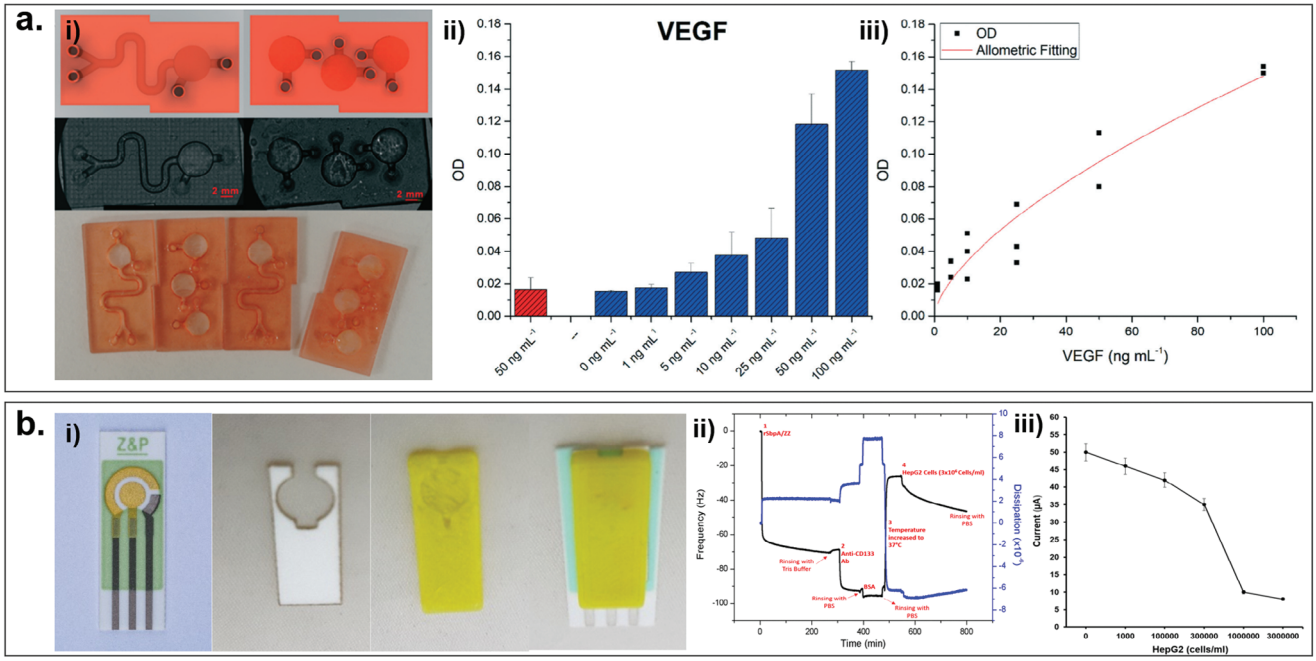

Figure 26. a) Demonstration of a 3D printed microfluidic device for rapid detection of VEGF and Ang-2 from the blood. Digital photographs of the printed device (i) showing the detection properties of the VEGF under physiological conditions (ii, iii).[359] Copyright 2020, Royal Society of Chemistry. b) Demonstration of a gold electrode-based electrochemical sensor for early detection of HepG2 biomarkers. i) Digital photographs of the gold electrode (left), adhesive sticker (middle), and printed microfluidic component (right) of the device; ii) change in frequency over time in the presence of anti-CD133/rSbpA/ZZ/Au, and iii) the relative current change after addition of HepG2 cells showing the excellent sensing ability.[360] Copyright 2017, Elsevier.

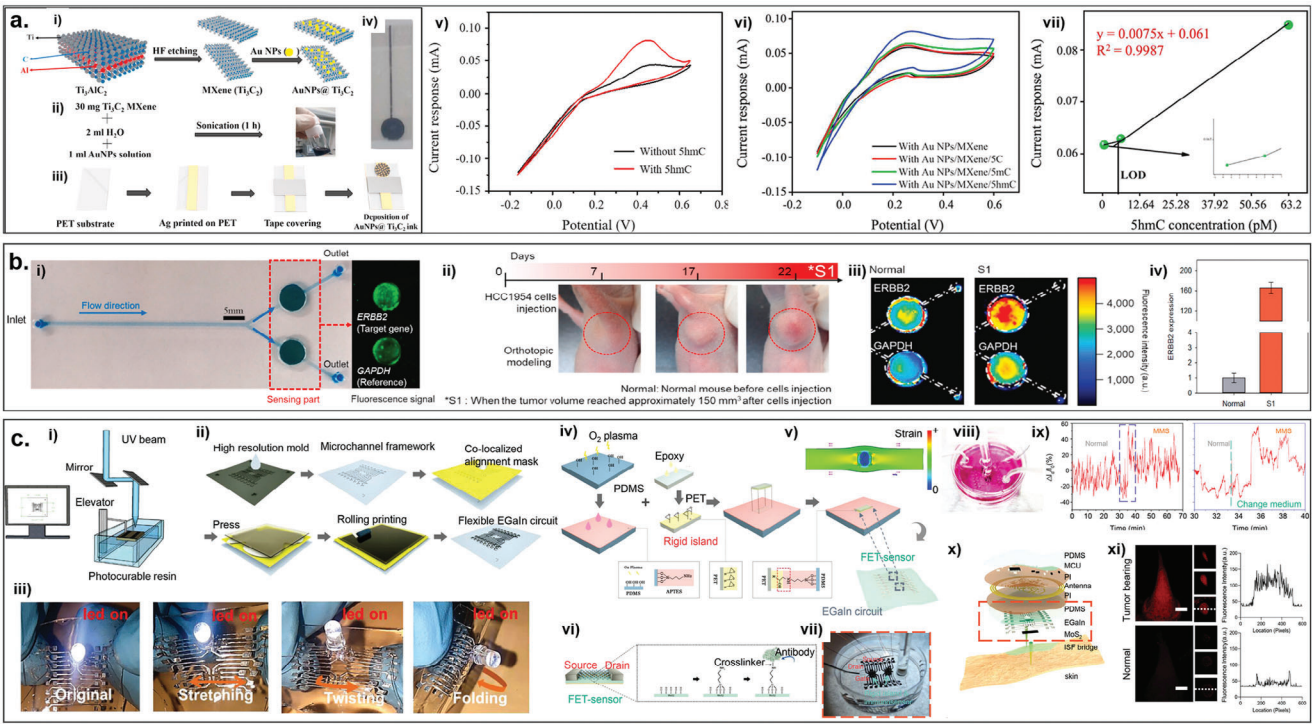

Figure 27. Demonstration of 3D micro/nano hybrid platforms for detecting nucleic acids and exosomes from tumor tissues. a) Illustration of an Au/MXene hydrogel-based 3D printed microfluidic platform for electrochemical detection of 5hmC (i-iv). The relative change in current density after adding 5hmC and the device's detection limit (v-vii). 5mC was taken as the positive control.[362] Copyright 2022, Elsevier. b) Demonstration of the working principle of the ExoNA chip. Digital and fluorescence images of the device (i) and the captured exosome (HER2 positive). GAPDH was taken as the control gene. In vivo sensing potential of the ExoNA chip showing the excellent sensing ability of the liquid biopsy samples (ii-iv). HCC1954 (HER2 positive) breast cancer cells were used for the in vivo experiments.[363] Copyright 2022, Elsevier. c) Schematic illustration of the self-healing and sensing circuit fabrication via micro-stereolithography (i-iii). Schematic diagram for the hybridization process of FET-based sensing platform for detecting ctDNA (iv-vii). In vitro (viii, ix) and in vivo (x, xi) DNA methylation biosensing using the fabricated immunosensor. Copyright 2022, Wiley-VCH.

architecture and self-assembled structure, offering the most suitable and biocompatible biopolymer for bioelectronics fabrication. Besides, the protein-based biopolymers with naturally occurring RGD (arginine, glycine, and aspartic acid) adhesive domain also ensure high adhesive and mechanical Then, we discussed the use of conventional chemically-derived biopolymers (e.g., polyaniline, polypyrrole, and PEDOT:PSS), frequently used for the fabrication of various sensory elements, such as electrodes, chips, and coils. Next, we discussed the necessity of 3D printing technology for stretchable and conductive hydrogel electronics with detailed information regarding the use of 3D printers, hydrogel design strategies, and choice of suitable conductive nanomaterials, which can significantly affect the stretchability, durability, conductivity, sensing ability, and biocompatibility towards "E-skin" patch development. Such a multi-material hydrogel could be easily used for the fabrication of tactile sensors, piezoelectric sensors, piezoresistive sensors, triboelectric sensors, and microfluidic chips for multi-faceted applications, such as motion sensing (e.g., finger, wrist, eye, leg, and many others), ECG/EGG monitoring, body temperature, pH, glucose, lactate, and even for cancer biomarkers detection. Therefore, a conventional printable hydrogel may differ from an advanced conductive hydrogel in three different ways: 1) choosing suitable combination of biopolymers to improve printability and stability (e.g., choosing a combination of natural and chemically-derived conductive biopolymers), 2) identifying proper nanomaterials/nanofillers for improving conductivity and biocompatibility (e.g., GO, CNTs, MXene, metal nanoparticles, and many others), and 3) the material post-processing (e.g., cross-linking strategy, cyclic performance, device accuracy, clinical applicability). Finally, we demonstrated the application of various 3D printable conductive biopolymers and their nanocomposites for precision medicine, focusing on wearable biosensing and cancer diagnosis. We discussed the current status and advancements in 3D-printed hydrogel bioelectronics in the present study; however, there is still room for future improvements before delivering those technologies to clinics. The key future research and development (R&D) must focus on enhancing biodegradation, physico-chemical properties, scalability, materials chemistry, multi-modal strategy, and artificial intelligence (AI)-based strategies for precisely monitoring human health via deep learning and computing. The future of wearable bioelectronics with innovative healthcare monitoring systems is schematically represented in **Figure** 28a.

7.2. Perspectives

With the advent of ground-breaking additive manufacturing technology, the thrust for wearable bioelectronics has been increasing rapidly, and extensive research is required to make it

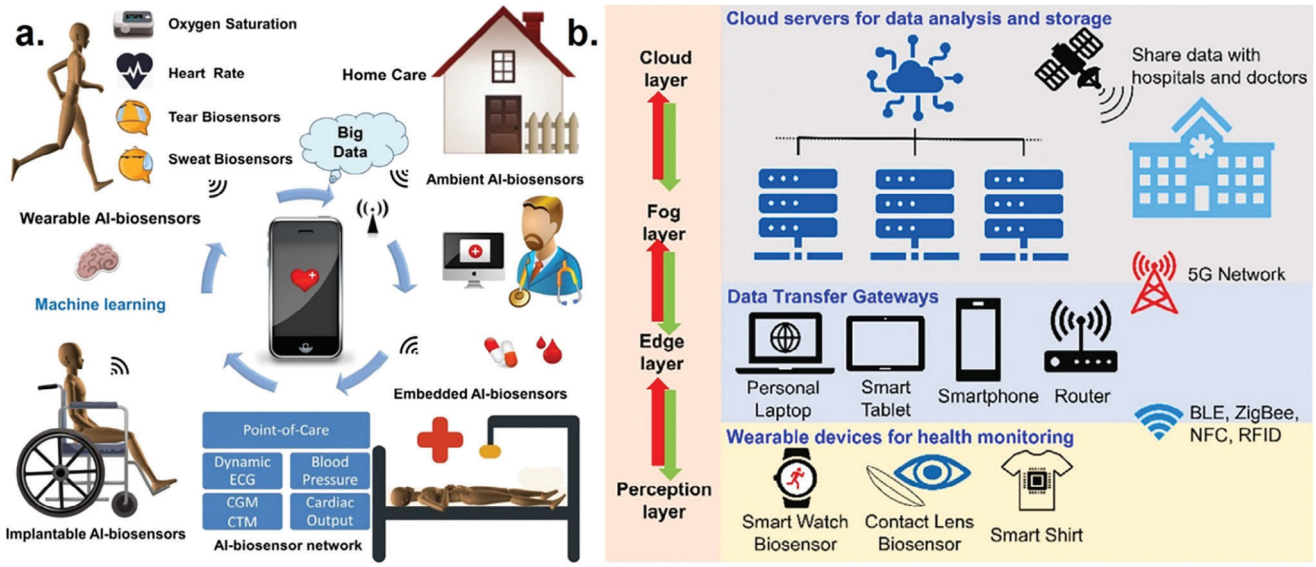

Figure 28. a) Schematic illustration of the AI-based smart bioelectronics for precision medicine.[370] Copyright 2020, Elsevier. b) Cloud computing as a smart future technology for wearable bioelectronics.[371] Copyright 2023, Elsevier.

available in the commercial market. The necessity of multiple stimuli-responsive bioelectronic devices has always been of great importance in the medical community. Despite many advances in wearable hydrogel electronics, commercial application is still hindered owing to the limitation in scalable manufacturing of those sensing devices, making it ideal for early research but not for clinical application. To address this shortcoming, a few things must be clarified before successful commercialization. The specific problem statements and their troubleshooting for future bioelectronics development are discussed below:

7.2.1. Enhancement of Physicochemical Properties

Scalability: Large-scale industrial manufacturing of printed electrodes and bioelectronics is crucial for expanding the healthcare market. As discussed earlier, most FDA-approved bioelectronic devices are not 3D printed and only rely on metal/alloy electrodes, which are not available to attach to the skin surface. Besides, conductive metal-based hydrogels use various metal ions (e.g., Al, Au, AG, Zn, and many others), which are highly conductive but display high manufacturing costs. Similarly, the CNT-based nanocomposites are also expensive, and fabrication of CNT-based biosensors and chips will come with high price tags, which is practically inappropriate for commercialization. To accelerate the manufacturing process with cost margin, future research must focus on developing novel nano/bio-fabricated hydrogels in combination with natural and chemical biopolymers with good conductivity and sensing ability to surpass this challenge.

Controllable Biodegradation: Controlled biodegradation is another supreme factor for the eco-friendly management of printed bioelectronics. Most printed bioelectronics are attached to the skin surface to monitor the body's physiology. Therefore, the attached skin electronic device can be easily peeled off after successful application or recovery without harming the skin tissue. However, the bioelectronic devices implanted inside the body (e.g., organ-specific electronic chips and devices) must be removed after certain time points or may be able to self-degrade in the presence of body fluids. Most durable and tough 3D-printed bioelectronics are developed through one- or two-step cross-linking techniques, which are sometimes non-biodegradable when implanted inside the living system. Thus, precise monitoring of the implanted devices' degradation ability and good sensing properties must be considered before successful clinical trials.

Choice of Adhesive Biomaterials, Durability, and Shelf-Life: A hydrogel patch with excellent adhesive properties is highly desirable for skin or tissue bioelectronics. Soft Adhesive hydrogels help adhere to the skin surface and behave like a flexible conductor. The ultimate adhesive strength and flexibility of any biomaterial-based hydrogel are directly connected to the mechanical strength and durability of the bioelectronics. Although several researches have been shown to improve bioelectronics' mechanical and adhesive properties, a few reports explain the durability and longevity as one of the critical drawbacks for clinical applications. The key challenge is that when the hydrogel patch is attached to the skin surface, it dehydrates due to exposure to the open environment and atmospheric moisture. This results in degradation, dryness, loss of adhesive and mechanical properties with decreased conductivity and sensing ability. Therefore, future research must focus on developing hydrogel bioelectronics with protective shielding features to enhance performance. Researchers must test their sensing device in various climatic conditions to cope with extreme environments (e.g., high temperature, pressure, or high altitude). Taken together, these shortcomings must be taken into consideration before successful commercialization.

Molecular and Chemical Design: Hydrogel inks with tunable surfaces and molecular functionalities for improving electrical

conductivity, mechanical and biological properties are highly desirable for developing next-generation soft wearables. In particular, rational design in naturally derived conductive biopolymers should be considered rather than chemically derived complex biopolymers. Future research must focus on developing a new and optimized strategy for chemical modification of biopolymers, such as introducing various surface functional groups or incorporating various adhesive protein molecules and studying their physico-chemical properties before and after 3D printing for long-term stability, which is especially required for commercialization.

Bioinspired Strategy: Biomimicry is a process used in additive manufacturing, where biologically-inspired structures and designs are used to fabricate various sensors and actuators.[372,373] For example, mimicking the anisotropic collagen matrix of human skin could be used in 3D printing to fabricate aligned hydrogel scaffolds, enabling uniform electrical conductivity when adhering to the skin surface. Thus, engineers must mimic various tissues (e.g., bone, skin, nerve, and many others) and understand their structure to develop next-generation wearables.

7.2.2. Advanced Strategies for Therapeutic Advancement

Novel Ink Development: As discussed earlier, the hydrogel properties, such as conductivity, adhesiveness, stretchability, mechanical stiffness, and biocompatibility, are profoundly affected by the nature and type of conductive nanofillers in the hydrogel ink. The choice of proper Thus, understanding the material chemistry (e.g., material property, source, fabrication process, functionalization, post-processing) and proper choice of nano/biomaterials is an important key for developing high-shape fidelity printable inks with all-functional physicochemical properties (e.g., bioadhesion, anti-freezing, fatigue tolerance, and non-dehydrating) for wearable bioelectronics.

Multi-Stimuli-Assisted 3D Printing: Multiple stimuli-assisted biofabrication is a fascinating technology used in tissue engineering to fabricate various nanostructured scaffolds and implants.[374] Multi-stimuli-assisted 3D printing is the application of various physical stimulations (e.g., magnetic fields, electric fields, photoacoustic, ultrasound, temperature, and pulsatile pressure) during or after 3D printing of a test hydrogel. Using magnetic and conductive nanofillers during 3D printing would benefit magnetic or electric field-assisted 3D printing, enabling the spatial alignment of the nanofillers during filament extrusion. Surprisingly, robotically coupled six-axis dynamic 3D printing is fascinating for developing wearable electronic chips and devices with complex designs. Thus, integrating various physical stimuli, future research must focus on fabricating intelligent and 3D printable hydrogel inks for wearable bioelectronics.

Multimodal Therapy Using Bioelectronics: Most of the conductive Nanomaterials display multiple stimuli-responsiveness. For example, GO, rGO, and functionalized CNTs exhibited good near-infra-red (NIR) responsive properties upon stimulation with laser light (e.g., 808 nm or 1064 nm). Similarly, carbon dots exhibited superior excitation-dependent fluorescence emission properties, which could be used to fabricate glowing hydrogels for biosensing applications. Magnetic nanoparticles (paramagnetic SPIONs and ferromagnetic MNPs) exhibit magnetic and photoacoustic (PA) stimuli-responsive properties. MXene is a novel carbon material class that displays NIR and piezoelectric properties. Therefore, by combining one or more stimuli, the developed nanocomposite hydrogels can release various bioactive molecules (*e.g.*, protein, growth factors, drugs, and many others) through bioelectronics devices.

7.2.3. Artificial Intelligence (AI) and Machine Learning

With modern computing technology and machine learning algorithms, tissue engineering and regenerative medicine have considerably changed. The intelligent management and processing of electronic data with advanced AI-based biosensors enabled rapid interpretation and diagnosis of several diseases. The AI-based technology is mainly divided into three subcategories: 1) information collection in the form of sound, imaging, or any other stimuli, 2) external signal conversion into an electronic signal, and 3) data processing, interpretation based on a predesigned algorithm and cloud storage. Conventional 3D printing technology mainly relies on hydrogel printing and mathematical calculation of 3D printing performances, which is practically unreliable and time-consuming. Besides, the AI-based innovative system can detect and diagnose the 3D printing process precisely with the help of a multi-axis camera module equipped with computers. Recently, a variety of machine learning tools, such as Principle Component Analysis (PCA), Multiple Regression Test (MRT), Support Vector Machines (SVMs), and Artificial Neural Networks (ANN) are frequently programmed with AI-enabled biosensors for precise decision-making for medical doctors to formulate medication to the patients. An author should study the cited literature for more details regarding the AI and machine learning of biosensors.[370,375] Another essential tool highly required in healthcare and medicine is the use of cloud computing. Most bioelectronics devices accumulate bid data, including multiple medical images, streaming, and raw values; manual interpretation of those data is impossible. To address this issue, cloud computing and storing big data generated from the wearable device is highly desirable (Figure 28b). Nevertheless, many more challenges in developing 3D-printed wearable electronics must be clarified before clinical application. Looking forward, we hope that the fabrication of smart bioelectronic devices, reducing all the challenges mentioned above, will revolutionize medical nano-biotechnology.

Exploring Advanced Human–Machine Interfaces: The invention of the human–machine interface system (HMIS) has revolutionized various cutting-edge technologies in biomedical fields, especially in artificial organ development, such as bionic hands, prosthetics, and neural interfaces, enabling scientists and clinicians to understand the interaction between machines and the human body. In order to optimize operational efficiency, power consumption, and multitasking capabilities, it is essential to miniaturize the human-interactive device and streamline its architectural design. Nevertheless, current human-interactive technologies include a range of sensors that are physically linked to microprocessors. These sensors facilitate the transmission of information collected from the environment (input) to displays for user perception. Soft electroactive and biocompatible hydrogels can bridge electronic signal generation and the human body

surface in this context. Therefore, future research must focus on developing novel bioactive hydrogels that can be used as a sensory layer for the human body's stimulus recognition towards precision medicine.

Acknowledgements

This study was supported by the "Basic Science Research Program" through the "National Research Foundation of Korea" funded by the "Ministry of Education" (NRF-2018R1A16A1A03025582, NRF-2019R1D1A3A03103828, and NRF2022R1I1A3063302).

Conflict of Interest

The authors declare no conflict of interest.

Keywords

3D printing, bioelectronics, flexible hydrogels, precision medicine, skin-electronic interfaces

Received: November 3, 2023
Revised: December 15, 2023
Published online:

[1] W. Bai, T. Kuang, C. Chitrakar, R. Yang, S. Li, D. Zhu, L. Chang, *Biosens. Bioelectron.* **2018**, *122*, 189.
[2] R. Dahiya, Proceedings of the IEEE **2019**, *107*, 247.
[3] N. Yogeswaran, W. Dang, W. T. Navaraj, D. Shakthivel, S. Khan, E. O. Polat, S. Gupta, H. Heidari, M. Kaboli, L. Lorenzelli, G. Cheng, R. Dahiya, *Advanced Robotics* **2015**, *29*, 1359.
[4] Y. Liu, M. Pharr, G. A. Salvatore, *ACS Nano* **2017**, *11*, 9614.
[5] A. Kalkal, S. Kumar, P. Kumar, R. Pradhan, M. Willander, G. Packirisamy, et al., *Additive Manufacturing.* **2021**, *46*, 102088.
[6] H. C Ates, P. Q. Nguyen, L. Gonzalez-Macia, E. Morales-Narváez, F. Güder, J. J. Collins, C. Dincer, *Nat. Rev. Mater.* **2022**, *7*, 887.
[7] N. Weigel, M. J. Männel, J. Thiele, *ACS Appl. Mater. Interfaces* **2021**, *13*, 31086.
[8] W. Gao, H. Ota, D. Kiriya, K. Takei, A. Javey, *Acc. Chem. Res.* **2019**, *52*, 523.
[9] S. Tansaz, A. Baronetto, R. Zhang, A. Derungs, O. Amft, *IEEE Pervasive Computing* **2019**, *18*, 38.
[10] J. A. Rogers, T. Someya, Y. Huang, *Science* **2010**, *327*, 1603.
[11] T. Someya, Z. Bao, G. G. Malliaras, *Nature* **2016**, *540*, 379.
[12] D. J. Lipomi, M. Vosgueritchian, B. C-K. Tee, S. L. Hellstrom, J. A. Lee, C. H. Fox, Z. Bao, *Nat. Nanotechnol.* **2011**, *6*, 788.
[13] L. Nokes, D. Jennings, T. Flint, B. Turton, Introduction to medical electronics applications, Butterworth-Heinemann, **1995**.
[14] P. Lukowicz, T. Kirstein, G. Tröster, *Methods Inf Med* **2004**, *43*, 232.
[15] S. N. Khan, E. Tomin, J. M. Lane, *Orthop Clin North Am* **2000**, *31*, 389.
[16] Y. Khan, A. E. Ostfeld, C. M. Lochner, A. Pierre, A. C. Arias, *Adv. Mater.* **2016**, *28*, 4373.
[17] Z. Ma, S. Li, H. Wang, W. Cheng, Y. Li, L. Pan, Y. Shi, *J. Mater. Chem. B* **2019**, *7*, 173.
[18] A. Chortos, J. Liu, Z. Bao, *Nat. Mater.* **2016**, *15*, 937.
[19] B. C. Tee, C. Wang, R. Allen, Z. Bao, *Nat. Nanotechnol.* **2012**, *7*, 825.
[20] U. Khan, T. H. Kim, H. Ryu, W. Seung, S. W. Kim, *Adv Mater* **2017**, *29*, 1603544.
[21] D.-H. Kim, N. Lu, R. Ghaffari, J. A. Rogers, *NPG Asia Mater.* **2012**, *4*, e15.
[22] S. Wang, M. Li, J. Wu, D.-H. Kim, N. Lu, Y. Su, Z. Kang, Y. Huang, J. A. Rogers, *J Appl Mech.* **2012**, *79*.
[23] C. Liu, N. Huang, F. Xu, J. Tong, Z. Chen, X. Gui, Y. Fu, C. Lao, *Polymers* **2018**, *10*, 629.
[24] X. Wang, L. Dong, H. Zhang, R. Yu, C. Pan, Z. L. Wang, *Adv. Sci.* **2015**, *2*, 1500169.
[25] Y. S. Rim, S. H. Bae, H. Chen, M. N. De, Y. Yang, *Adv. Mater.* **2016**, *28*, 4415.
[26] S. Chen, K. Jiang, Z. Lou, D. Chen, G. Shen, *Adv. Mater. Technol.* **2018**, *3*, 1700248.
[27] Z. Zou, C. Zhu, Y. Li, X. Lei, W. Zhang, J. Xiao, *Sci. Adv.* **2018**, *4*, eaaq0508.
[28] S. Bauer, S. Bauer-Gogonea, I. Graz, M. Kaltenbrunner, C. Keplinger, R. Schwödiauer, *Adv. Mater.* **2014**, *26*, 149.
[29] W. Taube Navaraj, C. García Núñez, D. Shakthivel, V. Vinciguerra, F. Labeau, D. H. Gregory, et al., *Front Neurosci.* **2017**, *11*, 501.
[30] J. Heikenfeld, A. Jajack, J. Rogers, P. Gutruf, L. Tian, T. Pan, R. Li, M. Khine, J. Kim, J. Wang, J. Kim, *Lab Chip.* **2018**, *18*, 217.
[31] S. Yao, P. Swetha, Y. Zhu, *Adv. Healthcare Mater.* **2018**, *7*, 1700889.
[32] H. Yuk, B. Lu, X. Zhao, *Chem. Soc. Rev.* **2019**, *48*, 1642.
[33] H. Yuk, B. Lu, S. Lin, K. Qu, J. Xu, J. Luo, X. Zhao, *Nat. Commun.* **2020**, *11*, 1.
[34] H. Tetsuka, L. Pirrami, T. Wang, D. Demarchi, S. R. Shin, *Adv. Funct. Mater.* **2022**, *32*, 2202674.
[35] A. A. Alsharif, N. S. Milan Cucuri, R. B. Mishra, N. El-Atab, *Adv. Mater. Technol.* **2023**, 2201677.
[36] T. Košir, J. Slavič, *Addit. Manuf.* **2023**, *73*, 103699.
[37] H. Nassar, R. Dahiya, *Advanced Intelligent Systems* **2021**, *3*, 2100102.
[38] P. A. Lopes, B. C. Santos, A. T. de Almeida, M. Tavakoli, *Nat. Commun.* **2021**, *12*, 4666.
[39] T. J. Wallin, L.-E. Simonsen, W. Pan, K. Wang, E. Giannelis, R. F. Shepherd, Y. Mengüç, *Nat. Commun.* **2020**, *11*, 4000.
[40] W. C. Liu, V. H. Y. Chou, R. P. Behera, H. Le Ferrand, *Nat. Commun.* **2022**, *13*, 5015.
[41] H. Liu, C. Du, L. Liao, H. Zhang, H. Zhou, W. Zhou, T. Ren, Z. Sun, Y. Lu, Z. Nie, F. Xu, J. Zhu, W. Huang, *Nat. Commun.* **2022**, *13*, 3420.
[42] S. R. Dabbagh, M. R. Sarabi, R. Rahbarghazi, E. Sokullu, A. K. Yetisen, S. Tasoglu, *iScience* **2021**, *24*, 102012.
[43] R. Su, S. H. Park, X. Ouyang, S. I. Ahn, M. C. McAlpine, *Sci. Adv.* **2022**, *8*, eabl8798.
[44] C. Michas, M. Ç Karakan, P. Nautiyal, J. G. Seidman, C. E. Seidman, A. Agarwal, K. Ekinci, J. Eyckmans, A. E. White, C. S. Chen, *Sci. Adv.* **2022**, *8*, eabm3791.
[45] Y. H. Cho, Y. G. Park, S. Kim, J. U. Park, *Adv. Mater.* **2021**, *33*, 2005805.
[46] J. Guo, Y. Wang, H. Zhang, Y. Zhao, *Adv. Mater.* **2022**, *34*, 2110024.
[47] F. Ershad, S. Patel, C. Yu, *Npj Flex Electron* **2023**, *7*, 32.
[48] C. M. Noller, Y. A. Levine, T. M. Urakov, J. P. Aronson, M. S. Nash, *Front Neurosci.* **2019**, *13*, 911.
[49] A. Hossain, S. Roy, P. S. Guin, *Asian Journal of Research in Chemistry* **2017**, *10*, 441.
[50] D. Joung, N. S. Lavoie, S. Z. Guo, S. H. Park, A. M. Parr, M. C. McAlpine, *Adv. Funct. Mater.* **2020**, *30*, 1906237.
[51] Y. Wang, H. Haick, S. Guo, C. Wang, S. Lee, T. Yokota, T. Someya, *Chem. Soc. Rev.* **2022**, *51*, 3759.
[52] L. Wang, T. Xu, X. Zhang, *Trends Analyt Chem.* **2021**, *134*, 116130.
[53] L. Jiang, J. Wu, *Prog. Mater. Sci.* **2023**, 101110.
[54] Z. Wang, H. Wei, Y. Huang, Y. Wei, J. Chen, *Chem. Soc. Rev.* **2023**.
[55] A. Martinelli, A. Nitti, G. Giannotta, R. Po, D. Pasini, *Mater. Today Chem.* **2022**, *26*, 101135.
[56] R. Pradhan, S. Rahman, A. Qureshi, A. Ullah, *Biopolym. Their Ind. Appl.* **2021**, 281.

[57] C. Wang, T. Yokota, T. Someya, *Chem. Rev.* **2021**, *121*, 2109.
[58] J. Zhou, S. Vijayavenkataraman, *Int. J. Bioprint.* **2021**, *24*, e00166.
[59] J. Liu, L. Sun, W. Xu, Q. Wang, S. Yu, J. Sun, *Carbohydr. Polym.* **2019**, *207*, 297.
[60] M. A. S. R. Saadi, A. Maguire, N. T. Pottackal, M. S. H Thakur, M. M. Ikram, A. J Hart, P. M. Ajayan, M. M. Rahman, *Adv. Mater.* **2022**, *34*, 2108855.
[61] S. D. Dutta, D. K. Patel, K.-T. Lim, *J. Biol. Eng.* **2019**, *13*, 1.
[62] D. K. Patel, S. D. Dutta, J. Hexiu, K. Ganguly, K.-T. Lim, *Carbohydr. Polym.* **2022**, *281*, 119077.
[63] D. K. Patel, K. Ganguly, S. D. Dutta, T. V. Patil, K.-T. Lim, *Carbohydr. Polym.* **2023**, *303*, 120464.
[64] E. Pinto, W. N. Aggrey, P. Boakye, G. Amenuvor, Y. A. Sokama-Neuyam, M. K. Fokuo, et al., *Scientific African.* **2022**, *15*, e01078.
[65] K. Ouyang, J. Zhuang, C. Chen, X. Wang, M. Xu, Z. Xu, *Biomacromolecules* **2021**, *22*, 5033.
[66] R. Yang, X. Chen, Y. Zheng, K. Chen, W. Zeng, X. Wu, *J. Mater. Chem. C* **2022**, *10*, 5380.
[67] K. Li, D. Zhang, H. Zhang, D. Wang, Z. Xu, H. Cai, et al., *ACS Appl. Mater. Interfaces* **2023**.
[68] B. Alonso-Lerma, L. Barandiaran, L. Ugarte, I. Larraza, A. Reifs, R. Olmos-Juste, N. Barruetabeña, I. Amenabar, R. Hillenbrand, A. Eceiza, R. Perez-Jimenez, *Communications Materials* **2020**, *1*, 57.
[69] H. Kargarzadeh, M. Ioelovich, I. Ahmad, S. Thomas, A. Dufresne, *Handb. Nanocellul. Cellul. Nanocompos.* **2017**, *1*, 1.
[70] B. R. Hunde, A. D. Woldeyohannes, *Results Eng.* **2022**, 100478.
[71] D. Trache, A. F. Tarchoun, M. Derradji, T. S. Hamidon, N. Masruchin, N. Brosse, M. H Hussin, *Front Chem.* **2020**, *8*, 392.
[72] T. Uto, T. Yui, *ACS Omega* **2018**, *3*, 8050.
[73] P. Heidarian, S. Gharaie, H. Yousefi, M. Paulino, A. Kaynak, R. Varley, et al., *Carbohydr. Polym.* **2022**, *291*, 119545.
[74] D. K. Patel, K. Ganguly, S. D. Dutta, T. V. Patil, A. Randhawa, K.-T. Lim, *Int. J. Biol. Macromol.* **2023**, *229*, 105.
[75] H. Koga, K. Nagashima, K. Suematsu, T. Takahashi, L. Zhu, D. Fukushima, Y. Huang, R. Nakagawa, J. Liu, K. Uetani, M. Nogi, T. Yanagida, Y. Nishina, *ACS Nano.* **2022**, *16*, 8630.
[76] T. Liu, R. Liang, H. He, Y. Zeng, Z. Hou, Y. Liu, J. Yuan, B. Luo, S. Zhang, C. Cai, S. Wang, D. Lu, S. Nie, *Nano Energy* **2023**, *112*, 108480.
[77] P.-C. Lai, S.-S. Yu, *Polymers* **2021**, *13*, 688.
[78] G. Zhu, L. Giraldo Isaza, B. Huang, A. Dufresne, *ACS Sustainable Chem. Eng.* **2022**, *10*, 2397.
[79] Z. Chen, Y. Hu, G. Shi, H. Zhuo, M. A. Ali, E. Jamróz, H. Zhang, L. Zhong, X. Peng, *Adv. Funct. Mater.* **2023**, 2214245.
[80] M. N. R. Kumar, *React. Funct. Polym.* **2000**, *46*, 1.
[81] S. Islam, M. R. Bhuiyan, M. Islam, *J. Polym. Environ.* **2017**, *25*, 854.
[82] I. Aranaz, M. Mengíbar, R. Harris, P. I. nos, B. Miralles, N. Acosta, G. Galed, A. Heras, *Curr. Chem. Biol.* **2009**, *3*, 203.
[83] S. Wu, S. Wu, X. Zhang, T. Feng, L. Wu, *Biosensors* **2023**, *13*, 93.
[84] Y. Liang, Y. Shen, X. Sun, H. Liang, *Int. J. Biol. Macromol.* **2021**, *193*, 629.
[85] R. Jin, J. Xu, L. Duan, G. Gao, *Carbohydr. Polym.* **2021**, *268*, 118240.
[86] S. D. Dutta, J. Hexiu, D. K. Patel, K. Ganguly, K.-T. Lim, *Int. J. Biol. Macromol.* **2021**, *167*, 644.
[87] J. Sun, H. Tan, *Materials* **2013**, *6*, 1285.
[88] F. Abasalizadeh, S. V. Moghaddam, E. Alizadeh, E. Akbari, E. Kashani, S. M. B. Fazljou, et al., *J. Biol. Eng.* **2020**, *14*, 1.
[89] S. Yang, L. Jang, S. Kim, J. Yang, K. Yang, S.-W. Cho, J. Y. Lee, *Macromol. Biosci.* **2016**, *16*, 1653.
[90] S. Reakasame, A. R. Boccaccini, *Biomacromolecules* **2018**, *19*, 3.
[91] W. Lu, D. Bao, F. Ta, D. Liu, D. Zhang, Z. Zhang, Z. Fan, *ACS Omega* **2020**, *5*, 17152.
[92] M. M. Hasani-Sadrabadi, P. Sarrion, S. Pouraghaei, Y. Chau, S. Ansari, S. Li, T. Aghaloo, A. Moshaverinia, *Sci. Transl. Med.* **2020**, *12*, eaay6853.
[93] Y. Ohm, C. Pan, M. J. Ford, X. Huang, J. Liao, C. Majidi, *Nat. Electron.* **2021**, *4*, 185.
[94] J. Zhang, Y. Wang, Q. Wei, Y. Wang, M. Li, D. Li, L. Zhang, *Int. J. Biol. Macromol.* **2022**, *219*, 1216.
[95] D. Kang, Z. Liu, C. Qian, J. Huang, Y. Zhou, X. Mao, Q. Qu, B. Liu, J. Wang, Z. Hu, Y. Miao, *Acta Biomater.* **2023**, *165*, 19.
[96] H. Zheng, B. Zuo, *J. Mater. Chem. B* **2021**, *9*, 1238.
[97] Z.-L. Wang, Y.-H. Shen, X. Sun, Z.-H. Li, X.-Y. Wang, Z. Zhao, *Microchem. J.* **2020**, *157*, 105036.
[98] N. Johari, L. Moroni, A. Samadikuchaksaraei, *Eur. Polym. J.* **2020**, *134*, 109842.
[99] Z. Li, Q. Wang, G. Liu, *Micromachines* **2022**, *13*, 528.
[100] D. Chouhan, L. Tu, P. K. Samudrala, B. B. Mandal, *Adv. Healthcare Mater.* **2018**, *7*, 1801092.
[101] N. Gorenkova, I. Osama, F. P. Seib, H. V. Carswell, *ACS Biomater. Sci. Eng.* **2018**, *5*, 859.
[102] D. Chen, Z. Yin, F. Wu, H. Fu, S. C. Kundu, S. Lu, *J. Appl. Polym. Sci.* **2017**, *134*, 45050.
[103] H. H. Hwang, W. Zhu, G. Victorine, N. Lawrence, S. Chen, *Small Methods* **2018**, *2*, 1700277.
[104] P. Dorishetty, R. Balu, A. Sreekumar, L. de Campo, J. P. Mata, N. R. Choudhury, et al., *ACS Sustainable Chem. Eng.* **2019**, *7*, 9257.
[105] N. Wu, H. Yu, M. Sun, Z. Li, F. Zhao, Y. Ao, H. Chen, *ACS Appl. Bio Mater.* **2019**, *3*, 721.
[106] O. Hasturk, K. E. Jordan, J. Choi, D. L. Kaplan, *Biomaterials* **2020**, *232*, 119720.
[107] Y. P. Singh, A. Bandyopadhyay, B. B. Mandal, *ACS Appl. Mater. Interfaces* **2019**, *11*, 33684.
[108] L. Ning, R. Mehta, C. Cao, A. Theus, M. Tomov, N. Zhu, et al., *ACS Appl. Mater. Interfaces* **2020**, *12*, 44563.
[109] D. Kang, Z. Liu, C. Qian, J. Huang, Y. Zhou, X. Mao, et al., *Acta Biomater.* **2022**.
[110] X. Wang, Z. Bai, M. Zheng, O. Yue, M. Hou, B. Cui, et al., *J. Sci.: Adv. Mater. Devices* **2022**, *7*, 100451.
[111] Y. Li, Y. Liu, B. Peng, X. Li, T. Fang, S. Liu, J. Liu, B. Li, F. Li, *Biomater Adv.* **2022**, *143*, 213172.
[112] H. Shirahama, B. H. Lee, L. P. Tan, N.-J. Cho, *Sci. Rep.* **2016**, *6*, 31036.
[113] Y. Zhang, Y. Dai, F. Xia, X. Zhang, *Nano Energy* **2022**, *104*, 107977.
[114] J. M. Cabot, L. Y. Daikuara, Z. Yue, P. Hayes, X. Liu, G. G. Wallace, et al., *Sci. Rep.* **2020**, *10*, 7120.
[115] S. Feroz, N. Muhammad, J. Ratnayake, G. Dias, *Bioact Mater.* **2020**, *5*, 496.
[116] A. Sarma, *Int. J. Biol. Macromol.* **2022**, 395.
[117] T. R. Ham, R. T. Lee, S. Han, S. Haque, Y. Vodovotz, J. Gu, L. R. Burnett, S. Tomblyn, J. M. Saul, *Biomacromolecules* **2016**, *17*, 225.
[118] D. R. Goddard, *J. Biol. Chem.* **1935**, *112*, 361.
[119] K. Katoh, T. Tanabe, K. Yamauchi, *Biomaterials* **2004**, *25*, 4255.
[120] A. L. Smith, M. Harris, *J Res Natl Bur Stand(US).* **1936**, *17*, 97.
[121] P. M. Schrooyen, P. J. Dijkstra, R. C. Oberthür, A. Bantjes, J. Feijen, *J. Colloid Interface Sci.* **2001**, *240*, 30.
[122] C. Earland, C. Knight, *Bioch. Biophys. Acta* **1955**, *17*, 457.
[123] H. Xie, S. Li, S. Zhang, *Green Chem.* **2005**, *7*, 606.
[124] Y. Ren, X. Yu, Z. Li, D. Liu, X. Xue, *J. Photochem. Photobiol., B* **2020**, *202*, 111676.
[125] A. Hasan, A. Khattab, M. A. Islam, K. A. Hweij, J. Zeitouny, R. Waters, M. Sayegh, M. M. Hossain, A. Paul, *Adv. Sci.* **2015**, *2*, 1500122.
[126] S. Zhu, Q. Zhou, J. Yi, Y. Xu, C. Fan, C. Lin, J. Wu, Y. Lin, *Adv. Sci.* **2023**, *10*, 2207400.
[127] B. G. Davis, *Chem. Rev.* **2002**, *102*, 579.
[128] D. Ince, T. M. Lucas, S. A. Malaker, *Curr. Opin. Chem. Biol.* **2022**, *69*, 102174.

[129] Z. Yang, A. K. Sarkar, N. Amdursky, *Biomacromolecules* **2023**, *24*, 1111.
[130] W. Shen, S. Das, F. Vitale, A. Richardson, A. Ananthakrishnan, L. A. Struzyna, et al., *Microsyst. Nanoeng.* **2018**, *4*, 30.
[131] J. H. Tsui, A. Leonard, N. D. Camp, J. T. Long, Z. Y. Nawas, R. Chavanachat, A. S. T. Smith, J. S. Choi, Z. Dong, E. H. Ahn, A. Wolf-Yadlin, C. E. Murry, N. J. Sniadecki, D.-H. Kim, *Biomaterials* **2021**, *272*, 120764.
[132] K. Namsheer, C. S. Rout, *RSC Adv* **2021**, *11*, 5659.
[133] P. Sakunpongpitiporn, K. Phasuksom, N. Paradee, A. Sirivat, *RSC Adv* **2019**, *9*, 6363.
[134] H. Wang, H. Wen, B. Hu, G. Fei, Y. Shen, L. Sun, D. Yang, *Sci Rep* **2017**, *7*, 43694.
[135] V. Gautam, K. P. Singh, V. L. Yadav, *Int. J. Biol. Macromol.* **2018**, *111*, 1124.
[136] B. P. Dwivedee, S. Soni, J. K. Laha, U. C. Banerjee, *Int. J. Biol. Macromol.* **2018**, *119*, 8.
[137] V. K. Singh, C. S. Kushwaha, S. Shukla, *Int. J. Biol. Macromol.* **2020**, *147*, 250.
[138] G. Liao, Y. Gong, C. Yi, Z. Xu, *Chinese Journal of Chemistry.* **2017**, *35*, 1157.
[139] V. C. Menzel, I. Tudela, *Curr. Opin. Chem. Eng.* **2022**, *35*, 100742.
[140] E. Shirzaei Sani, C. Xu, C. Wang, Y. Song, J. Min, J. Tu, et al., *Sci. Adv.* **2023**, *9*, eadf7388.
[141] L. Montaina, R. Carcione, F. Pescosolido, M. Montalto, S. Battistoni, E. Tamburri, *ACS Appl. Electron. Mater.* **2023**, *5*, 164.
[142] S. Bhadra, D. Khastgir, N. K. Singha, J. H. Lee, *Prog. Polym. Sci.* **2009**, *34*, 783.
[143] C. Teh, R. Rozaidi, D. Rusli, H. Sahrim, *Polym.-Plast. Technol. Eng.* **2008**, *48*, 17.
[144] K. R. Ryan, M. P. Down, N. J. Hurst, E. M. Keefe, C. E. Banks, *eScience* **2022**.
[145] A. El Jaouhari, A. El Asbahani, M. Bouabdallaoui, Z. Aouzal, D. Filotás, E. A. Bazzaoui, L. Nagy, G. Nagy, M. Bazzaoui, A. Albourine, D. Hartmann, *Synth. Met.* **2017**, *226*, 15.
[146] E. De Giglio, M. Guascito, L. Sabbatini, G. Zambonin, *Biomaterials* **2001**, *22*, 2609.
[147] J. G. de Castro, B. V. M. Rodrigues, R. Ricci, M. M. Costa, A. F. C. Ribeiro, F. R. Marciano, A. O. Lobo, *RSC Adv.* **2016**, *6*, 32615.
[148] E. N. Zare, T. Agarwal, A. Zarepour, F. Pinelli, A. Zarrabi, F. Rossi, M. Ashrafizadeh, A. Maleki, M.-A. Shahbazi, T. K. Maiti, R. S. Varma, F. R. Tay, M. R. Hamblin, V. Mattoli, P. Makvandi, *Appl. Mater. Today* **2021**, *24*, 101117.
[149] C. García-Cabezón, V. Godinho, C. Pérez-González, Y. Torres, *Mater. Today Chem.* **2023**, *29*, 101433.
[150] S. D. Dutta, K. Ganguly, A. Randhawa, T. Patil, D. K. Patel, K.-T. Lim, *Biomaterials* **2023**, 121999.
[151] K. Yamada, Y. Magori, S. Akimoto, J. Sone, *Microsystem Technologies* **2019**, *25*, 2051.
[152] A. Keirouz, Y. L. Mustafa, J. G. Turner, E. Lay, U. Jungwirth, F. Marken, H. S. Leese, *Small* **2023**, *19*, 2206301.
[153] B. Lu, H. Yuk, S. Lin, N. Jian, K. Qu, J. Xu, X. Zhao, *Nat. Commun.* **2019**, *10*, 1043.
[154] V. R. Feig, H. Tran, M. Lee, Z. Bao, *Nat. Commun.* **2018**, *9*, 2740.
[155] J. Liu, J. Garcia, L. M. Leahy, R. Song, D. Mullarkey, B. Fei, A. Dervan, I. V. Shvets, P. Stamenov, W. Wang, F. J. O'Brien, J. N. Coleman, V. Nicolosi, *Adv. Funct. Mater.* **2023**, 2214196.
[156] X. Xie, Z. Xu, X. Yu, H. Jiang, H. Li, W. Feng, *Nat. Commun.* **2023**, *14*, 4289.
[157] N. Lopez-Larrea, M. Criado-Gonzalez, A. Dominguez-Alfaro, N. Alegret, I. D. Agua, B. Marchiori, D. Mecerreyes, *ACS Appl. Polym. Mater.* **2022**, *4*, 6749.
[158] C. Zhang, M. Wang, C. Jiang, P. Zhu, B. Sun, Q. Gao, C. Gao, R. Liu, *Nano Energy* **2022**, *95*, 106991.
[159] A. C. Da Silva, J. Wang, I. R. Minev, *Nat. Commun.* **2022**, *13*, 1353.
[160] D. Ji, J. M. Park, M. S. Oh, T. L. Nguyen, H. Shin, J. S. Kim, D. Kim, H. S. Park, J. Kim, *Nat. Commun.* **2022**, *13*, 3019.
[161] I. Perkucin, K. S. Lau, T. Chen, S. N. Iwasa, H. E. Naguib, C. M. Morshead, *Adv. Healthcare Mater.* **2022**, *11*, 2201164.
[162] I. K. Han, K.-I. Song, S.-M. Jung, Y. Jo, J. Kwon, T. Chung, S. Yoo, J. Jang, Y.-T. Kim, D. S. Hwang, Y. S. Kim, *Adv. Mater.* **2023**, *35*, 2203431.
[163] C. Yu, X. Ying, M.-A. Shahbazi, L. Yang, Z. Ma, L. Ye, W. Yang, R. Sun, T. Gu, R. Tang, S. Fan, S. Yao, *Biomaterials* **2023**, *301*, 122266.
[164] F. Furlani, E. Campodoni, N. Sangiorgi, M. Montesi, A. Sanson, M. Sandri, S. Panseri, *Int. J. Biol. Macromol.* **2023**, *224*, 266.
[165] C.-T. Liu, J. Yu, M.-H. Lin, K.-H. Chang, C.-Y. Lin, N.-C. Cheng, et al., *Biomacromolecules.* **2023**.
[166] J. Sun, X. Wu, J. Xiao, Y. Zhang, J. Ding, J. Jiang, et al., *ACS Appl. Mater. Interfaces* **2023**, *15*, 5897.
[167] F. Zhang, H. Cheng, K. Qu, X. Qian, Y. Lin, Y. Zhang, S. Qian, N. Huang, C. Cui, M. Chen, *Mater. Today Bio.* **2023**, *20*, 100626.
[168] E. Cheah, M. Bansal, L. Nguyen, A. Chalard, J. Malmström, S. J. O'Carroll, B. Connor, Z. Wu, D. Svirskis, *Acta Biomater.* **2023**, *158*, 87.
[169] M. Zhang, Y. Wang, K. Liu, Y. Liu, T. Xu, H. Du, et al., *Carbohydr. Polym.* **2023**, *305*, 120567.
[170] X. Pan, J. Li, N. Ma, X. Ma, M. Gao, *Chem. Eng. J.* **2023**, *461*, 142062.
[171] X. Chai, J. Tang, Y. Li, Y. Cao, X. Chen, T. Chen, et al., *ACS Appl. Mater. Interfaces* **2023**, *15*, 18262.
[172] Z. Karimzadeh, M. Mahmoudpour, A. Jouyban, E. Rahimpour. Hydrogels for Wearable Electronics. Hydrogels, CRC Press, **2023**. pp. 293.
[173] M. I. Shekh, G. Zhu, W. Xiong, W. Wu, F. J. Stadler, D. Patel, C. Zhu, *Int. J. Biol. Macromol.* **2023**, *224*, 604.
[174] B. Yao, H. Wang, Q. Zhou, M. Wu, M. Zhang, C. Li, G. Shi, *Adv. Mater.* **2017**, *29*, 1700974.
[175] S. Zhang, Y. Chen, H. Liu, Z. Wang, H. Ling, C. Wang, J. Ni, B. Çelebi-Saltik, X. Wang, X. Meng, H.-J. Kim, A. Baidya, S. Ahadian, N. Ashammakhi, M. R. Dokmeci, J. Travas-Sejdic, A. Khademhosseini, *Adv. Mater.* **2020**, *32*, 1904752.
[176] J. He, M. Shi, Y. Liang, B. Guo, *Chem. Eng. J.* **2020**, *394*, 124888.
[177] P. He, J. Wu, X. Pan, L. Chen, K. Liu, H. Gao, H. Wu, S. Cao, L. Huang, Y. Ni, *J. Mater. Chem. A* **2020**, *8*, 3109.
[178] K. Li, J. Zhao, A. Zhussupbekova, C. E. Shuck, L. Hughes, Y. Dong, S. Barwich, S. Vaesen, I. V. Shvets, M. Möbius, W. Schmitt, Y. Gogotsi, V. Nicolosi, *Nat. Commun.* **2022**, *13*, 6884.
[179] Y. Zhao, S. Zhang, T. Yu, Y. Zhang, G. Ye, H. Cui, C. He, W. Jiang, Y. Zhai, C. Lu, X. Gu, N. Liu, *Nat. Commun.* **2021**, *12*, 4880.
[180] P. Xue, C. Valenzuela, S. Ma, X. Zhang, J. Ma, Y. Chen, et al., *Advanced Functional Materials.* **2023**, 2214867.
[181] C. A. R. Chapman, E. A. Cuttaz, B. Tahirbegi, A. Novikov, K. Petkos, S. Koutsoftidis, E. M. Drakakis, J. A. Goding, R. A. Green, *Adv. Nanobiomed. Res.* **2022**, *2*, 2100102.
[182] Q. Zhuang, K. Yao, M. Wu, Z. Lei, F. Chen, J. Li, Q. Mei, Y. Zhou, Q. Huang, X. Zhao, Y. Li, X. Yu, Z. Zheng, *Sci. Adv.* **2023**, *9*, eadg8602.
[183] M. S. Brown, L. Somma, M. Mendoza, Y. Noh, G. J. Mahler, A. Koh, *Nat. Commun.* **2022**, *13*, 3727.
[184] H. Min, S. Baik, J. Kim, J. Lee, B.-G. Bok, J. H. Song, M.-S. Kim, C. Pang, *Adv. Funct. Mater.* **2022**, *32*, 2107285.
[185] Y. Hui, Y. Yao, Q. Qian, J. Luo, H. Chen, Z. Qiao, Y. Yu, L. Tao, N. Zhou, *Nat. Electron.* **2022**, *5*, 893.
[186] T. J. Hinton, A. Hudson, K. Pusch, A. Lee, A. W. Feinberg, *ACS Biomater. Sci. Eng.* **2016**, *2*, 1781.
[187] J. R. Tumbleston, D. Shirvanyants, N. Ermoshkin, R. Janusziewicz, A. R. Johnson, D. Kelly, K. Chen, R. Pinschmidt, J. P. Rolland, A.

Ermoshkin, E. T. Samulski, J. M. DeSimone, *Science* **2015**, *347*, 1349.
[188] G. Scordo, V. Bertana, L. Scaltrito, S. Ferrero, M. Cocuzza, S. L. Marasso, S. Romano, R. Sesana, F. Catania, C. F. Pirri, *Mater. Today Commun.* **2019**, *19*, 12.
[189] Q. Yi, S. Najafikhoshnoo, P. Das, S. Noh, E. Hoang, T. Kim, R. Esfandyarpour, *Adv. Mater. Technol.* **2022**, *7*, 2101034.
[190] M. Takenouchi, M. Mukai, T. Furukawa, S. Maruo, *Polymers.* **2022**, *14*, 4949.
[191] J. W. Phillips, A. Prominski, B. Tian, *View* **2022**, *3*, 20200157.
[192] Y. Yan, Y. Jiang, E. L. L. Ng, Y. Zhang, C. Owh, F. Wang, Q. Song, T. Feng, B. Zhang, P. Li, X. J. Loh, S. Y. Chan, B. Q. Y. Chan, *Mater. Today Adv.* **2023**, *17*, 100333.
[193] L. del-Mazo-Barbara, M.-P. Ginebra, *J. Eur. Ceram. Soc.* **2021**, *41*, 18.
[194] H. He, Y. Yang, Y. Pan, *J. Manuf. Syst.* **2019**, *50*, 236.
[195] B. Grigoryan, D. W. Sazer, A. Avila, J. L. Albritton, A. Padhye, A. H. Ta, et al., *Sci. Rep.* **2021**, *11*, 3171.
[196] (Eds: Z. Li, A. S. Rathore, C. Song, S. Wei, Y. Wang, W. Xu), Proceedings of the 2018 ACM sigsac conference on computer and communications security, **2018**.
[197] N. K. Roy, D. Behera, O. G. Dibua, C. S. Foong, M. A. Cullinan, *Microsyst. Nanoeng.* **2019**, *5*, 64.
[198] P. Fu, H. Li, J. Gong, Z. Fan, A. T. Smith, K. Shen, et al., *Prog Polym Sci* **2022**, 101506.
[199] M. H. Ali, S. Kurokawa, E. Shehab, M. Mukhtarkhanov, *Int. J. Lightweight Mater. Manuf.* **2023**, *6*, 198.
[200] A. Wazeer, A. Das, A. Sinha, K. Inaba, S. Ziyi, A. Karmakar, *Prog. Addit. Manuf.* **2022**, 1.
[201] C. Tong, C. Tong, *Advanced Materials for Printed Flexible Electronics* **2022**, 597.
[202] Y. G. Park, I. Yun, W. G. Chung, W. Park, D. H. Lee, J. U. Park, *Adv. Sci.* **2022**, *9*, 2104623.
[203] J. C. Yang, J. Mun, S. Y. Kwon, S. Park, Z. Bao, S. Park, *Adv. Mater.* **2019**, *31*, 1904765.
[204] M. R. Khosravani, T. Reinicke, *Sens. Actuators, A* **2020**, *305*, 111916.
[205] W. Zhao, Z. Wang, J. Zhang, X. Wang, Y. Xu, N. Ding, Z. Peng, *Adv. Mater. Technol.* **2021**, *6*, 2001218.
[206] H. Quan, T. Zhang, H. Xu, S. Luo, J. Nie, X. Zhu, *Bioact. Mater.* **2020**, *5*, 110.
[207] I. Bahnini, M. Rivette, A. Rechia, A. Siadat, A. Elmesbahi, *Int. J. Adv. Manuf. Technol.* **2018**, *97*, 147.
[208] F. Pahlevanzadeh, R. Emadi, A. Valiani, M. Kharaziha, S. A Poursamar, H. R. Bakhsheshi-Rad, A. F. Ismail, S. RamaKrishna, F. Berto, *Materials* **2020**, *13*, 2663.
[209] J. Lemarchand, N. Bridonneau, N. Battaglini, F. Carn, G. Mattana, B. Piro, S. Zrig, V. Noël, *Angew. Chem., Int. Ed.* **2022**, *61*, e202200166.
[210] K. Cho, T. Lee, S. Chung, *Nanoscale Horiz.* **2022**, *7*, 1161.
[211] A. H. Espera, J. R. C. Dizon, Q. Chen, R. C. Advincula, *Progress in Additive Manufacturing* **2019**, *4*, 245.
[212] Y. Ji, C. Luan, X. Yao, J. Fu, Y. He, *Advanced Intelligent Systems* **2021**, *3*, 2000271.
[213] T. Zandrini, S. Florczak, R. Levato, A. Ovsianikov, *Trends Biotechnol.* **2022**.
[214] A. Zennifer, S. Manivannan, S. Sethuraman, S. G. Kumbar, D. Sundaramurthi, *Biomater. Adv.* **2022**, *134*, 112576.
[215] Y. Ze, R. Wang, H. Deng, Z. Zhou, X. Chen, L. Huang, Y. Yao, *Biomater Adv.* **2022**, 213053.
[216] C. Wang, K. Xia, H. Wang, X. Liang, Z. Yin, Y. Zhang, *Adv. Mater.* **2019**, *31*, 1801072.
[217] M. Leschok, I. Cheibas, V. Piccioni, B. Seshadri, A. Schlüter, F. Gramazio, et al., *Automation in Construction.* **2023**, *152*, 104918.
[218] J. M. Lee, W. Y. Yeong, *Adv. Healthcare Mater.* **2016**, *5*, 2856.
[219] H. Li, G. Gao, Z. Xu, D. Tang, T. Chen, *Macromol. Rapid Commun.* **2021**, *42*, 2100480.
[220] K. FUJII, *Trans. Inst. Electron., Inf. Commun. Eng., Sect. E* **2005**, *88*, 2401.
[221] P. Zhu, H. Peng, A. Y. Rwei, *Med. Nov. Technol. Devices* **2022**, *14*, 100118.
[222] Z. Liu, Y. Ma, H. Ouyang, B. Shi, N. Li, D. Jiang, F. Xie, D. Qu, Y. Zou, Y. Huang, H. Li, C. Zhao, P. Tan, M. Yu, Y. Fan, H. Zhang, Z. L. Wang, Z. Li, *Adv. Funct. Mater.* **2019**, *29*, 1807560.
[223] H. Peng, X. Qian, L. Mao, L. Jiang, Y. Sun, Q. Zhou, *Appl. Phys. Lett.* **2019**, *115*.
[224] J. Serup, G. B. Jemec, G. L. Grove, Handbook of non-invasive methods and the skin, CRC press, **2006**.
[225] J. Joseph, C. Feher, W. Anderson, D. Charles, Quantitative Human Physiology: an Introduction, Elsevier Academic Press, **2012**.
[226] Q. Zhang, X. Liu, L. Duan, G. Gao, *Chem. Eng. J.* **2019**, *365*, 10.
[227] T. Q. Trung, N. E. Lee, *Adv. Mater.* **2016**, *28*, 4338.
[228] W. Heng, S. Solomon, W. Gao, *Adv. Mater.* **2022**, *34*, 2107902.
[229] Y. Ma, Y. Zhang, S. Cai, Z. Han, X. Liu, F. Wang, Y. Cao, Z. Wang, H. Li, Y. Chen, X. Feng, *Adv. Mater.* **2020**, *32*, 1902062.
[230] H. Yousef, M. Boukallel, K. Althoefer, *Sens. Actuators, A* **2011**, *167*, 171.
[231] M. R. Cutkosky, W. Provancher, Springer Handbook of Robotics, Springer, **2016**. pp. 717–736.
[232] S. Z. Guo, K. Qiu, F. Meng, S. H. Park, M. C. McAlpine, *Adv. Mater.* **2017**, *29*, 1701218.
[233] S. Chun, A. Hong, Y. Choi, C. Ha, W. Park, *Nanoscale* **2016**, *8*, 9185.
[234] H.-B. Yao, J. Ge, C.-F. Wang, X. Wang, W. Hu, Z.-J. Zheng, Y. Ni, S.-H. Yu, *Adv. Mater.* **2013**, *25*, 6692.
[235] S. Z. Guo, F. Gosselin, N. Guerin, A. M. Lanouette, M. C. Heuzey, *Small* **2013**, *9*, 4118.
[236] R. L. Truby, J. A. Lewis, *Nature* **2016**, *540*, 371.
[237] R. D. Farahani, M. Dubé, D. Therriault, *Adv. Mater.* **2016**, *28*, 5794.
[238] S.-Z. Guo, M.-C. Heuzey, D. Therriault, *Langmuir* **2014**, *30*, 1142.
[239] Y. L. Kong, M. K. Gupta, B. N. Johnson, M. C. McAlpine, *Nano Today* **2016**, *11*, 330.
[240] B. Guo, P. X. Ma, *Biomacromolecules* **2018**, *19*, 1764.
[241] A. Chortos, Z. Bao, *Mater. Today* **2014**, *17*, 321.
[242] Y. Lee, J. Y. Oh, T. R. Kim, X. Gu, Y. Kim, G.-J. N Wang, H.-C. Wu, R. Pfattner, J. W. F. To, T. Katsumata, D. Son, J. Kang, J. R. Matthews, W. Niu, M. He, R. Sinclair, Y. Cui, J. B.-H. Tok, T.-W. Lee, Z. Bao, *Adv. Mater.* **2018**, *30*, 1704401.
[243] G.-J. N. Wang, F. Molina-Lopez, H. Zhang, J. Xu, H.-C. Wu, J. Lopez, L. Shaw, J. Mun, Q. Zhang, S. Wang, A. Ehrlich, Z. Bao, *Macromolecules* **2018**, *51*, 4976.
[244] M. T. Chorsi, E. J. Curry, H. T. Chorsi, R. Das, J. Baroody, P. K. Purohit, H. Ilies, T. D. Nguyen, *Adv. Mater.* **2019**, *31*, 1802084.
[245] K. S. Ramadan, D. Sameoto, S. Evoy, *Smart Mater. Struct.* **2014**, *23*, 033001.
[246] S. Emamian, B. B. Narakathu, A. A. Chlaihawi, B. J. Bazuin, M. Z. Atashbar, *Sens. Actuators, A* **2017**, *263*, 639.
[247] A. Adami, R. S. Dahiya, C. Collini, D. Cattin, L. Lorenzelli, *Sens. Actuators, A* **2012**, *188*, 75.
[248] E. S. Kolesar, C. S. Dyson, *J. Microelectromech. Syst.* **1995**, *4*, 87.
[249] Y. Wang, J. Zheng, G. Ren, P. Zhang, C. Xu, *Smart Mater. Struct.* **2011**, *20*, 045009.
[250] C. Baur, J. R. DiMaio, E. McAllister, R. Hossini, E. Wagener, J. Ballato, S. Priya, A. Ballato, D. W. Smith, *J. Appl. Phys.* **2012**, *112*, 124104.
[251] L. Persano, C. Dagdeviren, Y. Su, Y. Zhang, S. Girardo, D. Pisignano, Y. Huang, J. A. Rogers, *Nat. Commun.* **2013**, *4*, 1.
[252] S.-H. Park, H. B. Lee, S. M. Yeon, J. Park, N. K. Lee, *ACS Appl. Mater. Interfaces* **2016**, *8*, 24773.
[253] Y. K. Fuh, B. S. Wang, C.-Y. Tsai, *Sci Rep* **2017**, *7*, 1.
[254] K. Senthil Kumar, P.-Y. Chen, H. Ren, *Research* **2019**, 2019.

[255] S. Guerin, A. Stapleton, D. Chovan, R. Mouras, M. Gleeson, C. McKeown, M. R. Noor, C. Silien, F. M. F. Rhen, A. L. Kholkin, N. Liu, T. Soulimane, S. A. M. Tofail, D. Thompson, *Nat. Mater.* **2018**, *17*, 180.
[256] M. Minary-Jolandan, M.-F. Yu, *Nanotechnology* **2009**, *20*, 085706.
[257] T. Yucel, P. Cebe, D. L. Kaplan, *Adv. Funct. Mater.* **2011**, *21*, 779.
[258] V. Basavalingappa, S. Bera, B. Xue, J. O'Donnell, S. Guerin, P.-A. Cazade, H. Yuan, E. U. Haq, C. Silien, K. Tao, L. J. W. Shimon, S. A. M. Tofail, D. Thompson, S. Kolusheva, R. Yang, Y. Cao, E. Gazit, *ACS Nano* **2020**, 7025.
[259] A. Kholkin, N. Amdursky, I. Bdikin, E. Gazit, G. Rosenman, *ACS Nano* **2010**, *4*, 610.
[260] T. Someya, Stretchable electronics, John Wiley & Sons, **2012**.
[261] A. Lund, **2013**.
[262] G. da Cunha Rodrigues, P. Zelenovskiy, K. Romanyuk, S. Luchkin, Y. Kopelevich, A. Kholkin, *Nat. Commun.* **2015**, *6*, 1.
[263] M. Wajahat, S. Lee, J. H. Kim, W. S. Chang, J. Pyo, S. H. Cho, et al., *ACS Appl. Mater. Interfaces* **2018**, *10*, 19999.
[264] Z. Wang, X. Guan, H. Huang, H. Wang, W. Lin, Z. Peng, *Adv. Funct. Mater.* **2019**, *29*, 1807569.
[265] W. Deng, T. Yang, L. Jin, C. Yan, H. Huang, X. Chu, Z. Wang, D. Xiong, G. Tian, Y. Gao, H. Zhang, W. Yang, *Nano Energy* **2019**, *55*, 516.
[266] S. Wang, J. Xu, W. Wang, G.-J. N. Wang, R. Rastak, F. Molina-Lopez, J. W. Chung, S. Niu, V. R. Feig, J. Lopez, T. Lei, S.-K. Kwon, Y. Kim, A. M. Foudeh, A. Ehrlich, A. Gasperini, Y. Yun, B. Murmann, J. B.-H. Tok, Z. Bao, *Nature* **2018**, *555*, 83.
[267] B. Gorissen, D. Reynaerts, S. Konishi, K. Yoshida, J. W. Kim, M. De Volder, *Adv. Mater.* **2017**, *29*, 1604977.
[268] M. Amjadi, K. U. Kyung, I. Park, M. Sitti, *Adv. Funct. Mater.* **2016**, *26*, 1678.
[269] J. T. Muth, D. M. Vogt, R. L. Truby, Y. Mengüç, D. B. Kolesky, R. J. Wood, J. A. Lewis, *Adv. Mater.* **2014**, *26*, 6307.
[270] V. Correia, J. Oliveira, N. Perinka, P. Costa, E. Sowade, K. Y. Mitra, R. R. Baumann, S. Lanceros-Mendez, *ACS Appl. Electron. Mater.* **2020**, *2*, 1470.
[271] C. J. Hohimer, G. Petrossian, A. Ameli, C. Mo, P. Pötschke, *Addit. Manuf.* **2020**, 101281.
[272] S. J. Leigh, R. J. Bradley, C. P. Purssell, D. R. Billson, D. A. Hutchins, *PLoS One* **2012**, *7*, e49365.
[273] C. Yan, J. Wang, W. Kang, M. Cui, X. Wang, C. Y. Foo, K. J. Chee, P. S. Lee, *Adv. Mater.* **2014**, *26*, 2022.
[274] J. Park, Y. Lee, J. Hong, M. Ha, Y.-D. Jung, H. Lim, S. Y. Kim, H. Ko, *ACS Nano* **2014**, *8*, 4689.
[275] G. Schwartz, B. C.-K. Tee, J. Mei, A. L. Appleton, D. H. Kim, H. Wang, Z. Bao, *Nat. Commun.* **2013**, *4*, 1859.
[276] M. Amjadi, A. Pichitpajongkit, S. Lee, S. Ryu, I. Park, *ACS Nano* **2014**, *8*, 5154.
[277] S. Gong, W. Schwalb, Y. Wang, Y. Chen, Y. Tang, J. Si, B. Shirinzadeh, W. Cheng, *Nat. Commun.* **2014**, *5*, 1.
[278] K. K. Kim, S. Hong, H. M. Cho, J. Lee, Y. D. Suh, J. Ham, S. H. Ko, *Nano Lett.* **2015**, *15*, 5240.
[279] Y. Tong, Z. Feng, J. Kim, J. L. Robertson, X. Jia, B. N. Johnson, *Nano Energy* **2020**, 104973.
[280] Y. C. Lai, J. Deng, S. L. Zhang, S. Niu, H. Guo, Z. L. Wang, *Adv. Funct. Mater.* **2017**, *27*, 1604462.
[281] F. R. Fan, W. Tang, Z. L. Wang, *Adv. Mater.* **2016**, *28*, 4283.
[282] W. Zeng, L. Shu, Q. Li, S. Chen, F. Wang, X. M. Tao, *Adv. Mater.* **2014**, *26*, 5310.
[283] Q. Zhang, Z. Zhang, Q. Liang, F. Gao, F. Yi, M. Ma, Q. Liao, Z. Kang, Y. Zhang, *Nano Energy.* **2019**, *55*, 151.
[284] R. I. Haque, O. Chandran, S. Lani, D. Briand, *Nano Energy* **2018**, *52*, 54.
[285] M.-L. Seol, J.-W. Han, D.-I. Moon, K. J. Yoon, C. S. Hwang, M. Meyyappan, *Nano Energy* **2018**, *44*, 82.
[286] H.-J. Yoon, D.-H. Kim, W. Seung, U. Khan, T. Y. Kim, T. Kim, S.-W. Kim, *Nano Energy* **2019**, *63*, 103857.
[287] C. Qian, L. Li, M. Gao, H. Yang, Z. Cai, B. Chen, Z. Xiang, Z. Zhang, Y. Song, *Nano Energy* **2019**, *63*, 103885.
[288] J. Kim, A. S. Campbell, B. E.-F. de Ávila, J. Wang, *Nat. Biotechnol.* **2019**, *37*, 389.
[289] N. P. Shetti, A. Mishra, S. Basu, R. J. Mascarenhas, R. R. Kakarla, T. M. Aminabhavi, *ACS Biomater. Sci. Eng.* **2020**, *6*, 1823.
[290] P. Yáñez-Sedeño, S. Campuzano, J. M. Pingarrón, *Biosensors* **2020**, *10*, 76.
[291] B. C. Gross, J. L. Erkal, S. Y. Lockwood, C. Chen, D. M. Spence, *Meml. Serv. Exploit. Ind. Tab. Allumettes, Ser. B* **2014**.
[292] S. Wang, L. Ge, X. Song, J. Yu, S. Ge, J. Huang, F. Zeng, *Biosens. Bioelectron.* **2012**, *31*, 212.
[293] C. M. B. Ho, S. H. Ng, K. H. H. Li, Y.-J. Yoon, *Lab on a Chip.* **2015**, *15*, 3627.
[294] B. P. Lechêne, M. Cowell, A. Pierre, J. W. Evans, P. K. Wright, A. C. Arias, *Nano Energy* **2016**, *26*, 631.
[295] E. Macdonald, R. Salas, D. Espalin, M. Perez, E. Aguilera, D. Muse, R. B. Wicker, *IEEE access* **2014**, *2*, 234.
[296] S. L. Zhang, D. J. Roach, S. Xu, P. Wang, W. Zhang, H. J Qi, Z. L. Wang, *Adv. Mater. Technol.* **2020**, 2000368.
[297] T. Chen, Q. Shi, M. Zhu, T. He, L. Sun, L. Yang, C. Lee, *ACS Nano* **2018**, *12*, 11561.
[298] B. García-Farrera, L. F. Velásquez-García, *ACS Appl. Mater. Interfaces* **2019**, *11*, 29167.
[299] X. Chen, X. Qian, K.-H. Lam, C. T. Chiu, R. Chen, Z. Chen, K. K Shung, P. Yu, Q. Zhou, *Adv. Funct. Mater.* **2019**, *29*, 1902912.
[300] H. Cui, R. Hensleigh, D. Yao, D. Maurya, P. Kumar, M. G. Kang, S. Priya, X. Zheng, *Nat. Mater.* **2019**, *18*, 234.
[301] J. Z. Gul, M. Sajid, K. H. Choi, *J. Mater. Chem. C* **2020**, *8*, 2597.
[302] J. F. Christ, N. Aliheidari, P. Pötschke, A. Ameli, *Polymers* **2019**, *11*, 11.
[303] S.-H. Min, G.-Y. Lee, S.-H. Ahn, *Composites, Part B* **2019**, *161*, 395.
[304] Y. Luo, D. Wu, Y. Zhao, Q. Chen, Y. Xie, M. Wang, L. Lin, L. Wang, D. Sun, *Org. Electron.* **2019**, *67*, 10.
[305] S. Mousavi, D. Howard, S. Wu, C. Wang, arXiv preprint arXiv:181009236 **2018**.
[306] O. Y. Kweon, S. J. Lee, J. H. Oh, *NPG Asia Mater.* **2018**, *10*, 540.
[307] J.-K. Lee, H.-H. Kim, J.-W. Choi, K.-C. Lee, S. Lee, *Int J Control Autom Syst* **2018**, *16*, 929.
[308] K. Kim, J. Park, J-h Suh, M. Kim, Y. Jeong, I. Park, *Sens. Actuators, A* **2017**, *263*, 493.
[309] S. Lathers, M. Mousa, J. La Belle, *3D Print. Addit. Manuf.* **2017**, *4*, 30.
[310] S. Agarwala, G. L. Goh, Y. L. Yap, G. D. Goh, H. Yu, W. Y. Yeong, T. Tran, *Sens. Actuators, A* **2017**, *263*, 593.
[311] K. Kim, M. Jung, B. Kim, J. Kim, K. Shin, O.-S. Kwon, S. Jeon, *Nano Energy* **2017**, *41*, 301.
[312] J. Y. Kim, S. Ji, S. Jung, B.-H. Ryu, H.-S. Kim, S. S. Lee, Y. Choi, S. Jeong, *Nanoscale* **2017**, *9*, 11035.
[313] P. Vasandani, B. Gattu, J. Wu, Z. H. Mao, W. Jia, M. Sun, *Adv. Mater. Technol.* **2017**, *2*, 1700014.
[314] J. A. Hondred, Z. Johnson, J. C. Claussen, *J. Mater. Chem. C* **2020**, 11376.
[315] M. A. Ali, C. Hu, E. A. Yttri, R. Panat, *Adv. Funct. Mater.* **2022**, *32*, 2107671.
[316] K. A. Deo, M. K. Jaiswal, S. Abasi, G. Lokhande, S. Bhunia, T.-U. Nguyen, M. Namkoong, K. Darvesh, A. Guiseppi-Elie, L. Tian, A. K. Gaharwar, *ACS Nano* **2022**, *16*, 8798.
[317] T. Kim, Q. Yi, E. Hoang, R. Esfandyarpour, *Adv. Mater. Technol.* **2021**, *6*, 2001021.

[318] D. H. Ho, P. Hong, J. T. Han, S. Y. Kim, S. J. Kwon, J. H. Cho, *Adv. Sci.* **2020**, *7*, 1902521.
[319] C. Lim, Y. J. Hong, J. Jung, Y. Shin, S.-H. Sunwoo, S. Baik, O. K. Park, S. H. Choi, T. Hyeon, J. H. Kim, S. Lee, D.-H. Kim, *Sci. Adv.* **2021**, *7*, eabd3716.
[320] Q. Wang, X. Pan, C. Lin, H. Gao, S. Cao, Y. Ni, X. Ma, *Chem. Eng. J.* **2020**, *401*, 126129.
[321] E. Parvini, A. Hajalilou, P. A. Lopes, M. S. M. Tiago, A. T. de Almeida, M. Tavakoli, *Soft Matter* **2022**, *18*, 8486.
[322] F. Fu, J. Wang, H. Zeng, J. Yu, *ACS Mater. Lett.* **2020**, *2*, 1287.
[323] X. Xiong, Y. Chen, Z. Wang, H. Liu, M. Le, C. Lin, G. Wu, L. Wang, X. Shi, Y.-G. Jia, Y. Zhao, *Nat. Commun.* **2023**, *14*, 1331.
[324] S. Pal, Y.-Z. Su, Y.-W. Chen, C.-H. Yu, C.-W. Kung, S.-S. Yu, *ACS Appl. Mater. Interfaces* **2022**, *14*, 28247.
[325] S. Peng, Q. Guo, N. Thirunavukkarasu, Y. Zheng, Z. Wang, L. Zheng, L. Wu, Z. Weng, *Chem. Eng. J.* **2022**, *439*, 135593.
[326] B. Hildebrandt, P. Wust, O. Ahlers, A. Dieing, G. Sreenivasa, T. Kerner, et al., *Crit. Rev. Oncol./Hematol.* **2002**, *43*, 33.
[327] H. Charaya, T. G. La, J. Rieger, H. J. Chung, *Adv. Mater. Technol.* **2019**, *4*, 1900327.
[328] J.-H. Lee, H. Chen, E. Kim, H. Zhang, K. Wu, H. Zhang, et al., *Mater. Horiz.* **2021**, *8*, 1488.
[329] T. Li, B. Liang, Z. Ye, L. Zhang, S. Xu, T. Tu, Y. Zhang, Y. Cai, B. Zhang, L. Fang, X. Mao, S. Zhang, G. Wu, Q. Yang, C. Zhou, X. Cai, X. Ye, *Biosens. Bioelectron.* **2022**, *198*, 113855.
[330] M. Parrilla, A. Vanhooydonck, M. Johns, R. Watts, K. De Wael, *Sens. Actuators, B* **2023**, *378*, 133159.
[331] S. Zhang, S. S. Rana, T. Bhatta, G. B. Pradhan, S. Sharma, H. Song, S. Jeong, J. Y. Park, *Nano Energy* **2023**, *106*, 108110.
[332] J. Wei, J. Xie, P. Zhang, Z. Zou, H. Ping, W. Wang, et al., *ACS Appl. Mater. Interfaces* **2021**, *13*, 2952.
[333] Z. Wang, H. Song, L. Chen, W. Li, D. Yang, P. Cheng, H. Duan, *ACS Appl. Electron. Mater.* **2022**, *4*, 5199.
[334] Y. Zhang, L. Chen, M. Xie, Z. Zhan, D. Yang, P. Cheng, H. Duan, Q. Ge, Z. Wang, *Mater. Today Phys.* **2022**, *27*, 100794.
[335] T.-H. Kang, H. Chang, D. Choi, S. Kim, J. Moon, J. A. Lim, K.-Y. Lee, H. Yi, *Nano Lett.* **2019**, *19*, 3684.
[336] Q. Chang, Y. He, Y. Liu, W. Zhong, Q. Wang, F. Lu, M. Xing, *Adv. Funct. Mater.* **2020**, *30*, 1910080.
[337] Z. Zhu, H. S. Park, M. C. McAlpine, *Sci. Adv.* **2020**, *6*, eaba5575.
[338] L.-W. Lo, J. Zhao, H. Wan, Y. Wang, S. Chakrabartty, C. Wang, *ACS Appl. Mater. Interfaces* **2021**, *13*, 21693.
[339] Z. Deng, T. Hu, Q. Lei, J. He, P. X. Ma, B. Guo, *ACS Appl. Mater. Interfaces* **2019**, *11*, 6796.
[340] M. Seong, S. Kondaveeti, G. Choi, S. Kim, J. Kim, M. Kang, et al., *ACS Appl. Mater. Interfaces* **2023**, *15*, 11042.
[341] S. NajafiKhoshnoo, T. Kim, J. A. Tavares-Negrete, X. Pei, P. Das, S. W. Lee, J. Rajendran, R. Esfandyarpour, *Adv. Mater. Technol.* **2023**, 2201655.
[342] Z. Shen, Z. Zhang, N. Zhang, J. Li, P. Zhou, F. Hu, Y. Rong, B. Lu, G. Gu, *Adv. Mater.* **2022**, *34*, 2203650.
[343] G. L. Goh, S. Agarwala, W. Y. Yeong, *Adv. Mater. Interfaces* **2019**, *6*, 1801318.
[344] B. Herren, M. C. Saha, M. C. Altan, Y. Liu, *Composites, Part B* **2020**, *200*, 108224.
[345] D. Xiang, X. Zhang, Y. Li, E. Harkin-Jones, Y. Zheng, L. Wang, C. Zhao, P. Wang, *Composites, Part B* **2019**, *176*, 107250.
[346] J. S. Heo, M. F. Hossain, I. Kim, *Sensors* **2020**, *20*, 3927.
[347] Z. Tang, S. Jia, C. Zhou, B. Li, *ACS Appl. Mater. Interfaces* **2020**, *12*, 28669.
[348] Y. Song, R. Y. Tay, J. Li, C. Xu, J. Min, E. Shirzaei Sani, et al., *Sci. Adv.* **2023**, *9*, eadi6492.
[349] S. Liu, Y. Rao, H. Jang, P. Tan, N. Lu, *Matter* **2022**, *5*, 1104.
[350] D.-H. Kim, N. Lu, R. Ma, Y.-S. Kim, R.-H. Kim, S. Wang, et al., *Science* **2011**, *333*, 838.
[351] S. Xu, Y. Zhang, L. Jia, K. E. Mathewson, K.-I. Jang, J. Kim, H. Fu, X. Huang, P. Chava, R. Wang, S. Bhole, L. Wang, Y. J. Na, Y. Guan, M. Flavin, Z. Han, Y. Huang, J. A. Rogers, *Science* **2014**, *344*, 70.
[352] E. V. Robilotti, N. E Babady, P. A. Mead, T. Rolling, R. Perez-Johnston, M. Bernardes, Y. Bogler, M. Caldararo, C. J. Figueroa, M. S. Glickman, A. Joanow, A. Kaltsas, Y. J. Lee, A. Lucca, A. Mariano, S. Morjaria, T. Nawar, G. A. Papanicolaou, J. Predmore, G. Redelman-Sidi, E. Schmidt, S. K. Seo, K. Sepkowitz, M. K. Shah, J. D. Wolchok, T. M. Hohl, Y. Taur, M. Kamboj, *Nat. Med.* **2020**, *26*, 1218.
[353] H. Dillekås, M. S. Rogers, O. Straume, *Cancer Med.* **2019**, *8*, 5574.
[354] R. V. Devi, M. Doble, R. S. Verma, *Biosens. Bioelectron.* **2015**, *68*, 688.
[355] A. B. Chinen, C. M. Guan, J. R. Ferrer, S. N. Barnaby, T. J. Merkel, C. A. Mirkin, *Chem. Rev.* **2015**, *115*, 10530.
[356] F. Arshad, F. Nabi, S. Iqbal, R. H. Khan, *Colloids Surf., B* **2022**, *212*, 112356.
[357] J. Li, Y. Li, L. Pan, W. Pan, N. Li, B. Tang, *Trends Analyt. Chem.* **2022**, 116807.
[358] D. Crosby, S. Bhatia, K. M. Brindle, L. M. Coussens, C. Dive, M. Emberton, et al., *Early detection of cancer. Science.* **2022**, *375*, eaay9040.
[359] A. Chiadò, G. Palmara, A. Chiappone, C. Tanzanu, C. F. Pirri, I. Roppolo, F. Frascella, *Lab on a Chip.* **2020**, *20*, 665.
[360] S. Damiati, S. Küpcü, M. Peacock, C. Eilenberger, M. Zamzami, I. Qadri, H. Choudhry, U. B. Sleytr, B. Schuster, *Biosens. Bioelectron.* **2017**, *94*, 500.
[361] M. Berney, J. F. McGouran, *Nat. Rev. Chem.* **2018**, *2*, 332.
[362] K. S. Bhat, S. Byun, A. Alam, M. Ko, J. An, S. Lim, *Talanta* **2022**, *244*, 123421.
[363] J. Lim, B. Kang, H. Y. Son, B. Mun, Y.-M. Huh, H. W. Rho, T. Kang, J. Moon, J.-J. Lee, S. B. Seo, S. Jang, S. U. Son, J. Jung, S. Haam, E.-K. Lim, *Biosens. Bioelectron.* **2022**, *197*, 113753.
[364] H. Luo, W. Wei, Z. Ye, J. Zheng, R. Xu, *Trends Mol Med* **2021**, *27*, 482.
[365] W. Liang, Y. Zhao, W. Huang, Y. Gao, W. Xu, J. Tao, M. Yang, L. Li, W. Ping, H. Shen, X. Fu, Z. Chen, P. W. Laird, X. Cai, J.-B. Fan, J. He, *Theranostics* **2019**, *9*, 2056.
[366] D. Li, H. Chen, K. Fan, V. Labunov, S. Lazarouk, X. Yue, C. Liu, X. Yang, L. Dong, G. Wang, *Biosens. Bioelectron.* **2021**, *181*, 113147.
[367] S. Chang-Hao Tsao, J. Weiss, C. Hudson, C. Christophi, J. Cebon, A. Behren, et al., *Sci. Rep.* **2015**, *5*, 11198.
[368] R. Li, L. Zou, Y. Luo, M. Zhang, L. Ling, *Sci Rep* **2017**, *7*, 44212.
[369] B. Qiu, W. Guo, F. Zhang, F. Lv, Y. Ji, Y. Peng, X. Chen, H. Bao, Y. Xu, Y. Shao, F. Tan, Q. Xue, S. Gao, J. He, *Nat. Commun.* **2021**, *12*, 6770.
[370] X. Jin, C. Liu, T. Xu, L. Su, X. Zhang, *Biosens. Bioelectron.* **2020**, *165*, 112412.
[371] Y. Zhang, Y. Hu, N. Jiang, A. K. Yetisen, *Biosens. Bioelectron.* **2023**, *219*, 114825.
[372] M. Schaffner, J. A. Faber, L. Pianegonda, P. A. Rühs, F. Coulter, A. R. Studart, *Nat. Commun.* **2018**, *9*, 878.
[373] T. Li, J. Chang, Y. Zhu, C. Wu, *Adv. Healthcare Mater.* **2020**, *9*, 2000208.
[374] X. Zhou, L. Ren, Q. Liu, Z. Song, Q. Wu, Y. He, et al., *Macromol. Biosci.* **2022**, *22*, 2100332.
[375] D. Venkatesan, A. Elangovan, H. Winster, M. Y. Pasha, K. S. Abraham, J. Satheeshkumar, et al., *Biosens Bioelectron X* **2022**, *11*, 100188.

Sayan Deb Dutta is a postdoctoral research associate at Kangwon National University. He received his doctoral degree from the Department of Biosystems Engineering at Kangwon National University, South Korea. He reviewed his Master's degree from the University of Kalyani, India. His research interest is the synthesis of multifunctional nanomaterials for 3D printing and nanotheranostic applications for tissue engineering.

Keya Ganguly is a postdoctoral research associate at Kangwon National University. She received her doctoral degree from the Department of Biosystems Engineering at Kangwon National University, South Korea. She received her Master's degree from Presidency University, India. Her research interest is developing a multi-stimuli-assisted scaffolding platform for tissue engineering and biosensing.

Aayushi Randhawa is a doctoral student in Biosystems Engineering at Kangwon National University, South Korea. She received her master's degree from Bangalore University, India. Her research interest is the synthesis of 3D-printed structures for the healing and regeneration of damaged bone tissues.

Tejal V. Patil is a doctoral student of Biosystems Engineering at Kangwon National University, South Korea. She received her master's degree from the Institute of Chemical Technology, Mumbai, India. Her research interest is developing biomaterials for application in bacteria eradication and tissue regeneration.

Hojin Kim is a Master's student in Biosystems Engineering at Kangwon National University, South Korea. His research interest is Nanocellulose hydrogel for wound healing and sensing.

Rumi Acharya is a doctoral student in Biosystems Engineering at Kangwon National University, South Korea. She received her master's degree from Guru Ghasidas University, India. Her research interests are Nano biosensors and magnetogenetic therapy on cellular targets.

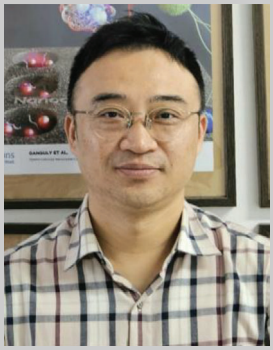

Ki-Taek Lim is a professor at the Department of Biosystems Engineering at Kangwon National University, South Korea. He received his doctoral degree from Seoul National University, South Korea, and joined as a postdoctoral research fellow at the University of Arkansas, USA. He has a strong knowledge of mechatronics and regenerative medicines. His research focuses on developing the bio-nanorobotics system with novel bioreactors and stem cell cultures for tissue-engineering applications.